Isolation and Characterization of Malondialdehyde Mimotopes of Oxidized LDL

Doctoral Thesis at the Medical University of Vienna
for obtaining the Degree

'Doctor of Philosophy - PhD'

Submitted by

Shahzada Amir, M.D., M.Sc.

Supervisors

Univ. Prof. Dr. med. Christoph J. Binder, PhD
O.Univ. Prof. Dr. med. Oswald Wagner

Department of Laboratory Medicine (KILM)
Medical University of Vienna

Research Center for Molecular Medicine (Ce-M-M)
of the Austrian Academy of Sciences
Lazarettgasse 14, AKH BT 25.3
1090 Vienna, Austria

Vienna, 27/06/2012

TABLE OF CONTENTS

1. ABSTRACT

1.1 Abstract – English

Atherosclerosis is a chronic-inflammatory disease of the vascular wall that is the underlying cause for myocardial infarction and stroke. It is characterized by the accumulation of oxidized LDL and apoptotic cells, both of which contain products of lipid peroxidation in their membranes. These oxidation products of LDL including malondialdehyde-adducts play a key role in the initiation and progression of atherosclerosis. Circulating autoantibodies specific for malondialdehyde-modified LDL (MDA-LDL) represent potential biomarkers to predict cardiovascular risk. Moreover, immunization of animal models of atherosclerosis with autologous MDA-LDL reduces atherosclerosis. However, MDA-LDL is a complex high variability antigen with limited reproducibility. Using an MDA-LDL-specific monoclonal antibody, I identified peptide mimotopes of MDA by peptide phage display. These MDA-mimotopes were specifically bound by murine and human MDA-specific monoclonal antibodies and were found to mimic MDA-epitopes on the surface of apoptotic cells. Immunization of mice with a selected mimotope resulted in the induction of MDA-LDL-specific antibodies, which strongly immunostained atherosclerotic lesions. Finally, autoantibodies to MDA-mimotopes in sera of healthy subjects and in patients with myocardial infarction and stable angina pectoris undergoing percutaneous coronary intervention were determined and found to correlate significantly with respective autoantibody titers against MDA-LDL. Thus, I identified mimotopes that can be exploited as standardized and reproducible antigens, which will be useful for diagnostic and therapeutic applications in cardiovascular disease.

1.2 Kurzfassung – Deutsch

Atherosklerose ist eine chronisch-entzündliche Erkrankung arterieller Gefäße, die sich mit klinischen Komplikationen, wie Myokardinfarkt und Schlaganfall, welche die häufigsten Todesursachen weltweit sind, manifestiert. Atherosklerose zeichnet sich durch die Ablagerung von oxidiertem LDL und apoptotischen Zellen aus, deren Membranen durch Lipid-Peroxidation hervorgerufene biochemischeVeränderungen aufweisen. Bei der Entstehung und dem Voranschreiten atherosklerostischer Gefäßveränderungen spielen Lipidperooxidationsprodukte, unter anderem Malondialdehyd-Addukte, eine wesentliche Rolle. So konnte gezeigt werden, dass die Spiegel zirkulierende Antikörper mit Spezifität für Malondialdehyd-modifiziertes LDL (MDA-LDL) potenzielle Biomarker für kardiovaskuläre Erkrankungen darstellen. Weiters konnte im Tierversuch gezeigt werden, dass die Immunisierung mit autologem MDA-LDL die Entstehung atherosklerotischer Plaques reduziert. Da MDA-LDL jedoch ein sehr komplexes Antigen mit großer Variabilität und limitierter Reproduzierbarkeit darstellt, war es bisher nicht möglich diese Immunantworten genauer zu charakterisieren. In dieser Arbeit konnten mit Hilfe eines MDA-LDL spezifischen monoklonalen Antikörpers Peptid-Mimotope von MDA-Addukten mittels Peptid-Phagen Display Technologie identifiziert werden, welche spezifisch von murinen und humanen MDA-spezifische Antikörpern erkannt werden. Weiters konnte gezeigt werden, dass diese MDA-Mimotope immunologisch MDA-Addukten an der Oberfläche apoptotischer Zellen entsprechen. Außerdem wurde gezeigt, dass Immunisierung von Mäusen mit einem der Mimotope zur Bildung von MDA-LDL spezifischen Antikörpern führt, welche immunhistochemisch atherosklerotische Läsionen spezifisch anfärbten. Zuletzt konnten auch gegen MDA-mimotope gerichtet Autoantikörper in Seren von gesunden Probanden und Patienten mit Myokard-Infarkt und stabiler Angina Pectoris, die sich einer perkutanen coronaren Intervention unterzogen haben, nachgewiesen werden. Die Serumspiegel dieser Antikörper wiesen eine signifikante Korrelation mit den Autoantikörper-Titern gegen MDA-LDL auf. Demnach konnten hoch spezifische MDA-Mimotope, die als standardisierte und reproduzierbare Antigene eingesetzt werden können, identifiziert werden, welchein Zukunft für diagnostische und therapeutische Zwecke verwendet werden können.

2. INTRODUCTION

2.1 Atherosclerosis

Atherosclerosis is the most common pathological process leading to cardiovascular disease (CVD), the leading cause of death in developed countries (1-3).The term "atherosclerosis" originates from the Greek words "*athero"* (meaning gruel) and "*sclerosis"* (meaning hardness) and is used to describe the chronic inflammatory lesions of large and medium-sized arteries, which can lead to clinical manifestations, such as coronary artery disease, peripheral vascular disease and stroke (4). Atherosclerotic plaques appear macroscopically as patchy deposits on the inside of the arterial wall that are formed by lipid-laden macrophages, smooth muscle cells, extracellular matrix, lipids and acellular lipid-rich debris. In the initial stage of plaque formation so-called "fatty streaks" are formed, which are characterized by the accumulation of lipid laden foam cells in the intima of arteries. As lesion formation progresses from fatty streaks to advanced plaques, foam cells that are unable to maintain the export of excess cholesterol undergo apoptosis and/or necrosis leading to the development of a necrotic core in the lesion (5, 6). Smooth muscle cell proliferation and collagen secretion stabilizes these lesions. However, sudden rupture of vulnerable lesions, which have a thin fibrous cap, can result in thrombus formation leading to clinical events such as heart attacks and strokes (7, 8). Inflammation has been found to play an important role in all these processes, and it is now well established that atherosclerosis is a chronic inflammatory disease (9, 10), in which certain immune functions have been found to modulate atherosclerotic lesion formation through cellular and non-cellular components of the immune system (11, 12).

Various risk factors such as hypertension, advanced age, male gender, smoking and diabetes contribute to CVD (13), but extensive evidence suggests that hypercholesterolemia is the key contributor in lesion development from initial fatty streaks to plaque rupture (14). High plasma levels of LDL-cholesterol result in the entrapment of LDL particles in the extracellular matrix of the intimal layer, in part because positively charged residues (Lys, Arg) of ApoB-100 bind to negatively charged glycosaminoglycan of proteoglycans. Interestingly, transgenic mice expressing mutated apoB-100 with less binding to glycosaminoglycan developed less atherosclerosis, thereby suggesting an important role for

LDL retention in the subendothelial space (15). The prolonged retention of LDL predisposes it to oxidative modification by enzymatic (myeloperoxidase, 12/15-lipoxygenase) as well as non-enzymatic mechanisms mediated by reactive oxygen species formed by NADPH oxidase and nitric oxide synthases (4, 16-19). In turn, products of LDL oxidation (OxLDL) initiate an inflammatory response and activate the normally non-adhesive and non-thrombogenic surface of endothelial cells (ECs) in lesion prone areas of the arteries. Activated ECs express intracellular adhesion molecule-1 (ICAM-1), E-selectin and P-selectin, fractalkine, vascular cell adhesion molecule-1(VCAM)-1, and synthesize monocyte chemoattractant protein-1 (MCP-1), interleukin-8 (IL-8) that results in the recruitment and adhesion of leukocytes, most prominently monocytes (20-22). In fact, the experimental inhibition/blockage of factors involved in the recruitment and differentiation of leukocytes (Fig. 1) has been shown to reduce the development of atherosclerotic lesions (23-28).

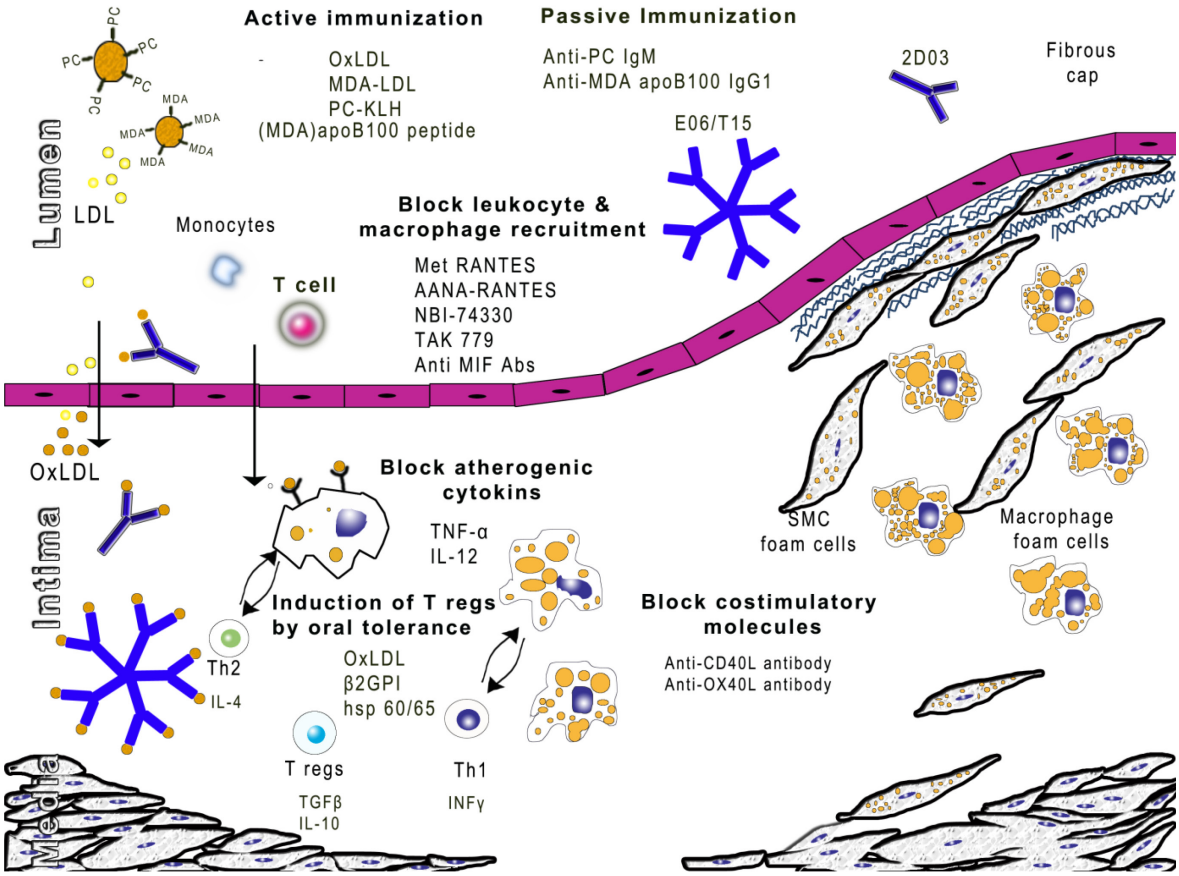

Fig. 1: Experimental immunotherapeutic strategies for inhibition of atherosclerosis.

Atherosclerosis can be reduced at various levels of its development by inducing or blocking components of the innate and adaptive immune response. Adapted from Amir et al. (29).

Subsequently, monocytes differentiate into macrophages, which engulf OxLDL leading to the formation of foam cells, hallmark cells of lesions of all stages (4, 30-33).

2.2 Immunity and atherosclerosis

In the past years, it has been shown that both innate and adaptive immune responses have the ability to modulate the course of atherosclerosis (12, 34, 35).

2.3 Innate Immune system in atherosclerosis

The prominent involvement of the innate immune system in atherosclerosis is characterized by the critical role of macrophages, which express germline encoded pattern recognition receptors (PRRs) such as scavenger receptors (SR) and toll-like receptors (TLR) (36-38). These receptors recognize both exogenous microbial pathogen-associated molecular patterns (PAMPs) as well as endogenous damage-associated molecular patterns (DAMPs (39, 40). Recent evidence has demonstrated that molecular structures that are generated in the course of lipid peroxidation represent an important class of DAMPs with critical importance for innate immune functions in atherosclerosis (41)

For example, scavenger receptors of macrophages including CD36, SR-A1 and -A2, SR-B1, LOX-1 bind OxLDL (42-44) and internalize it. Mice deficient in CD36 and/or SR-A1 develop less atherosclerosis in most – but not all - studies, suggesting the rate limiting role of scavenger receptors (44-50). Signalling PRRs such as TLRs are also expressed by various cells in atherosclerotic lesion and they actively contribute to the inflammatory responses (51, 52). Deletion of cell surface TLR2 and TLR4 in mice led to reduced plaque development (53), whereas local overexpression of both TLR2 and TLR4 in the intima of carotid arteries of hyperlipidemic rabbits significantly increased atherosclerosis (54, 55). Recently, it has been demonstrated that the genetic deletion of intracellular TLR3 in hypercholesterolemic $ApoE^{-/-}$ mice accelerated the onset of early atherosclerosis. These data suggest that cell surface TLRs

(TLR2, TLR4) may promote atherosclerosis, while intracellular TLR3 appear to protect from atherosclerosis.

In human epidemiological studies, a polymorphism in TLR4 (Asp299Gly) has been found to be associated with a decreased risk of carotid artery disease in one study (56), while another study reported inconsistent results (57). Recently, TLR4 has been shown to mediate pro-inflammatory effects of oxidized phospholipids and CD36 has been shown to trigger inflammatory signals in response to minimally oxidized LDL through the assembly of TLR4/6 heterodimer complex (58).

Apart from cellular PRRs, secreted pattern recognition proteins such as C-reactive protein, complement factor H, as well as natural IgM Abs may also be involved in atherogenesis, as they have been shown to bind oxidation-specific epitopes present in OxLDL (11, 59).

2.4 Adaptive immune system in atherosclerosis

Cells of the adaptive immune system such as T and B cells have extremely high diversity due to the somatic rearrangements (V(D)J recombination) of their receptors (60). B cells identify free antigens of any origin, whereas T cells identify peptide fragments of processed protein antigens. T cells become activated when T cell receptors recognize antigens bound either to MHC class II molecules ($CD4^+$ helper T cells) or to MHC class I molecules ($CD8^+$ T cells) on the surface of antigen presenting cells (APCs). It has been shown that cellular components of the adaptive immune response, most prominently T cells are present in lesions (61). $CD4^+$T helper cells (Th) can be classified into Th1, Th2 and Th17, and regulatory T (Treg) cells on the basis of distinct cytokine repertoire (62). Th1 cells are considered mainly proatherogenic, as they produce proinflammatory cytokines such as IFN-γ, TNF-α and TNF-β and IL-2 leading to the activation of macrophages (35, 62). In humans, 10% of the T cells extracted from human lesions were found to be specific for OxLDL and to secrete IFN-γ in response to activation (63). Th2 cells secrete IL-4, IL-5, IL-13 and are mainly involved in the activation of B cells, which subsequently leads to the secretion of antigen specific Abs (35, 62). Th2 cells are also present in the lesion, but the role of Th2 cytokines in atherogenesis is more complex. While IL-5 was found to be atheroprotective, IL-4 seems to have no effect or even a pro-atherogenic one (34, 64, 65). A third distinct subset of

Th cells, Th-17 cells, has also been found in the atherosclerotic plaque (66). Th17 cells secrete IL-17A, IL-17F, IL-21, IL-22, and IL-26 (35, 62). Recently, it has been reported that in patients with carotid artery atherosclerosis Th17 cells and plasma IL-17 levels were positively correlated with the severity and progression of carotid artery plaques (67). While blockade of IL-17A (68) or its receptor (69), and neutralization of IL-17 by administration of an anti-IL-17 antibody (70) in animal models of atherosclerosis protects against atherosclerosis, intravenous administration of recombinant IL-17A reduced early atherosclerosis in *Ldlr*$^{-/-}$ mice (71). The role of IL-17 in atherosclerosis is not completely elucidated (72). However, reduction in vascular inflammation and atherosclerosis in hypercholesterolemic *IL-17*$^{-/-}$*ApoE*$^{-/-}$ mice indicate a proinflammatory and proatherogenic role of Th17-cells (73). While Th1, Th17 subtypes of T cells aggravate atherosclerosis, Tregs subtype of T cells may prevent inflammation by supperessing and counterbalancing effects of other Th subtypes. Several lines of evidence indicate that different Tregs (Foxp3^{+}natural, inducible and Tr1 cells) exert immunoregulatory function through secretion of anti-inflammatory cytokines TGF-β, IL-10 and IL-35. The atheroprotective effect of Tregs has been demonstrated by experiments in which Tregs were depleted either by anti-CD25 Abs (74) or by immunization with Foxp3-transfected dendritic cells (75) In contrast, transfer of Tregs can inhibit T cells responses and can reduce atherosclerosis (76, 77). Moreover, blockage or deficiency of anti-inflammatory cytokines TGF-β and IL-10 significantly increases atherosclerosis (78-81). The role of other recently identified additional T-cell subtypes which include Tfh (T follicular helper cells), Th9 (T cells that produce IL-9) in atherosclerosis has not yet been investigated (82, 83).

B cells are also found in atherosclerotic plaques of mice and humans, though at much lower frequencies than T cells (84-86). Like T cells, also different subsets of B cells exist. The dominant population is represented by B2 cells that are present in adult spleens and lymph nodes and contribute to T-cell dependent antibody responses. In addition, a small population called B1 cells mainly found in pleural and peritoneal cavities exists. It has been further divided into B1a and B1b cells with respect to cell-surface CD5 expression. B1a cells in particular secrete germ line encoded natural IgM Abs, which contribute mainly to T-cell independent humoral immune responses and serve as a first line of defense against bacterial pathogens (87, 88). Initial studies suggested a protective function of B cells in atherosclerosis, as splenectomy aggravated atherosclerotic lesion formation in hypercholesterolemic *Apoe*$^{-/-}$ mice and adoptive transfer of splenic B cells from hypercholesterolemic *Apoe*$^{-/-}$ mice into

splenectomized *Apoe*$^{-/-}$ recipients mediated protection (89). Moreover, *Ldlr*$^{-/-}$ mice that were reconstituted with bone marrow from B-cell deficient μMT mice developed significantly more atherosclerosis (90). Two recent studies, however, demonstrated that depletion of B cells using CD20-antibodies significantly reduced atherosclerosis in *Ldlr*$^{-/-}$ and *Apoe*$^{-/-}$ mice (91, 92). This apparent discrepancy can be explained by the fact that different B-cell subsets have different functions in atherosclerosis (93). Recently, it has been reported that selective depletion of B2 with minimal effects on B1 cells in *BAFF-R*$^{-/-}$*ApoE*$^{-/-}$ resulted in reduction of arterial inflammation and atherosclerosis (94). Moreover, adoptive transfer of bone marrow cells from *BAFF-R*$^{-/-}$ mice into *Ldlr*$^{-/-}$ recipient mice also led to the reduction of lesion size and OxLDL specific IgG with preservation of IgM Abs (95). Moreover, it has been demonstrated that the transfer of natural IgM Abs producing B1a cells into splenectomized *Apoe*$^{-/-}$ mice resulted in the restoration of OxLDL specific IgM Abs and reduction of atherosclerotic lesions(96). Likewise the absence of serum IgM Abs significantly enhanced formation of atherosclerotic lesions in *sIgM*$^{-/-}$*Ldlr*$^{-/-}$ *mice*, pointing towards an atheroprotective role for NAbs (97). Thus, overall experimental data indicate that B2 cells aggravate atherosclerosis, whereas B1a cells and the natural IgM Abs they secrete have atheroprotective effects.

Immune responses to various antigens have been found to modulate atherosclerosis progressions to different degrees. Therefore, current immunological interventions to prevent atherogenesis aim at dampening atherogenic pro-inflammatory or boosting protective anti-inflammatory responses (Fig. 1).

2.5 Potential antigens in atherosclerosis

Several potential antigens have been suggested to trigger immune responses that influence atherosclerotic lesion formation (12, 98). These include bacterial and viral antigens, such as *Chlamydia pneumonia*, *Cytomegalovirus*, as well as (altered) self-antigens such as, heat shock protein 60 (including cross-reactive microbial homologues mHSP65 and cHSP60), β2gpI and oxidized LDL. Among all these antigens, epitopes of OxLDL appear to be prominent and immunodominant (35, 37). Oxidative modification of LDL has been shown to result in the generation of various oxidation specific epitopes (OSEs) that are recognized by specific Abs in a hapten-specific manner (99). These include lipid peroxidation breakdown

products such as malondialdehyde (MDA), which forms many different complex condensation products (see below), as well as the remaining "core aldehydes," such as 1-palmitoyl-2-(5-oxovaleroyl)-*sn*-glycero-3-phosphocholine (POVPC) (34, 41, 100). For the assessment of specific immune responses to such OSEs of OxLDL, two model antigens have been widely used, namely $CuSO_4$-oxidized LDL, which contains many different OSEs, and MDA-modified LDL, which is generated by the derivatization of LDL with various MDA-type adducts.

2.6 Malondidaldehyde adducts are prominent OSEs

MDA is believed to be the most abundant aldehyde resulting from lipid peroxidation and forms adducts with amino groups of lysine (101). Nevertheless, the MDA-modification of LDL and proteins is complex. In vitro, at neutral pH the most abundant form is the low reactive enolate ion which converts to β-hydroxyacrolein at lower pH and reacts with nucleophilic functional groups like primary amines in a Michael addition-type reaction. After spontaneous condensation enaminal adducts such as N^{ε}-(2-propenal) lysine (MDA-Lys; Fig. 2A) are generated (102). The aldehyde moiety of MDA-Lys reacts further with another ε-amino group of lysine which may further form non-fluorescent Schiff-bases intra- and inter-molecular covalent cross-linked 1-amino-3-iminopropene-type MDA-lysine adducts (MDA-$(Lys)_2$; Fig. 2B) (103). Moreover, in acidic conditions with excess of MDA, another cross-linking fluorescent product, 3,5-diformyl-1,4-dihydropyridine-4-yl-pyridinium (FHP; Fig. 2D) can be formed (104). MDA also contributes in the generation of so-called hybrid MAA adducts (105) which are formed from a Hantzsch reaction of MDA, acetaldehyde (AA) and the ε-amino group of lysine residues. The chemical structure of MAA adducts depends on the number of aldehydes involved in its formation (106). A linear non-fluorescent adduct, 2-formyl-3-(alkylamino)butanal (FAAB) forms when the ε-amino group of lysine contains acetaldehyde and MDA in 1:1 ratio, whereas in case of fluorescent cyclic adduct two MDA are present with one AA to form 4-methyl-1,4-dihydropyridine-3,5-dicarbaldehyde ($(MDA)_2$-AA-Lys; MDHDC; Fig. 2C) (105, 107, 108). The MDHDC adduct (109) has been demonstrated to be immunodominant and very immunogenic (110-112).

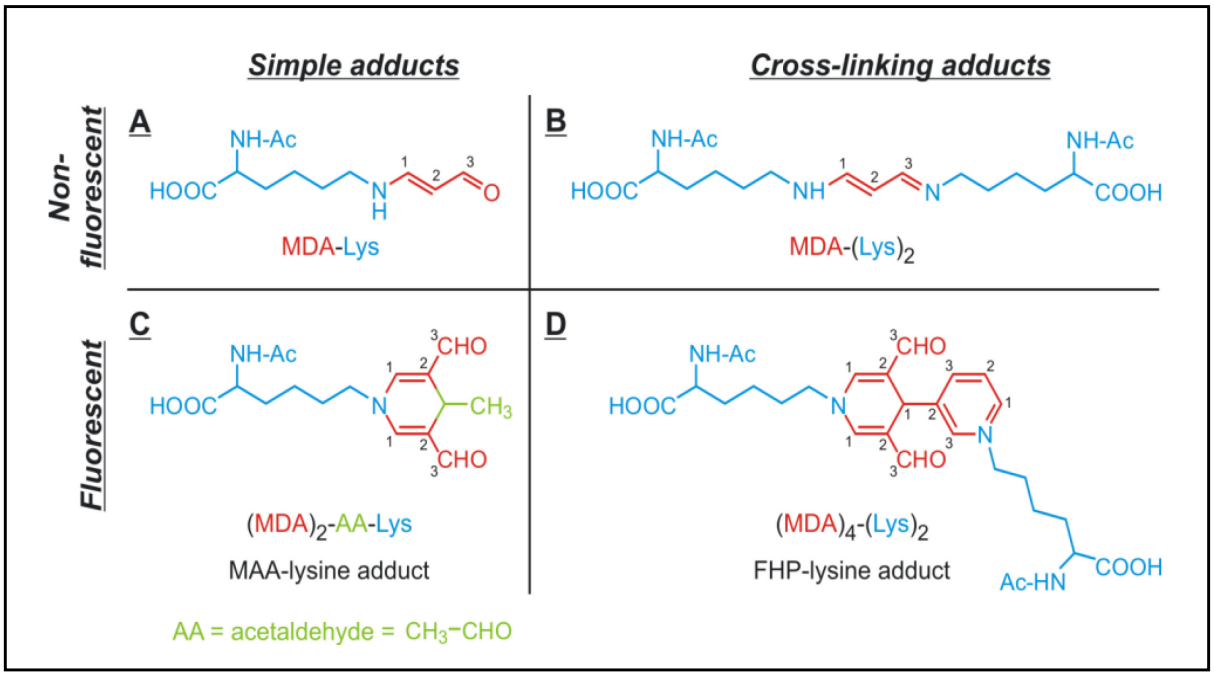

Fig 2: MDA-type adducts on a carrier molecule.

(A-D) Depending on the conditions (pH and ratio of MDA, AA and lysine residues) MDA generates various different adducts on a carrier molecule. MDA products are formed after condensation reactions of MDA with lysine and AA. **(A)** MDA-Lys (1:1, lysine:MDA stoichiochemistry) at pH 7.4. **(B)** MDA-$(Lys)_2$ (2:1, lysine:MDA stoichiochemistry) at pH 7.4. **(C)** $(MDA)_2$-lysine (1:2:1, lysine:MDA:AA stoichiochemistry) at pH 4.8. **(D)** FHP-lysine (1:2, lysine:MDA stoichiochemistry) at pH4.8 (Fig. courtesy of K. Hartvigsen).

2.7 Immune responses to OxLDL and MDA-LDL

Antibodies against these two models of OxLDL have been documented in lesions and plasma of patients and animal models of atherosclerosis (99, 113-115). In animal studies of atherogenesis, antibody titers to OSEs correlate strongly with the progression and regression of atherosclerosis (116-118).

In a large number of epidemiological studies elevated IgG titers to OxLDL and MDA-LDL were reported to be associated with progression of atherosclerosis (119-124). However, in other studies of patients with primary hypercholesterolemia (125) and with coronary artery

disease (126-132) this association was not confirmed. Abs to MDA-LDL have also been suggested to be a marker of plaque instability, as patients with acute coronary syndrome had higher IgG titers to MDA-LDL than patients with stable coronary artery disease and controls (133, 134). On the other hand, some studies report an inverse association between IgM titers to MDA-LDL and carotid atherosclerosis (125, 128, 135, 136). However, this was not consistently found (124, 127, 137).

Thus, many but not all epidemiological studies have demonstrated that IgG titers appear to correlate positively, whereas IgM titers are largely inversely associated with CVD events (128-132).

It is hypothesized that these IgM Abs are to a large extent natural IgM Abs. NAbs have germ line encoded variable regions with little or no nucleotide insertions and thus a limited repertoire of binding specificities for diverse antigens such as (phospho)lipids and carbohydrates (138). Their specificity for neoself-antigens provides NAbs with an important homeostatic "house-keeping" function to promote the clearance of potentially harmful self-antigens, such as OxLDL (88, 139). In fact, Chou et al. reported that OSEs are prominent targets for natural IgM Abs in mice and in humans (140). A prominent specificity of NAbs is PC of oxidized phospholipids, which is bound by the IgM Ab EO6. EO6 was originally cloned from the spleens of atherosclerotic *Apoe*$^{-/-}$ mice, which had high IgM titers to different epitopes of OxLDL (141). The variable region of EO6 was found to be 100% germline encoded and identical to the prototypic NAb T15, known to recognize PC epitopes present on *Streptococcus pneumonia* (11, 115). Functionally, EO6 has been shown to fully inhibit the binding and degradation of CuOx-LDL by mouse peritoneal macrophages, suggesting a role of NAbs in preventing foam cell formation in vivo (142). EO6 also recognizes oxidized phospholipids in the membranes of apoptotic cells (143), which have also been shown to express MDA-epitopes on their surface (140).

Importantly, it has been shown that approximately 12% of all natural IgM-secreting cells in mice were found to bind MDA-type adducts, identifying them as the single most dominant target of oxidation-specific natural IgM. MDA-specific IgM antibodies were also found to be enriched in human umbilical cord blood, which serves as surrogate for NAbs in humans (140). In analogy to the PC-specific mAb EO6, a number of MDA-LDL-specific IgM mAbs were also cloned either from the spleens of various mouse models: EN1 (chow-fed *Apoe*$^{-/-}$), LRO4 (fat-fed *Ldlr*$^{-/-}$), EO14 (fat-fed *Apoe*$^{-/-}$), and NA17 (B-1 cell reconstituted *Rag1*$^{-/-}$) IgM Abs (140, 141, 144, 145). All these IgM Abs stain atherosclerotic lesions (144).

The recently identified property of natural IgM to target various oxidation-specific structures in OxLDL and on the surface of apoptotic cells may provide important insights into the atheroprotective mechanisms of natural IgM. Indeed, the clearance of late apoptotic cells is assisted by IgM Abs through the activation of the classical pathway (146-149). IgM Abs are required for the efficient engulfment and clearance of apoptotic cells *in vivo* and their presence is essential for the immunomodulatory effects mediated by apoptotic cells, such as the induction of IL-10 secreting B cells (150).

2.8 Immunization with MDA antigens

To better understand the functional role of immune responses to OxLDL and MDA-LDL, a series of immunization studies have been carried out in which OxLDL-specific immune interventions were performed in animal models of atherosclerosis (29, 151, 152).

Immunization with homologous MDA-LDL: In a seminal study, the laboratory of Dr. Witztum made the surprising observation that immunization of *Ldlr*$^{-/-}$ rabbits with homologous MDA-LDL suspended in complete Freund's adjuvant (CFA) and subsequent booster immunizations of antigen in incomplete Freund's adjuvant (IFA) at monthly intervals for 6 months markedly reduced the extent of atherosclerosis compared to the controls. All MDA-LDL immunized animals developed robust specific anti-MDA-LDL IgG and IgM titers. This intervention demonstrated that certain components of MDA-specific immune responses have the potential to protect from atherosclerosis, though the mechanism by which immunization led to a protective effect remained unclear (153). Similarly, Nilsson and colleagues performed an immunization study in which NZW rabbits received only two injections of either native LDL or CuOx-LDL and demonstrated a significant reduction of lesion formation in LDL-immunized rabbits after 16-weeks of cholesterol-feeding (154).

In addition, immunization with homologous MDA-LDL emulsified in CFA/IFA has been shown to decrease atherosclerotic lesion formation in both *Apoe*$^{-/-}$ and *Ldlr*$^{-/-}$ mice (155, 156). In the same study, the authors demonstrate the induction of robust T-cell dependent IgG1 and IgG2a antibodies to MDA-LDL, but also IgG to other epitopes of OxLDL. Moreover, IgM titers to some of these also increased in response to immunization with MDA-LDL. Interestingly, the authors also reported a protective effect of immunization with native LDL, which was associated with a minimal but significant increase of IgG titers to oxidation-

specific epitopes (156). In another study, Zhou et al. also confirmed the protective effect of immunization with MDA-LDL, which they found associated with a robust induction of anti-MDA-LDL IgG. Moreover, they could document increased activation of $CD69^{+}CD4^{+}$ and $CD8^{+}$ T cells in lymph nodes from immunized mice after in vitro incubation with MDA-LDL (157). However, in a later study the authors demonstrated that the protective effect of MDA-LDL immunization does not depend on the presence of $CD4^{+}$ T cells, as immunization was still protective in $CD4^{-/-}apoE^{-/-}$ mice, although the importance of $CD4^{+}$ T cells for atherogenesis was demonstrated by the fact that $CD4^{-/-}apoE^{-/-}$ developed significantly less lesions than $apoE^{-/-}$ mice (158). To obtain better mechanistic insights into the protective effect of immunization, Binder et al. analyzed in more detail the immune response induced by immunization with MDA-LDL. In this study, immunization of $Ldlr^{-/-}$ mice with MDA-LDL led to the preferential induction IL-5 secreting T cells associated with a rise of Th2-dependent IgG1 titers but also IgM titers to MDA-LDL. Importantly, immunization with MDA-LDL was also found to increase the levels of the atheroprotective natural IgM T15/EO6 in an IL-5 dependent manner. Thus, MDA-LDL immunization induces a specific Th2 response that is dominated by IL-5, which provides non-cognate help for the expansion of natural IgM Abs by B-1 cells (64). However, the absolute role of IgM in the protective effect of this immunization still needs to be established. Similarly, the in vivo role of IgG antibodies with specificity for OxLDL has not been established. Unlike IgM, IgG are recognized by specific Fcγ-receptors and in vitro studies have shown that IgG-containing OxLDL-immune complexes promote lipid accumulation and pro-inflammatory responses in macrophages (159). Thus, unlike IgM antibodies, OxLDL-specific IgG antibodies (or certain subclasses) may well have pro-atherogenic effects.

2.9 Passive immunizations with MDA-specific antibodies

As most of the active immunization approaches were found to induce high titered antibodies against the respective model antigens, the therapeutic potential of isolated antibodies in atherosclerosis has been tested by passive immunization (Fig. 1) of animal models of atherosclerosis with MDA-specific Abs.

Anti-MDA-peptide IgG1: For example, the effectiveness of passive immunizations was tested using recombinant human IgG1 antibodies specific for MDA-modified apoB-100

peptides, which were identified from an antibody fragment phage display library screened with different peptides and then transformed into a full length IgG1λ. Passive transfer of one antibody, termed IEI-E3, showed an effect on lesion formation in *Apoe*$^{-/-}$ mice when administered weekly for the last three weeks of a 25-week feeding period. Interestingly, the authors demonstrated that the same antibody was shown to have the capacity to increase OxLDL binding and uptake by monocytes in vitro (160). In a follow-up study using *Apobec-1*$^{-/-}$*/Ldlr*$^{-/-}$ mice with established atherosclerosis the authors tested the potential of two human anti-peptide antibodies to stimulate regression. After 24 weeks of high fat diet, regression was induced by a change to regular chow diet for a for a 4-week period. During this time, mice received three weekly injections of two MDA-modified apoB-100 p45 peptide specific IgG1 (IEI-E3 or 2D03). Both therapeutic IgG1 Abs promoted the regression significantly, and 2D03 also stimulated the expression of ABCA-1 in the plaques, suggesting that induction of cholesterol efflux may be induced by the antibody (161). Goncalves et al. also demonstrated the presence of 2D03-reactive epitopes in human plaques (162). Thus, human anti-MDA-peptide IgG1 has a protective capacity in mouse models of atherosclerosis. As the functional properties of human IgG Abs are difficult to assess in murine models, interpretation of the exact mechanism by which these antibodies mediate protection are difficult. Recently, the 2D03 mAb in human (BI 204) has been proven to be safe in a phase I human trial and is currently being tested in the phase II GLACIER study for the assessment of its effect on vascular inflammation in the atherosclerotic blood vessel of patients with acute coronary syndromes (152).

Anti MDA-LDL Fab and scFv: Recently, Tsimikas et al. reported that intraperitoneal injections of IK17 Fab (2.5 mg/kg in PBS) to cholesterol-fed *Ldlr*$^{-/-}$ mice 3 times per week for 14 weeks decreased aortic lesion formation up to 29% compared to PBS treated mice (163). In a follow up study, *Ldlr*$^{-/-}$*Rag 1*$^{-/-}$ double-knockout mice were fed a high cholesterol diet and levels of plasma IK17-scFv were maintained by bi-weekly injections of Adv-IK-17-scFv expressing recombinant IK-17. After 16 weeks of treatment, a 46% decrease in *en face* atherosclerosis was observed in mice treated with Adv-IK17-scFv compared to the mice treated with adenovirus-enhanced green fluorescent protein vector. Moreover, peritoneal macrophages isolated from Adv-IK-17-scFv treated mice had decreased lipid accumulation compared with control group. Taken together, MDA-specific antibodies can reduce the progress of atherosclerosis, demonstrating their potential in treating cardiovascular disease in humans.

2.10 Specific background of research goals

One of the widely investigated products of lipid peroxidation, MDA, has been found in atherosclerotic lesions and plasma of humans and animal models of atherosclerosis (99, 113-115). Importantly, active and passive immunization of animal models with MDA-LDL or MDA-specific antibodies confers atheroprotection, indicating the importance of MDA-specific responses. Indeed, antibodies to MDA-LDL have been documented in plasma and atherosclerotic lesions, and both murine and human mAbs have been cloned. Autoantibodies specific for MDA-LDL may represent potential biomarkers to predict cardiovascular risk. However, published studies report inconsistent findings and even display diverging results regarding the prognostic role of autoAbs to OxLDL in CVD. Reasons for this may be manifold. Certainly, each population studied is unique with different study design and time points of assessment. In addition, the method of OxLDL-specific Ab determination often varies from one study to another and there is no universal reference standard available. However, this is important, as OxLDL preparations show great variability both within one laboratory and in-between several laboratories. On the one hand, the isolated LDL preparations that are used for the generation of CuOx-LDL or MDA-LDL are never identical; on the other hand, the generation of CuOx-LDL or MDA-LDL does not result in reproducible and fully comparable antigen preparations. Even MDA-modification can result in different adducts, as MDA is a highly reactive breakdown product of lipid peroxidation that can give rise to many different immunogenic epitopes. Recent evidence indicates that 4-methyl-1,4-dihydro-3,5-pyridinedicarboxaldehyde (MDHDC)-type adducts found in malondialdehyde-acetaldehyde (MAA)-modified proteins represent the immunogenic advanced MDA-adducts responsible for many biological effects (106, 110). However, due to the various condensation products of MDA, the reproducible generation of MDA-LDL as an antigen carrying the relevant epitopes with similar density is difficult (Fig. 2). Moreover, the stability of these structures is limited. All these factors may have contributed to the variable outcomes of the many studies assessing MDA-specific antibodies as risk factor for CVD. Thus, there is a great need to develop a reproducible and standardized antigen for the translation of MDA vaccine approach to humans and to understand the exact dynamics of MDA-specific IgG and IgM Abs responses in health and disease.

3. AIM OF THE STUDY

The aim of this thesis was to identify and characterize peptide mimotopes of MDA-LDL that could be used as antigens to improve the reproducible detection of MDA-specific autoantibody responses and to investigate their dynamics in health and disease. The second aim is to test whether shorter peptides can be developed as immunogenic mimics of MDA structures for the development of peptide based vaccines.

4. MATERIALS AND METHODS

4.1 Antigens

The following antigens were prepared as described previously (140, 164): Copper-oxidized LDL (CuOx-LDL) and malondialdehyde-modified LDL (MDA-LDL) was prepared from human LDL isolated from pooled plasma of healthy subjects. MAA-BSA was prepared by modification of bovine serum albumin (BSA) with MDA and acetaldehyde as described (107). BSA and KLH was purchased from Pierce Biotechnology.

Small MAA-modified peptides were prepared and provided by Dr. Karsten Hartvigsen (University of California San Diego). N-terminally biotinylated peptides contained the following basal primary sequence: Biotin-Gly-Asp-Gly-Asp-Gly-X(OH) (Bt-GDGDG-X, in which X consists of following 1-4 additional amino acids; H, R, N, K, KK, and KGGK). Binding to the constant spacer sequence of the peptides, GDGDG, by Abs was ruled out by substitution of Asp (D) with Ala (A). All biotinylated peptides where purchased from Biopeptide Co., Inc. (San Diego, CA, USA).

4.2 Antibodies

LRO4 and EN1 are monoclonal IgM Abs that were cloned from the spleens of cholesterol-fed *Ldlr*$^{-/-}$ and *Apoe*$^{-/-}$ mice fed regular chow, respectively, and selected for binding to MDA-LDL (165). EO6 is a germline-encoded PC-specific murine IgM mAb that binds to the PC of oxidized phospholipids (141, 142). MDA2 is a murine IgG monoclonal Ab raised against murine MDA-LDL in BALB/c mice (164). IK17 is a human IgG Fab fragment specific for an MDA-epitope present on MDA-LDL and CuOx-LDL (166). Pre-made recombinant CLL69 mAbs (human IgG1) specific to MAA-BSA were obtained from Que Xuchu in University of California San Diego.

4.3 Biopanning

In the biopanning process, specific binding clones from a peptide phage display library are selected by incubating the phage library with the coated target (LRO4 mAb), followed by washing steps to remove unbound phages, and competitive as well as non-competitive elution of bound phages. Eluted phages are subsequently amplified, titered, and used as input for a further round of biopanning (BPR).

For the identification of peptide mimics of MDA-epitopes in MDA-LDL, commercial random phage display peptide libraries, purchased from New England Biolabs (NEB) (Beverly, MA, USA), were screened using the MDA-specific IgM mAb LRO4. Two phage display peptide libraries were used: A combinatorial linear 12-mer (Ph.D.-12) library and a combinatorial cyclic 7-mer library flanked by cysteine residues (Ph.D.-C7C). In both cases peptides are fused to the outer minor phage coat protein (pIII) of the M13 phage. Library screening was performed according to NEB's instructions with some modifications. Fig. 3 depicts the steps involved in this procedure. Three BPR were performed, in which high specificity was obtained by increasing the concentration of Tween 20 (Sigma-Aldrich) in washing buffers as well as the number of washing steps with each BPR.

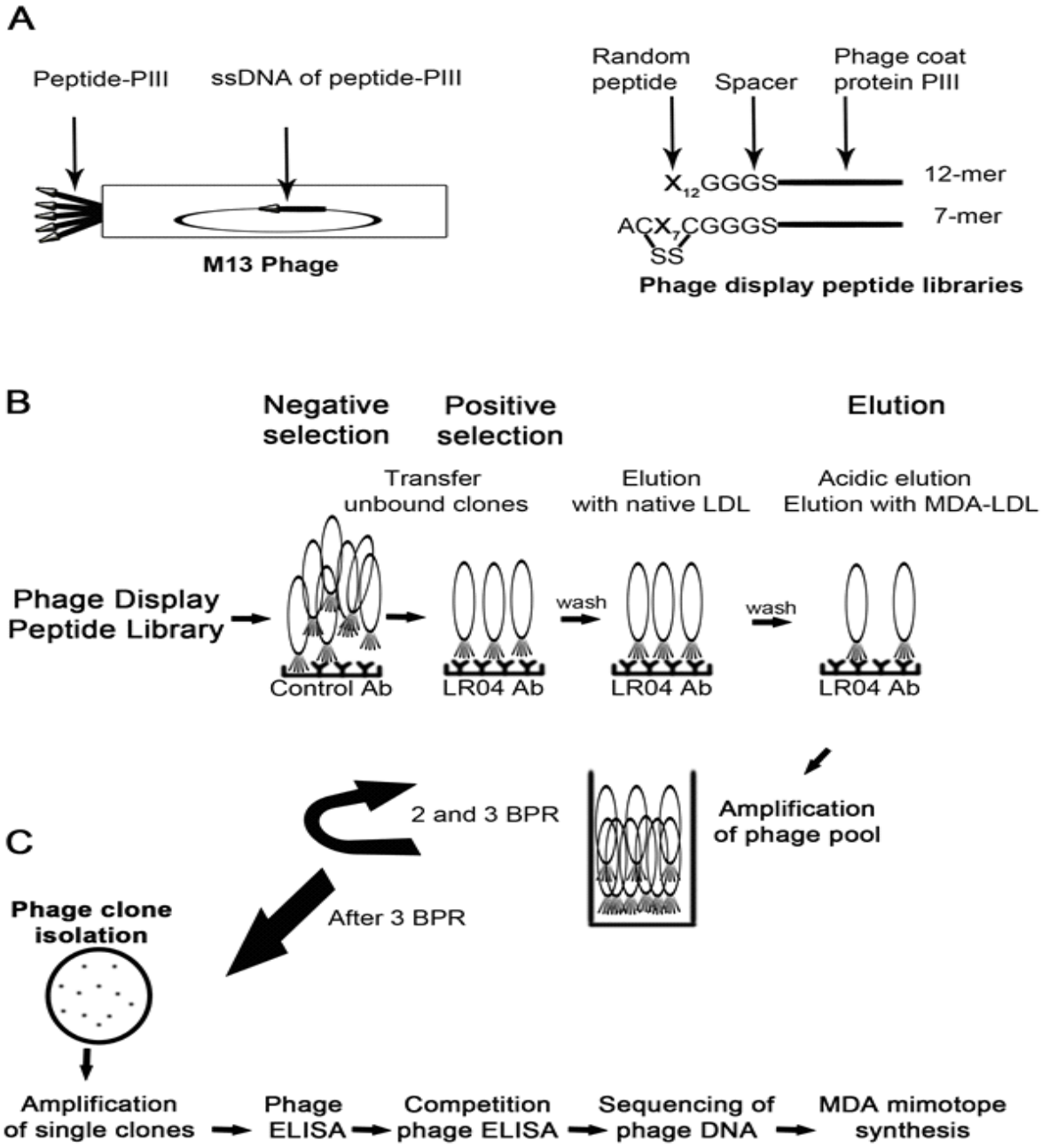

Fig. 3: Biopanning of phage display peptide libraries with LRO4.

(A) A random phage display library is a heterogeneous mixture of phage clones. Each phage carries a DNA fragment encoding for a random peptide fused to the DNA encoding for the outer phage coat protein pIII. Upon expression of the phage coat protein pIII, 5 copies of the random peptide sequence are also displayed. The Ph.D.-12 library consists of random linear peptides with 12 amino acid residues, whereas the Ph.D.-C7C library consists of heptameric peptides flanked by cysteine residues, which form a disulfide bond, thereby presenting peptides in a cyclic loop. All of the libraries contain a short linker sequence (Gly-Gly-Gly-

Ser) between the displayed peptide and outer phage coat protein pIII. The first residue in the peptide is the first randomized amino acid (Ph.D.-12 libraries), whereas in the Ph.D.-C7C library it is preceded by Ala-Cys. **(B)** For negative selection phages are incubated with isotype control antibodies. In a next step unbound phages are transferred to wells with LRO4 Abs (positive selection). After further washing steps and elution with native LDL, bound phages are eluted with elution buffer or with MDA-LDL and amplified in the *E. coli* strain ER2738 for application in the next BPR. **(C)** After the third BPR, selected single clones are amplified, screened in colony screening assays and by competition ELISA, and subsequently sequenced. Furthermore, specificity was increased by decreasing the concentration of coated LRO4 mAb as well as the incubation time of phages with LRO4.

Briefly, LRO4 or a control isotype IgM Ab (clone C48-6; specific for KLH; BD Bioscience-Pharmingen, USA) were coated in buffer containing 0.1 M $NaHCO_3$ (pH 8.5) on ELISA plates (Nunc Maxisorp, Roskilde, Denmark) overnight (ON) at 4°C at a concentration of 100 µg/mL for the first, 50 µg/mL for the second, and 10 µg/mL for the third BPR. The next day, wells were washed with TBS containing 0.05% v/v Tween 20 (TBS-T) and incubated with blocking buffer containing 0.1 M $NaHCO_3$ (pH 8.6) and 5 mg/mL BSA for 1 hour at room temperature (RT). After further washing with TBS-T, 10 µL of a library solution (containing 2×10^{12} phages) diluted in 100 µL of blocking buffer were first added to wells coated with control IgM (negative selection) and then unbound phages were transferred to wells coated with LRO4 (positive selection) and incubated at RT. The incubation time for negative or positive selection was reduced from 60 min for the first round to 30 min for the second as well as third BPR. Thereafter, plates were washed 5 times with TBS-T to remove unbound phages. To further elute nonspecifically bound phages, wells were incubated with 100 µL of 100 µg/mL of native LDL for 1 hour at RT. After washing up to 5 times with TBS-T, bound phages were eluted with 100 µL of elution buffer containing 0.2 M glycine–HCl (pH 2.2) and 1 mg/mL BSA. Eluates were transferred to microfuge tubes and neutralized with 15 µL of 1 M Tris-HCl (pH 9.1). The eluted phages were then titrated and amplified for the next round of panning as described (167). The second and third biopanning round were carried out using amplified eluates from the first and second round as input phages, respectively. To remove nonspecifically bound phages and to increase the affinity in the subsequent BPR, wells were washed 15 and 30 times with 0.1% TBS-T in the second and 0.5% TBS-T in the third BPR, respectively. In the last BPR, LRO4-bound phages were

competitively eluted with increasing concentrations (3-150 µg/mL) of MDA-LDL diluted in blocking buffer followed by elution using elution buffer.

4.4 Titration of M13 phage

The number of LRO4-reactive phages from each elution step was determined by a plaque forming units assay and was carried out as described in NEB's instructions. A fresh overnight culture of *Escherichia coli* ER2738 (NEB) was diluted in Luria broth (LB) medium and incubated at 37°C and 230 rpm shaking until the bacteria had reached mid-log phase (OD_{600}~0.6). Ten µL of each serially diluted phages were added to 200µl of mid-log ER2738 and incubated at 37°C for 10 min. In the meantime, top agar (LB containing 0.7% agarose) was melted and cooled to 45°C. The infected culture of *E. coli* ER2738 with phages was added to 3 mL of molten top agarose and was poured into pre-warmed LB/X-gal/IPTG agar plates. After 5 min at RT, plates were incubated overnight at 37°C. After 18 hours of incubation the number of blue plaques was counted on plates containing 25-200 plaques and the final titer was calculated after multiplying by the dilution factor (167, 168).

4.5 Amplification of phages

A fresh overnight culture of *E. coli* ER2738 was diluted 1:100 in LB medium and for amplification 100 µl of the phage eluate was added. The culture was incubated (37°C with 225 rpm) for 4.5 hours. Afterwards the bacteria were pelleted by centrifugation at 4°C (10 min, 10,000 rpm, Sorvall SS-34 rotor). The upper 80% supernatant was transferred to a fresh tube and clarified again by centrifugation. The upper 80% of the supernatant was transferred into a fresh tube and 1/6 volume of polyethylene glycol-8000 (PEG)/NaCl was added, mixed well and incubated at 4°C overnight. On the next day phages were pelleted again at 4°C (15 min, 10,000 rpm, Sorvall SS-34 rotor) and the supernatant was discarded. The pellet was resuspended in TBS and centrifuged again to pellet residual cells. Purified phages were added to 1/6 volume of 20% PEG/2.5 M NaCl, mixed and incubated at RT for 60 min. Afterwards phages were pelleted in a microfuge at 14,000 rpm for 10 min at 4°C. The dried pellet was

respun and resuspended in 200 µL of TBS. To pellet any insoluble material the supernatant was respun again and transferred to a fresh tube.

4.6 Phage single stranded DNA isolation

Individual phage clones were selected by plating for single plaques (titration steps described above). A well isolated blue plaque was picked using a sterile disposable Pasteur pipette and inoculated into 20 mL of *E. coli* ER2738 culture at an early log phase of gowth. Phages were amplified and centrifuged as described above. Single stranded phage DNA from amplified single phage clones was isolated using either Qiaprep spin M13 kit (Qiagen, Hilden Germany) or a sodium iodide-ethanol precipitation method. In this method phages were thoroughly suspended in 100 µL NaI buffer (10 mM Tris-Cl pH 8.0, 1mM EDTA, 4 M NaI). For the removal of phage coat proteins and phage DNA precipitation, 250 µL of ethanol was added and the mixture was incubated for 10 min at RT. After spinning in a microfuge at 14,000 rpm for 10 min at 4°C, the supernatant was discarded and the pellet was washed with 0.5 mL of 70% ethanol. After repeating washing steps with 70% ethanol, ssDNA was dried and resuspended in 30 µL distilled water.

4.7 Agarose gel electrophoresis

The DNA content was electrophoresed on a 1.2% agarose gel containing 0.01% ethidium bromide in TAE buffer (0.01 M Tris Base, 0.04 M Acetic Acid, 0.001 M EDTA). DNA samples were diluted in 5x loading dye (50% w/v sucrose, 40 mM Tris Base, 0.24% w/v of Bromophenol Blue, Xylene Cyanole, and Orange G) and were loaded on the gel. The DNA was electrophoresed at 120 V and bands were visualized by UV transillumination at 302 nm.

4.8 Phage capture and competition ELISA

Phage ELISA was performed as described by NEB with minor modifications. Ninety six-well ELISA plates (Nunc Maxisorp) were coated with 5 µg/mL LRO4 mAb or control IgM mAb in $NaHCO_3$ buffer (pH 8.6) at 50 µL/well ON at 4° C. Wells were washed with TBS containing 0.5% Tween 20 and then blocked with blocking buffer (TBS-T containing 1% BSA) at 200 µL/well for 1 hour at RT. After further washing, 10^{10} pfu/mL of phage amplificates diluted in blocking buffer were added to the wells at 50 µL/well for 2 hours at RT. Wells were washed again, and an HRP-labeled anti-M13 mAb conjugate (no. 27-9421-01; GE Healthcare, Amersham, UK) diluted 1:1,000 in blocking buffer was added for 1 h at RT followed by the addition of an 2,2'-azino-bis(3-ethylbenzothiazoline-6-sulphonic acid) (ABTS) (Sigma-Aldrich) substrate solution for 1 hour at RT. The binding reactivity of selected phage clones was measured at OD 405-490 nm using a BioTek Synergy 2 plate reader.

For competitive phage ELISA**,** plates were coated with 5 µg/mL LRO4 and binding of 25 µl of phage solution at $2x10^{10}$ pfu/mL was tested in the presence of 25 µL of MDA-LDL at 100 µg/mL. Bound phages were detected as described above and data expressed as values obtained in presence of competitor (B) divided by the values obtained in the absence of competitor (B_0). A reciprocal competition assay was performed in which 50 µl of 5 µg/mL MDA-LDL was coated on microtiter wells, and binding of LRO4 that was preincubated for 30 min at RT with a solution containing either no or $1x10^{10}$ pfu/mL phages with or without peptide inserts was tested by chemiluminescent ELISA as described (133, 140).

4.9 Phage sequencing and peptide synthesis

DNA sequencing was performed by VBC Biotech Service GmbH using 96 gIII sequencing primers (5′- ^{HO}CCC TCA TAG TTA GCG TAA CG –3′) corresponding to the phages' minor coat protein (pIII) gene sequence (NEB). The nucleotide sequence encoding for the peptide insert was identified by pIII gene sequence and translated into a protein sequence. Dodecamer and heptamer peptide sequences were aligned by a Clustal-W algorithm using MegAlign software (DNA Star Inc., Madison, WI) to obtain consensus sequences. A dodecameric linear peptide P1 (HSWTNSWMATFL), a cysteine-constrained heptameric cyclic peptide P2 (AC-NNSNMPL-C) and scrambled peptide of P2 (AC-SPNLNMN-C), and an irrelevant control peptide (IMGVGAVGAGAI) were synthesized by Peptide 2.0 Inc.

(Chantilly, VA, USA). A spacer (GGGS or GGGC or GGGK)-$CONH_2$ was added at each C-terminus. The purity of all the peptides was between 89-95% as assessed by high performance liquid chromatography and mass spectral analysis. For evaluation of its immunogenicity, P2 peptides were conjugated to KLH or BSA via the C-terminal cysteine.

4.10 Chemiluminescent ELISA

Binding of mAb as well as plasma Abs to respective antigens was measured by chemiluminescent ELISA as previously described (133, 140, 169). Antigens were coated at 5 µg/mL in PBS/EDTA (pH 7.4). Synthetic peptides were directly coated at 10 µg/mL (P1) or 5 µg/mL (P2) in 0.1 M $NaHCO_3$ buffer (pH 8.6), unless indicated differently. Biotinylated peptides were immobilized at indicated concentrations on wells pre-coated with 10 µg/mL neutravidin (Pierce, Rockford, IL, USA). Ab binding was measured using alkaline phosphatase (AP)-labeled secondary Abs (described below) followed by chemiluminescent detection. For the detection of human autoAbs, a 1:400 plasma dilution was used. For human assays, internal controls consisting of high and low standard plasma samples were included on each microtiter plate to detect potential variations between microtiter plates. The intra-assay coefficients of variation for all assays were 10 to 14%.

The following secondary Abs were used: Alkaline Phosphatase (AP)-labeled goat-anti-mouse IgM (µ-chain specific), IgG (γ-chain specific), IgG1 (Sigma-Aldrich) and IgG2c (Southern Biotech). For the detection of human Abs AP-labeled goat-anti-human IgG (γ-chain specific), IgM (µ-chain specific) (Sigma-Aldrich.) and biotinylated goat anti-human IgG1 (Southern Biotech) were used. Biotin-conjugated Abs were detected with AP-conjugated neutravidin (1:10,000; Pierce).

4.11 Competition immunoassays

The specific binding of LRO4 to mimotopes was determined by competition immunoassays as described previously (133, 140, 170). Fifty µl of 0.5 µg/mL MAA-BSA or 100 ng/mL of biotinylated peptides were plated as described above. After washing, LRO4 was added in 1% BSA-TBS with or without increasing concentrations of competitors (BSA,

MAA-BSA, P1, P2 and control peptide) and incubated for 30 min at RT. Binding of LRO4 was determined by chemiluminescent ELISA as described. The specificity of human plasma Ab binding to P1 was determined in a similar manner. In preliminary experiments, aliquots of pooled plasma samples (n=26) from a published cohort of healthy subjects (171) were diluted in 1% BSA-TBS to yield a limiting plasma dilution. Diluted plasma (1:1,000) and increasing concentrations of competitors were incubated overnight at 4°C. Samples were then centrifuged at 15,800 g for 45 min at 4°C to pellet immune complexes, and supernatants were analyzed for binding to plated P1 (10 μg/mL) by chemiluminescent ELISA as described above.

4.12 Immunization studies

To test the immunogenicity of mimotopes, two different carrier proteins and adjuvants were tested. Groups (n=3/group) of 5-weeks old male C57BL/6 mice (The Jackson Laboratory, Bar Harbor, ME) were immunized with either P2 conjugated to KLH (P2-KLH) or BSA (P2-BSA) or carriers (KLH, BSA) alone. Diluted conjugate P2-KLH was suspended 1:1 with Alum (Pierce) and mixed by vortexing at low speed for 30 min. Mice were injected intraperitoneally with 180 μg of P2-KLH or KLH in 100μL PBS, respectively. In subsequent 3 boosts, 90 μg of antigen was injected every two weeks.

To test the immunogenicity of P2-BSA, for the primary immunization, 100 μg of antigen (P2-BSA or BSA) in PBS was emulsified in equal volumes of complete Freund's Adjuvant (CFA; Sigma-Aldrich) and 50 μL of the homogenized suspension was injected subcutaneously at two sites. For the subsequent 4 booster immunizations every 2-3 weeks afterwards, 100μg of antigen was emulsified in Incomplete Freund's Adjuvant (IFA; Sigma-Aldrich) and 100 μL were injected intraperitoneally. Blood was taken on day 0 (preimmune serum), 21, 35, 47, and 70, and plasma stored at -80°C for further analyses. The experimental protocol was approved by the Animal Subjects Committee of the University of California, San Diego.

4.13 Plasma collection

Mice were bled either via the tail vein or via the retroorbital route. The blood was collected in EDTA containing tubes and was centrifuged at 13,000 rpm in a microfuge for 10 min. Plasma was pipetted off and stored at -20°C until use.

4.14 Immunohistochemistry

Immunostaining of formal sucrose-fixed, paraffin-embedded sections of aortas of atherosclerotic Watanabe heritable hyperlipidemic (WHHL) rabbits and human carotid atherosclerotic endarterectomy lesions was performed as described previously (153). Sections were blocked with PBS containing 5% horse serum and stained with diluted (1:200 or 1:400) pre- and post-immune sera from P2-BSA and BSA immunized mice, followed by addition of a biotinylated horse anti-mouse IgG (Jackson ImmunoResearch Laboratories, West Grove, PA, USA). A Vectastain ABC alkaline phosphatase kit and a Vector Red alkaline phosphatase chromogenic substrate (Vector Labs, Burlingame, CA, USA) were used to visualize Ab staining. Slides were counterstained with Weigert's Iron Hematoxylin (Richard-Allan Scientific, Kalamazoo, MI, USA). Immunostaining of adjacent sections in the absence of primary Abs or the MDA-specific mAb MDA2 (5 μg/mL) were used as negative and positive controls, respectively.

4.15 Flow cytometry

Binding of LRO4 IgM to apoptotic Jurkat T cells was assessed by flow cytometry. Apoptosis of Jurkat cells was induced by UV irradiation (UV Stratalinker, Stratagene, USA) at 20 mJ/cm^2, followed by further incubation of the cells in serum free medium for 14-16 hours. After washing in FACS buffer (PBS with 0.1% BSA) 10^6 cells were incubated with 1μg LRO4 in 100μl FACS buffer for 30 min at 4°C. In parallel experiments, cells were incubated with LRO4 in the presence of increasing concentrations of P1, P2, and an irrelevant control peptide. Following a washing step, cells were stained with FITC-labeled anti-mouse IgM (II/41, BD Biosciences-Pharmingen) in 100 μL staining buffer for 30 min at 4°C in darkness and washed again. Thereafter, cells were incubated with PE-labeled Annexin-V and 7-AAD (BD Bioscience-Pharmingen) in Annexin-V binding buffer for 15 min and

immediately analyzed by flow cytometry using a BD LSR II analyzer (BD Bioscience, San Jose, CA, USA). More than 5.0 x10^4 cells were aquired per sample, and data analysis was performed using Flow-Jo software (Tree Star Inc, San Carlos, CA, USA).

4.16 Human subjects

Human plasma samples from two independent studies were analyzed for the presence of anti-mimotope Abs. Details on the study cohorts are described elsewhere (169, 172) and research protocols were approved by the Human Research Protection Program at the University of California, San Diego. For these studies, autoAb titers to MDA-LDL as the antigen have already been reported (169, 172) and some figures from the original papers are reproduced (Fig. 16, 18), to allow ready comparisons to the new data generated here. Study 1 included 18 healthy subjects and 7 patients with acute coronary syndrome treated with primary percutaneous coronary intervention (PCI). Blood was obtained at baseline, and 1, 3, and 7 months thereafter. In addition, plasma from ACS patients was obtained at time of hospital discharge (approximately 4 days after admission). Study 2 included 114 patients with stable angina pectoris undergoing elective PCI. Blood samples were obtained before PCI, immediately after PCI, and 6 and 24 hours, 3 days, 1 week, 1, 3, and 6 months after PCI (169). For specificity assays (see above), plasma samples (n=26) from a published cohort of healthy subjects (171) was pooled and inhibition of human autoAbs to coated P1 was tested.

4.17 Statistical analysis

Statistical analyses were performed with GraphPad Prism 5 for Windows (GraphPad Software, Inc., San Diego, CA). Statistical analysis of two groups was performed using the Student's *t* test. For continuous variables, differences were evaluated by one-way analysis of variances (ANOVA). Spearman correlations were calculated to summarize the association between mimotope and MDA-LDL specific autoAbs. $P \leq 0.05$ was considered statistically significant. Data are presented as mean ± SD, if not indicated otherwise.

RESULTS

4.18 Enrichment of LRO4 binding phages by biopanning

To generate peptide mimotopes of MDA-epitopes present in MDA-LDL, I screened phage display peptide libraries by biopanning of phages with LRO4. LRO4 is a murine IgM mAb that was selected for its binding MDA-LDL. LRO4 binds to MDA-LDL and to a much lesser degree to CuOx-LDL, but not to native LDL (Fig. 4A). Moreover, LRO4 also binds MAA-modified BSA, but not unmodified BSA, demonstrating specificity for advanced MDA-lysine adducts independent of the carrier (Fig. 2 and 4A). In immunocompetition assays, I confirmed the specificity of LRO4 for MDA-adducts, as binding to coated MDA-LDL was efficiently competed by increasing concentrations of soluble MDA-LDL as well as MAA-BSA, but not native LDL or unmodified BSA (Fig. 4B). Because CuOx-LDL contains various late OSEs that are generated due to the vigorous lipid peroxidation. CuOx-LDL also showed slight binding and moderate competition, consistent with the presence of minimal amounts of MDA-adducts in these preparations (Fig. 4A-B).

I screened two different phage peptide libraries, one displaying 12-mer linear peptides (Ph.D-12) and one displaying cyclic 7-mer peptides constrained by flanking cysteines (Ph.D.7C7) for binding to coated LRO4 in three sequential BPRs. After amplification of eluted phages from each biopanning round, I tested the enrichment of LRO4-binding phages in the mixed pool of phage amplificates. A 336- and 400-fold enrichment of phage titers was found after three rounds of selection with the Ph.D.7C7 library and the Ph.D.-12 library, respectively (Table 1A-B). The decrease in enrichment of LRO4 binding phages in the third biopanning round was due to the increased stringency conditions during BPRs. This finding was confirmed by phage ELISA using phage amplificates from each BPR. The interaction of purified phage amplificates to LRO4, but not a control IgM Ab, was increased with each BPR indicating successful enrichment of LRO4 binding phage clones **(**Fig. 4 C-D**).**

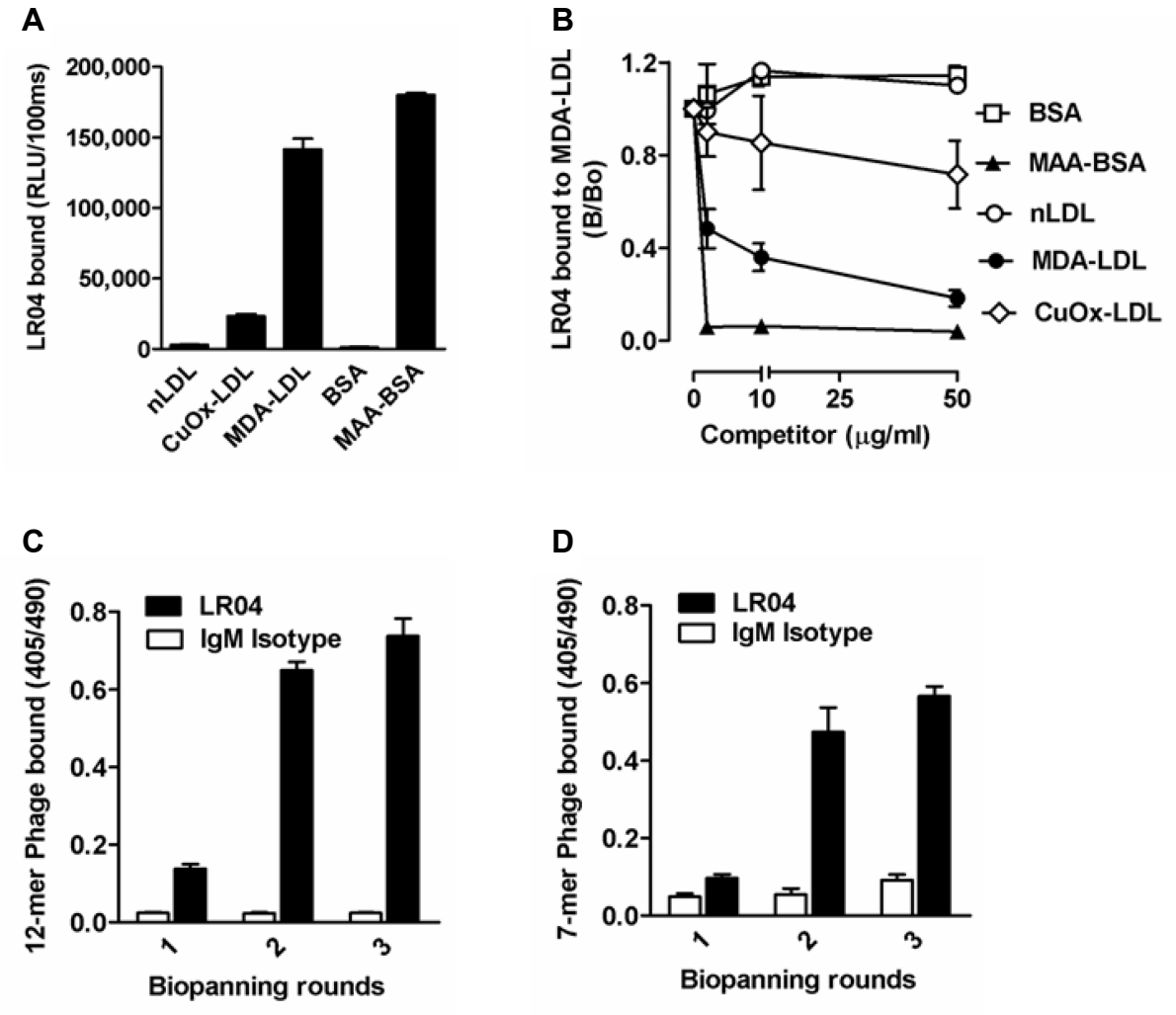

Fig. 4: Biopanning of phage display peptide libraries with monoclonal antibody LRO4

(A) ELISA for binding of the murine IgM mAb LRO4 (5 μg/mL) to native LDL (nLDL), CuOx-LDL, MDA-LDL, BSA, and MAA-modified BSA. Values are given as relative light units (RLU) per 100 ms and represent the mean±SD of triplicate determinations. Data are representative of at least three independent experiments. **(B)** Competition immunoassay for the specificity of LRO4 binding to MDA-LDL. Data are expressed as a ratio of binding in the presence of competitor (B) divided by absence of competitor (B_0) and represent the mean±SD of triplicate determinations. Data are representative of three independent experiments. **(C, D)** ELISA for the binding of eluted phages to LRO4. After each BPR, the binding of 10^{10} pfu/mL phage amplificates from the Ph.D.-12 library **(C)** and the Ph.D.7C7 library **(D)** to LRO4 (black bars) and an isotype control IgM (white bars) was tested as described in Methods. Values are given as absorbance measured at 405 and 490nm and represent the mean±SD of triplicate determinations.

Table 1A

Round	Input (PFU/ml)	Output (PFU/ml)	Ratio (Output/Input)	Phage Enrichment
1	2×10^{11}	11×10^{4}	$0{,}55\times10^{-6}$	
2	2×10^{12}	37×10^{7}	$18{,}5\times10^{-5}$	336
3	2×10^{12}	39×10^{7}	$19{,}5\times10^{-5}$	1
				336

Table 1B

Round	Input (PFU/ml)	Output (PFU/ml)	Ratio (Output/Input)	Phage Enrichment
1	2×10^{11}	$1{,}9\times10^{5}$	$0{,}95\times10^{-6}$	
2	2×10^{11}	152×10^{5}	76×10^{-6}	80
3	2×10^{11}	780×10^{5}	390×10^{-6}	5
				400

Table 1: Enrichment of phage titers following each BPR

Titers of eluted phages carrying LRO4-reactive phagotopes from the Ph.D.7C7 library **(A)** and the Ph.D.-12 library **(B)** were determined after each BPR by a plaque forming units assay, as described in Methods. Input indicates the number of phages applied to wells coated with LRO4. Output indicates the number of eluted phages. The ratio indicates the fraction of the number of eluted phages after each BPR divided by the number of phages applied at respective BPR. Phage enrichment is calculated as the multiplier of the output/input ratio from one round to the next. PFU = plaque forming units.

4.19 Phages displaying MDA-mimotopes bind specifically to LRO4

To identify individual LRO4-binding phages after the third BPR, eluted phages were plated in pre-warmed LB/X-gal/IPTG agar plates and 132 single clones of the Ph.D.-12 and 30 clones of the Ph.D.-C7C libraries were randomly selected and amplified. To overcome the preferential selection of single phagotopes with the same sequence, elutions from the third

biopanning round were plated 2-3 times on LB-X-gal-IPTG plates and clones were selected for amplification. To ensure that these selected phage clones were reactive to the variable region of the antibody, single phage amplificates were tested for reactivity with LRO4 as well as an irrelevant isotype control IgM by ELISA. Clones specifically binding to LRO4 were selected using a cutoff absorbance of thrice that of the binding to an irrelevant antibody. Forty-two unique phage clones (25 dodecamers and 17 heptamers) showed significantly higher binding to LRO4 compared to control IgM (Table 2A-B).

No binding of control phages (i.e. without a peptide insert) to LRO4 or control IgM was observed (data not shown). I further demonstrated the mimicry of selected phagotopes with MDA-epitopes using competitive phage ELISA, where binding of LRO4 to MDA-LDL (the cognate antigen) was tested in the absence and presence of selected phages. The ability of all phage clones to inhibit binding of LRO4 to MDA-LDL was >75% (Table 2A-B). Control phages did not show any inhibition in this assay (data not shown). Selected phage clones with the highest binding capacity and specificity were amplified, sequenced, and amino acid sequences were deduced (Table 2A-B).

Table 2A

Phage clones	Binding of phages to control IgM	Binding of phages to LR04	Inhibition of binding to LR04 (B/Bo)	Peptide sequence
A40	0,04	0,89	0,10	NSWTNASLSTFH
A34	0,11	0,82	0,11	NSRTNNSQWTFQ
A36,B41 * M35	0,03	1,16	0,14	ESWTNSWAHYFG
M2	0,03	1,17	0,20	ESWTNSWAMYFG
M19	0,03	1,67	0,25	QSYTNDDVLRIS
A31	0,08	0,85	0,25	QNMNNWTLASIM
M30	0,03	1,04	0,06	EVMNNWTLASIM
M15	0,04	1,34	0,15	ASISNLTLSRFM
A32	0,02	0,98	0,18	HSWSNYWGHQHA
G4	0,04	1,45	0,10	HRISNYAMELHS
M31	0,03	1,35	0,40	HSLTNTQMTQLS
M10,G8 *	0,03	1,16	0,10	HSLSNIQMATLA
A38	0,21	0,64	0,10	HRMTNAMHHFMG
M6,G10 *	0,03	1,56	0,20	HRMTNNAMDVFM
M3,M5 *	0,03	1,56	0,10	HRLTNSEQAALP
M8	0,04	1,57	0,20	TAVTNSMMERLW
A39	0,05	1,19	0,19	GWGNKTPSQDVH
M36	0,01	1,47	0,07	DYTNSVSMRYLS
A33	0,05	0,63	0,14	HQLSNKDEQTPQ
M7	0,03	1,37	0,10	ADPFSPTNRIPL

Table 2B

Phage clones	Binding of phages to control IgM	Binding of phages to LR04	Inhibition of binding to LR04 (B/Bo)	Peptide sequence
Ca1,Ca7*	0,1	0,8	0,04	NNWNMPL
Ca59,Cb1*	0,1	0,8	0,06	NNRNMPL
Cb589	0,1	0,8	0,03	NNYNMPL
Cb9	0,01	0,7	0,02	NNQNMPL
Cb4	0,1	0,6	0,02	NNWKMPL
Ca9,Cb3* Ca8,Ca10	0,2	0,9	0,04	NNSHMPL
Ca4	0,1	0,9	0,13	KNSXQPL
Ca6	0,0	0,7	0,04	NNSXMPL
Ca3	0,1	0,5	0,04	QNSHMPL
Cb10	0,2	0,6	0,02	NNSNMPL
Ca2	0,2	0,8	0,12	NNSKMRL
Cb2	0,2	1,0	0,03	DWAPHFT

Table 2: Binding characteristics of MDA-phagotopes.

Sequences and binding characteristics of selected phagotopes from **(A)** the Ph.D.-12 and **(B)** the Ph.D.7C7 libraries, respectively. Individual phages were selected and amplified after the third BPR, and binding to an isotype control IgM, LRO4, and LRO4 in the presence of 50 μg/mL MDA-LDL was measured by phage ELISA, as described in Methods. Numbers indicate OD values or for inhibition studies the fraction of OD values obtained in the absence and presence of soluble MDA-LDL (B/B_o). Sequences indicate amino acid residues in peptide sequences that were deducted from the DNA sequence of each phagotope. "X" indicates an unidentified amino acid at this position. * for clones with identical sequence representative data of one clone are provided.

4.20 Binding characteristics of synthetic MDA-mimotopes

Based on the amino acid sequences deduced, I determined consensus sequences from each library and synthesized a dodecameric peptide P1 (HSWTNSWMATFL) (Fig.5A) and a cyclic heptameric peptide P2 (ACNNSNMPLC) (Fig.5B). Synthetic peptides with a spacer were designed to reproduce the free N-terminal end of the phage pIII protein following the template XXXXXXXGGGS for linear and ACXXXXXXXCGGGS for cyclic peptides. The N-terminus of peptides remained free and the C-terminus was amidated to block the negative charge of the carboxyl group. Peptides were directly plated onto microtiter wells at increasing concentrations and the binding of LRO4 was tested.

Both plated peptides, P1 and P2, but not an irrelevant control peptide (IMGVGAVGAGAI) were bound by LRO4 as well as another murine MDA-specific monoclonal IgM Ab, EN1, in a dose-dependent manner (Fig. 5C-D). A scrambled peptide of P2 (ACSPNLNMNC) was not recognized by LRO4 either (Fig. 5E). Moreover, binding of LRO4 to the plated peptides was similar to the binding to MDA-LDL and MAA-BSA (Fig. 5E). The PC-specific IgM mAb EO6 (142), which binds CuOx-LDL, did not react with either P1 or P2 (Fig. 5F).

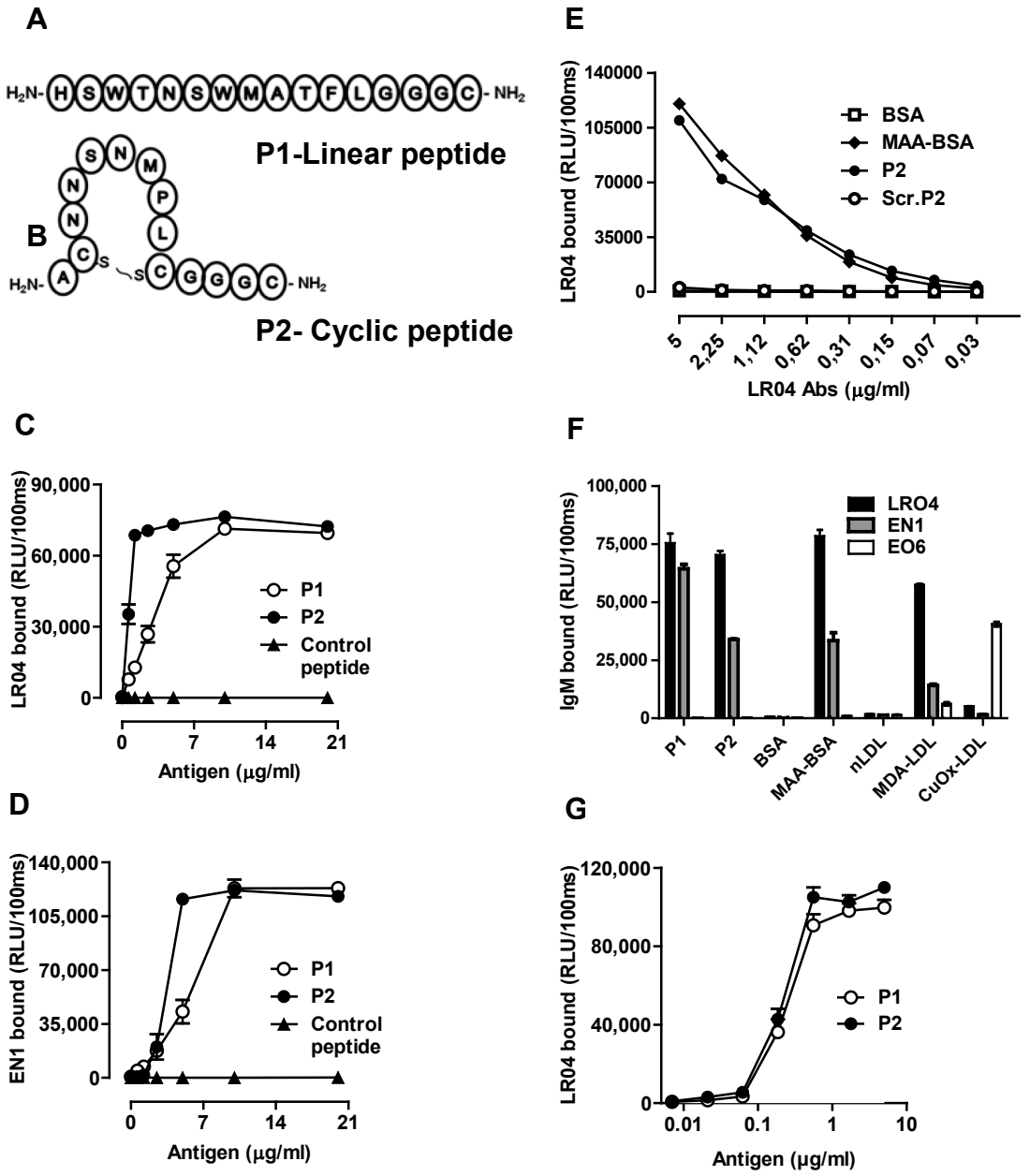

Fig. 5: Linear P1 and cyclic P2 are recognized by MDA-specific Abs

Schematic representation of synthesized peptides carrying the consensus sequence from phages identified with the Ph.D.-12 and Ph.D.C7C library, respectively. **(A)** P1 is a linear dodecameric peptide (HSWTNSWMATFL) and **(B)** P2 is a cyclic heptameric peptide (CNNSNMPLC). The peptides' C-terminus containing a GGGC-spacer was amidated. **(C, D, E)** ELISA for the binding of MDA specific Abs to P1 and P2, scrambled peptide and an irrelevant control peptide. **(C)** Binding of LRO4 and **(D)** EN1 to P1 and P2. Peptides P1, P2, and an irrelevant control peptide were coated at indicated concentrations. Binding of LRO4 (5 µg/mL) was determined by chemiluminescent ELISA. **(E)** ELISA for the the binding of LRO4 to BSA, MAA-BSA, the P2 mimotope (ACNNSNMPLC-GGGS) and a scrambled peptide (ACSPNLNMNC-GGGS) of P2 (Scr. P2). Peptides were coated at 20µg/mL, BSA and MAA-BSA at 5µg/mL, and binding of indicated concentrations of LRO4 was determined by chemiluminescent ELISA. **(F)** ELISA for binding of LRO4, EN1 and EO6. P1, P2, BSA, MAA-BSA, nLDL, MDA-LDL, and CuOx-LDL were coated at 5-10 µg/mL. Binding of

LRO4, EN1 and EO6 (all at 5 μg/mL) was determined by chemiluminescent ELISA. **(G)** Indicated concentrations of biotinylated peptides were captured on wells pre-coated with 10 μg/mL of neutravidin, and binding of LRO4 (5 μg/mL) was determined as described in Methods. Data represent the mean±SD of triplicate determinations and are representative of three independent experiments.

To confirm the binding of LRO4 to the peptides in their native configuration, I designed peptides with a short spacer at the respective C-terminus (GGGK), which was linked to a biotin group. Biotinylated peptides where captured on neutravidin-coated wells and binding of LRO4 to increasing amounts of captured peptides was determined by ELISA. LRO4 recognized both peptides equally well even at concentrations as low as 100 ng/mL (Fig. 5G).

4.21 Interaction of LRO4 with MDA-mimotopes is specific

To further test the binding specificity of LRO4 to P1 and P2 and evaluate their function as peptide mimotopes of MDA-epitopes, I performed a series of competition immunoassays. Binding of LRO4 to captured biotinylated P1 (Fig. 6A) and P2 (Fig. 6B) was fully competed by increasing concentrations of soluble MAA-BSA, but not unmodified BSA. Moreover, increasing concentrations of P2 fully competed for LRO4 binding to captured P2 as well as P1. Interestingly, soluble P1 did not compete for LRO4 binding to P1 or P2, respectively (Fig. 6A-B). The irrelevant control peptide and scrambled peptide of P2 had no effect (Fig. 6A-C). In a reciprocal competition experiment, LRO4 binding to coated MAA-BSA was effectively competed by increasing concentrations of MAA-BSA as well as P2, whereas again, P1 did not have an effect (Fig. 6D). Thus, it appears that when plated, the linear peptide P1 serves as an excellent mimotope for MDA-epitopes, but when in solution it loses this property, presumably due to conformational changes (173-175). In contrast, the cyclic peptide P2 is an excellent mimotope of MDA-epitopes when plated and in solution.

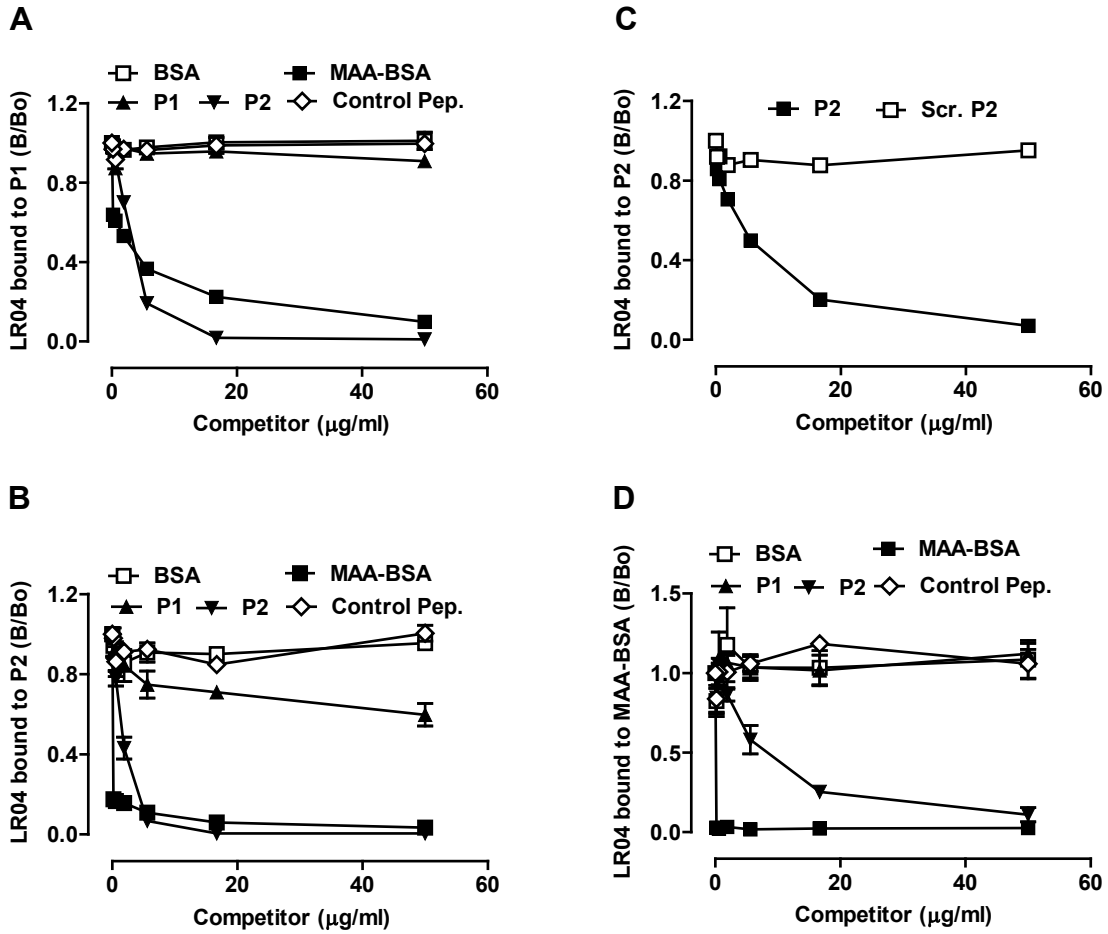

Fig. 6: Linear P1 and cyclic P2 peptides mimic a specific MDA-epitope.

(A, B, C, D) Immunocompetition assays for the antigenic properties of P1 and P2. Binding of 0.5 µg/mL LRO4 to 100 ng/mL captured biotinylated peptides P1 **(A)** or P2 **(B, C)** or to 0.5 µg/mL coated MAA-BSA **(D)** was measured by ELISA in the presence of increasing concentrations of indicated competitors. Data represent the mean±SD of triplicate determinations and are representative of three independent experiments.

4.22 MDA-mimotopes mimic an epitope present on apoptotic cells

To test whether the peptide mimotopes truly mimic epitopes occurring *in vivo*, I tested the ability of P2 to inhibit the binding of LRO4 to apoptotic cells. In my thesis laboratory it has been shown that MDA-epitopes are generated when cells undergo apoptosis, and that

MDA-epitopes are a major OSE on the surface of apoptotic cells (140, 176). Consistent with these reports, I showed that LRO4 binds to the surface of early and particularly to late apoptotic cells, as indicated by Annexin-V and 7-AAD staining (Fig. 7A-B). In these experiments, the staining of Annexin-V and 7-AAD was used to separate viable, early and late apoptotic cells by flow cytometry. LRO4 did not bind to normal viable cells (Q1) and only slight binding to early apoptotic cells (Q2) was observed. However, LRO4 prominently bound to late apoptotic cells (Q3). Importantly, in the presence of increasing concentrations of soluble P2, but not of an irrelevant control peptide, binding of LRO4 to apoptotic cells was fully inhibited (Fig. 7C). These data demonstrate that the peptide mimotope of MDA, P2, mimics MDA epitopes on the surface of dying cells.

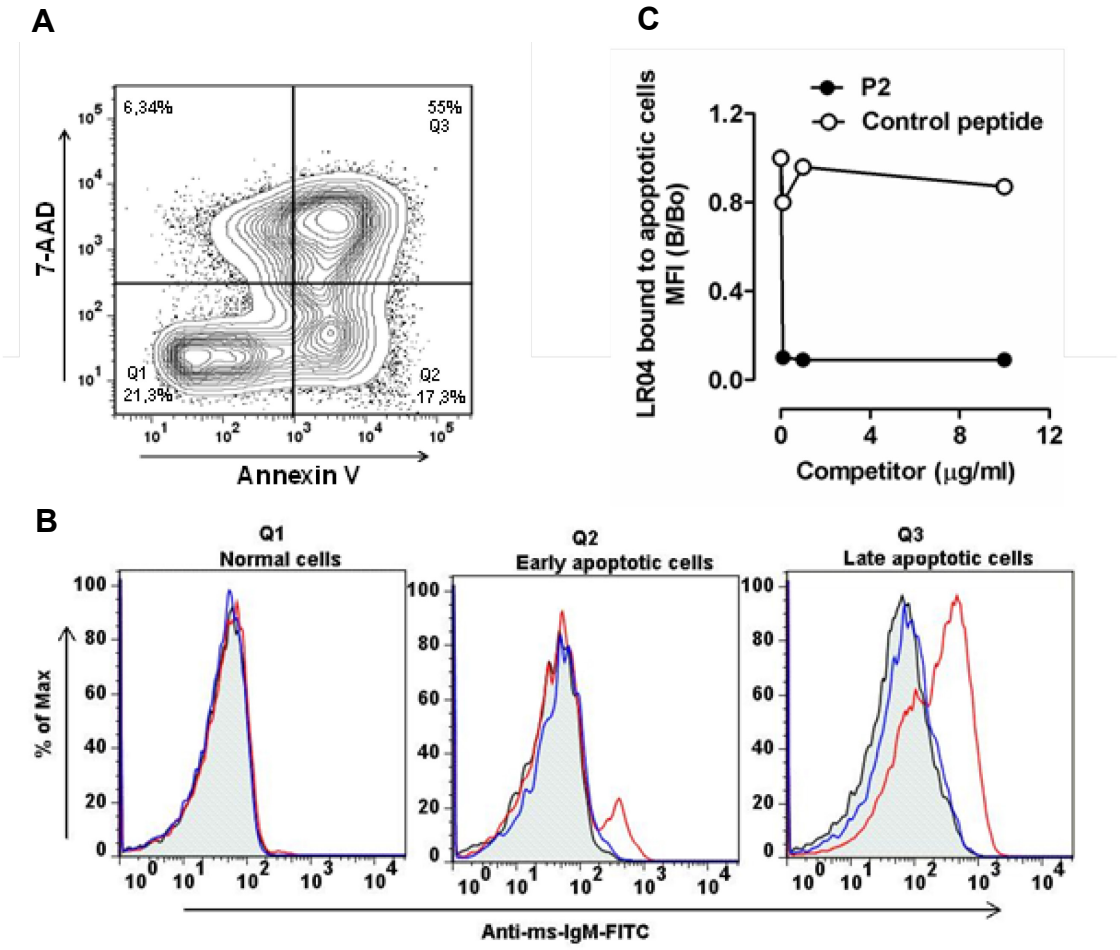

Fig. 7: Mimotopes mimic MDA-epitopes on apoptotic cells.

(A) Representative flow cytometry plot of apoptotic Jurkat T cells. Apoptosis of Jurkat T cells was induced by 20 mJ/cm^2 UV irradiation, and cells were stained with PE-labeled Annexin-V and 7-AAD to determine Annexin-V$^-$ 7-AAD$^-$ viable cells (Q1), Annexin-V$^+$ early apoptotic (Q2) and Annexin-V$^+$ 7-AAD$^+$ late (Q3) apoptotic cells. **(B)** Representative flow cytometry histogram plot for the binding of apoptotic cells by LRO4. Apoptotic cells were induced as

described in (A) and stained with either LRO4, isotype IgM, or no primary Ab, followed by detection using a FITC-conjugated anti-mouse IgM Ab as "secondary Ab" (Sec. Ab). Subsequently, cells were stained with PE-labeled Annexin-V and 7-AAD. The left panel represents staining of viable cells (Q1), the middle panel staining of early apoptotic cells (Q2), and the right panel staining of late apoptotic cells (Q3). **(C)** Inhibition of LRO4 binding to apoptotic cells by P2. Apoptotic cells were stained with LRO4 in the absence or presence of increasing amounts of P2 or an irrelevant control peptide, as indicated. Data represent the ratio of LRO4 binding as mean fluorescence intensity (MFI) obtained in the presence or absence of competitors (B/B_0). Results are representative of two independent experiments.

4.23 Mimotope immunization induces antibodies against MDA-LDL

Based on the preceding characterizations, I chose the cyclic P2 peptide to test for its immunogenic and antigenic properties. P2 was conjugated to KLH (P2-KLH) or BSA (P2-BSA) as a carrier protein, which did not affect its reactivity and specificity for LRO4 (Fig. 8A-C and data not shown). Interestingly, EN1 antibody did not bind to any peptide-carrier conjugate, suggesting subtle differences in binding specificity between LRO4 and EN1 (Fig. 8D). Due to the higher molecular weight and high number of primary amines for coupling haptens, KLH was selected as a first choice as a carrier. C57BL/6 mice were immunized with either P2-KLH (n=3) or KLH (n=3) alone suspended in Alum adjuvant. Ab titers were determined in the plasma obtained after the last boost. Only mice immunized with P2-KLH, but not KLH, developed IgG Ab titers to P2. Importantly, 2 out of 3 mice immunized with P2-KLH displayed increased IgG titers to MAA-BSA compared to KLH-immunized mice, which also had elevated titers to MAA-BSA (Fig. 9A). There was no difference in IgM Abs to either P2 or MAA-BSA in mice immunized with KLH or P2-KLH (Fig. 9B). These data suggested that immunization with P2 could also induce Abs to MAA-epitopes.

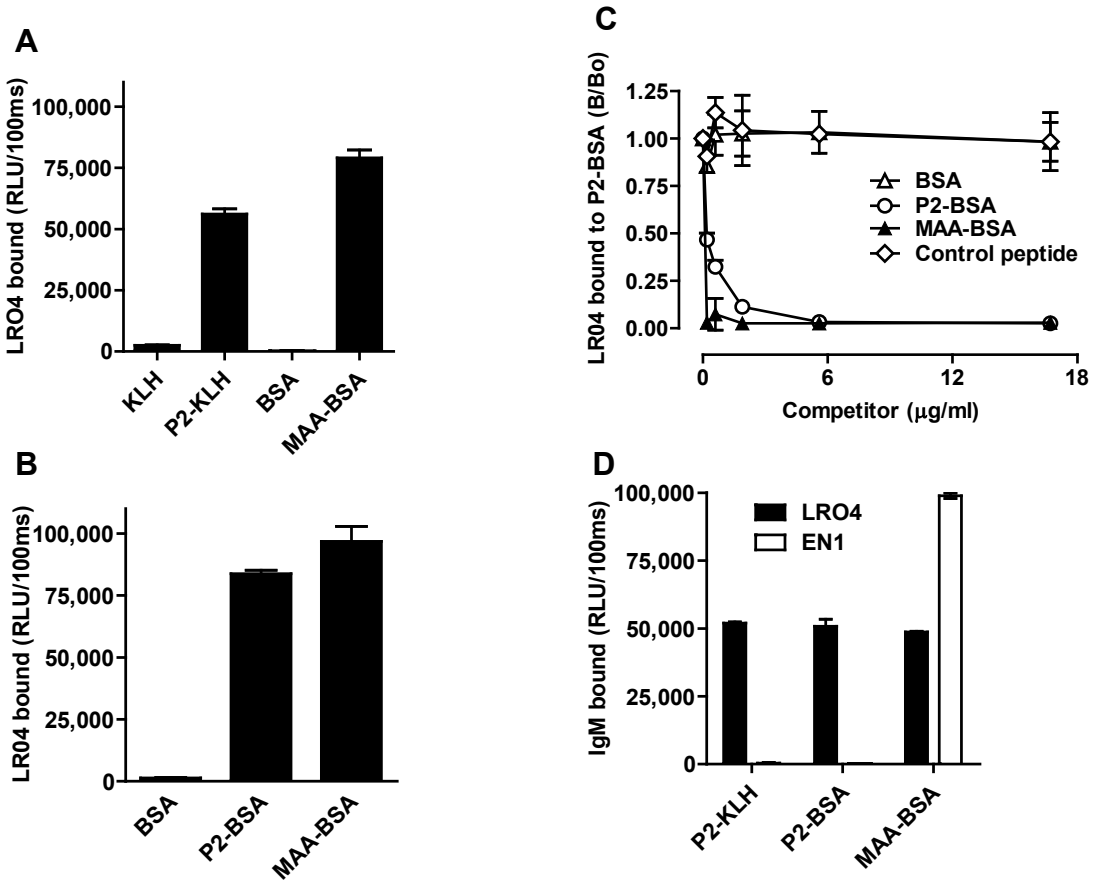

Fig. 8: Specificity of LRO4 binding to peptide-mimotopes P2-carrier conjugates.

(A-B) ELISA for binding of LRO4 to P2-KLH, P2-BSA, BSA, and MAA-BSA, which were coated at 5 µg/mL. Binding of LRO4 (5 µg/mL) was determined by chemiluminescent ELISA. **(C)** Immunocompetition assays for the specificity of LRO4 binding to P2-BSA. P2-BSA was coated at 5 µg/mL and binding of LRO4 was determined in the absence or presence of soluble BSA, MAA-BSA, P2-BSA, P2, and an irrelevant control peptide at indicated concentrations. Data are expressed as a ratio of binding in the presence of competitor (B) divided by the binding in the absence of competitor (B_0) and represent the mean±SD of triplicate determinations. **(D)** ELISA for binding of LRO4 and EN1 Abs to P2-KLH, P2-BSA and MAA-BSA, which were coated at 5-10 µg/mL. Binding of LRO4 (5 µg/mL) was determined by chemiluminescent ELISA. **(A, B, D)** Values are given as relative light units (RLU) per 100 ms and represent the mean of triplicate determinations. All data are representative of at least three independent experiments.

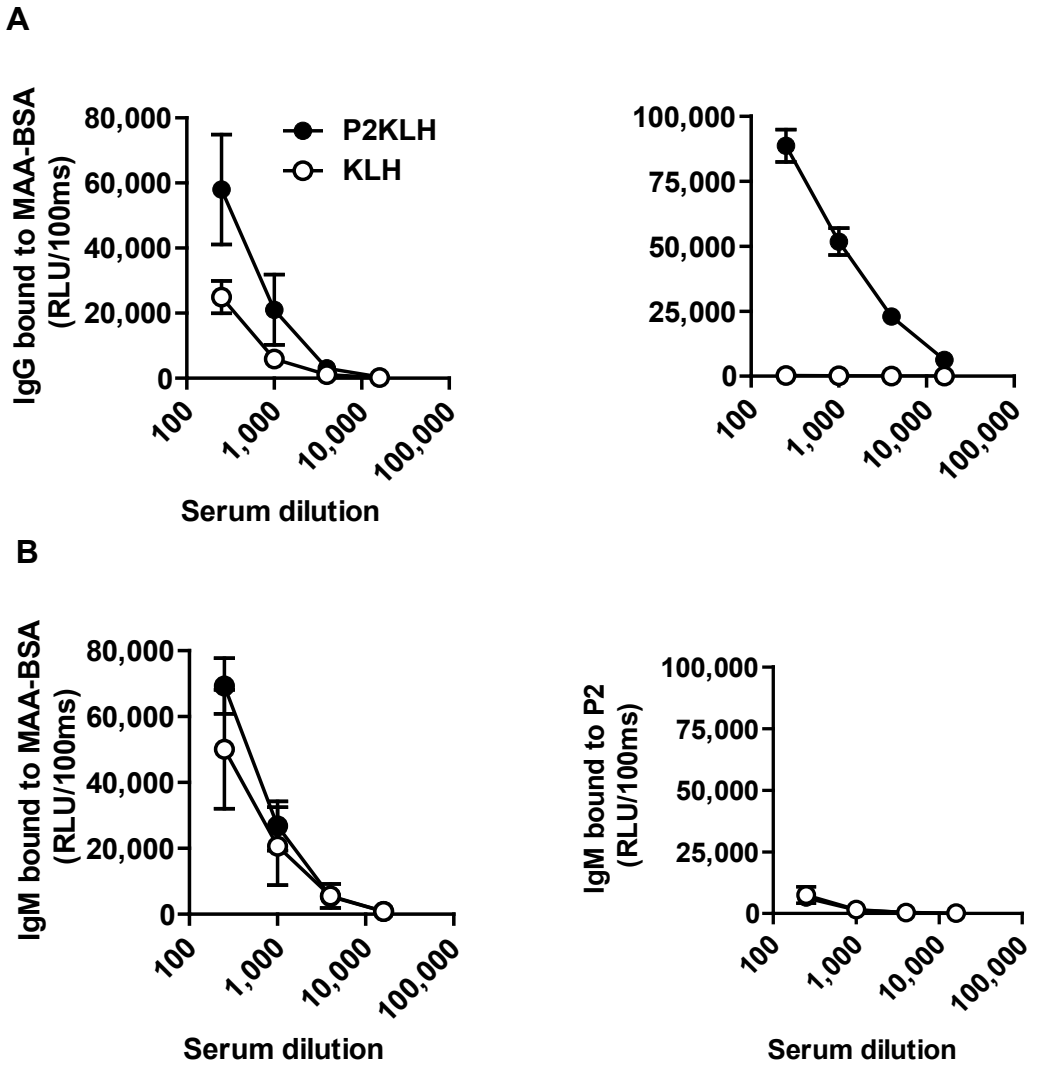

Fig. 9: P2-KLH immunization induces MDA-specific antibody responses

(A-B) ELISA for the binding of serum Abs of immunized mice to MAA-BSA and P2. C57BL/6 mice were immunized with P2-KLH (n=3) or KLH (n=3) as described in Methods. Dilution curves of IgG and IgM binding to indicated antigens in post-immune plasma was determined by chemiluminescent ELISA. **(A)** Dilution curve of IgG binding. **(B)** Dilution curve of IgM binding. Values are given as relative light units (RLU) per 100 ms and represent the mean±SEM of each group. Stars indicate significance in two-tailed Student's *t-test*; **P<0.05*, ***P*<0.005, ****P*<0.0005.

To obtain further insights into the fine specificity of the induced Abs, the reactivity of the antisera was further evaluated by using synthetic peptides modified with MAA as antigens. Biotinylated GDGDG-X peptides were used, in which X consists of 1-4 additional

amino acids such as H, R, N, K, KK, or KGGK. Antibodies in plasma of P2-KLH immunized mice only bound modified synthetic peptides containing lysine residues, but not unmodified peptides or modified-peptides containing H, R, or N residues. Moreover, plasma of mice immunized with P2-KLH exhibited a marked rise in IgG Abs against peptides with MAA-modified lysine residues, i.e. K-MAA, KK-MAA, etc. (Fig. 10). Thus, P2 exhibits immunogenic mimicry with advanced MDA-adducts such as MAA, and is independent of the amount of K-residues modified.

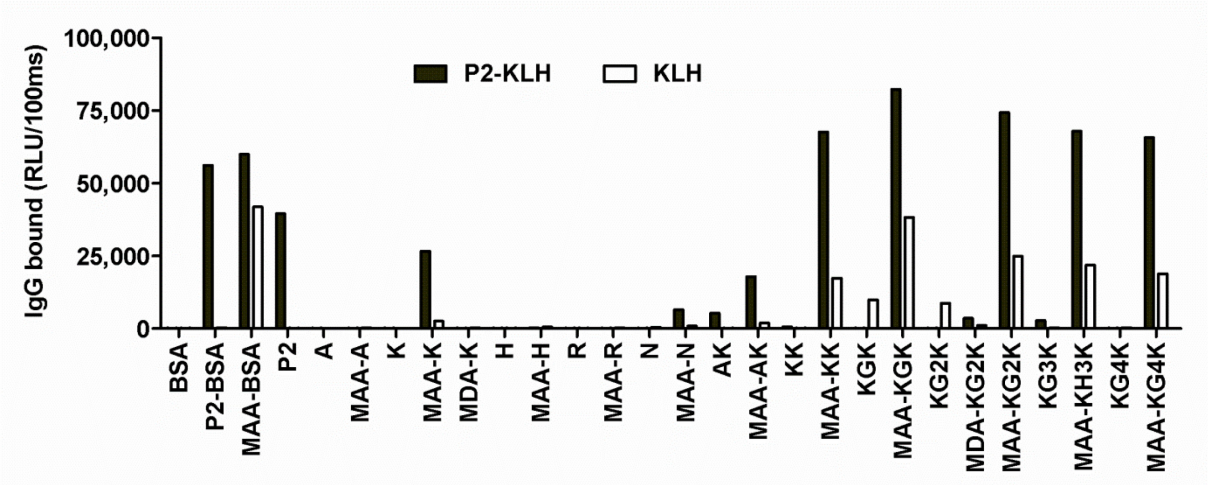

Fig. 10: MAA-modified peptides are recognized by antiboides induced by P2-KLH immunization.

ELISA for the binding of serum Abs of immunized mice to peptides modified with MDA and MAA. Representative plasma samples of mice immunized with P2-KLH or KLH were screened for the presence of Abs binding to MDA- and MAA-modified peptides as indicated. Biotinylated peptides (25 nmol/mL) were captured on wells pre-coated with 10 µg/mL of neutravidin, and binding of IgG in 1:200 diluted post-immune plasma was determined by chemiluminescent ELISA. Background binding of Abs to neutravidin was subtracted. Values represent the mean of triplicate determinationsand are given as relative light units (RLU) per 100ms.

In order to further evaluate the immunogenic mimicry between MDA-epitopes and P2, and to obtain data using a different potentially more suitable carrier, I performed immunization studies using P2-BSA and BSA as antigens, respectively. C57BL/6 mice were immunized with P2-BSA (n=3) or BSA (n=3) alone emulsified in Freund's adjuvant. Mice immunized with P2-BSA developed high IgG1 titers to BSA (data not shown) and P2 (Fig.

11), whereas mice immunized with BSA alone only developed IgG1 titers to BSA (data not shown) but not P2 (Fig. 11A). Importantly, mice immunized with P2-BSA displayed a robust IgG1 (Fig. 11A) and IgG2c (data not shown) response to MDA-LDL and MAA-LDL, which was not observed in control mice immunized with BSA alone. In addition, the immunization with P2-BSA also induced IgM titers to MDA-LDL and more prominently to MAA-LDL (Fig. 11B). Thus, immunization of mice with P2 mimotopes results in the induction of MDA-specific Abs, similar to that observed following immunization with homologous MDA-LDL (64)

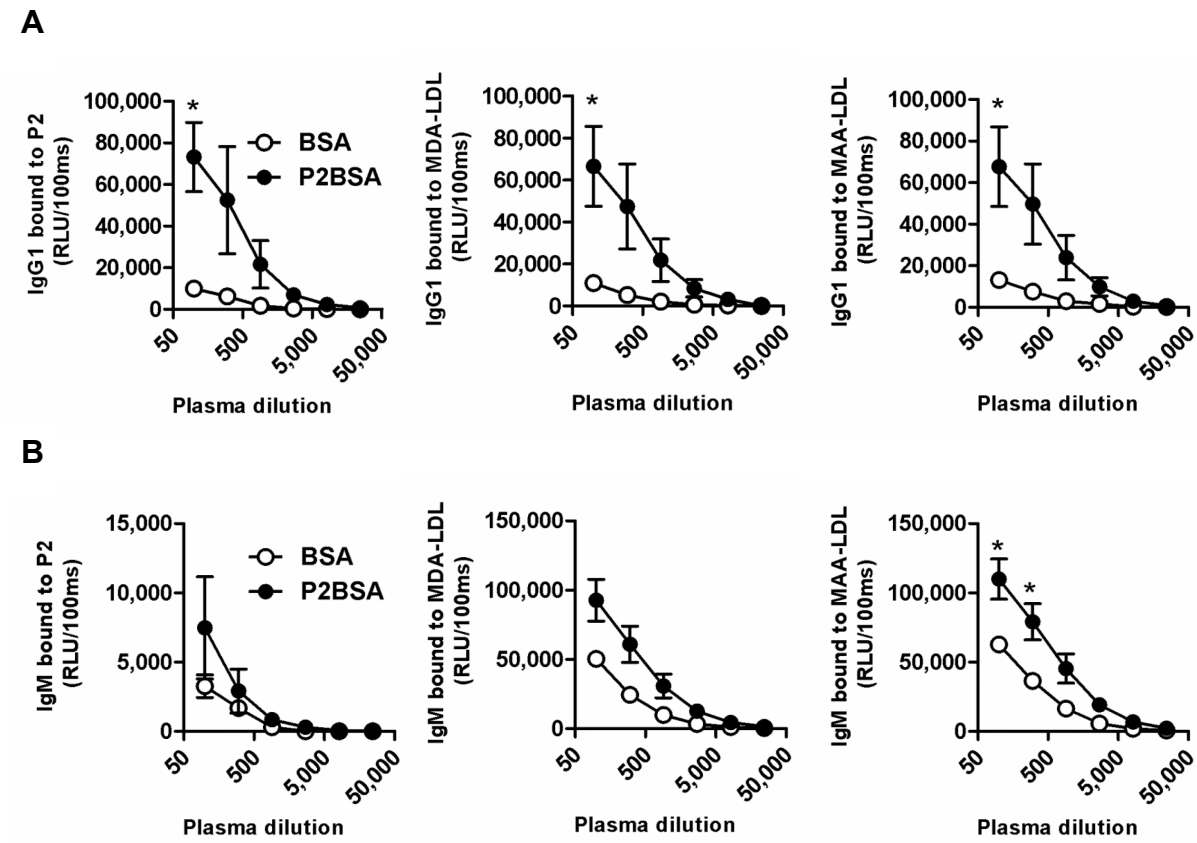

Fig. 11: P2-BSA immunization induces MDA-specific antibody responses

(A-B) ELISA for the binding of plasma Abs of immunized mice to MDA-LDL, MAA-LDL, and P2. C57BL/6 mice were immunized with P2-BSA (n=3) or BSA (n=3) as described in Methods. Dilution curves of IgG1 and IgM binding to indicated antigens in post-immune plasma was determined by chemiluminescent ELISA. **(A)** Dilution curve of IgG1 binding. **(B)** Dilution curve of IgM binding. Values are given as relative light units (RLU) per 100 ms and represent the mean±SEM of each group.

4.24 Antisera recognize epitopes in atherosclerotic lesions

To demonstrate the specificity of the Abs induced by mimotope immunization for epitopes in atherosclerotic lesions, I immunostained human carotid endarterectomy specimens and lesions of WHHL rabbits with plasma from immunized mice. Post-immune IgG of P2-BSA immunized mice showed high reactivity with epitopes in both human (Fig. 12B) and rabbit atherosclerotic lesions (Fig. 13B). A similar staining pattern was achieved with the MDA-specific monoclonal Ab MDA2 (Fig. 12C). In contrast, post-immune IgG of BSA immunized mice failed to stain the atherosclerotic lesion (Fig. 13D). These data indicate that the Abs induced by mimotope immunization are specific for epitopes that occur in atherosclerotic lesions *in vivo*.

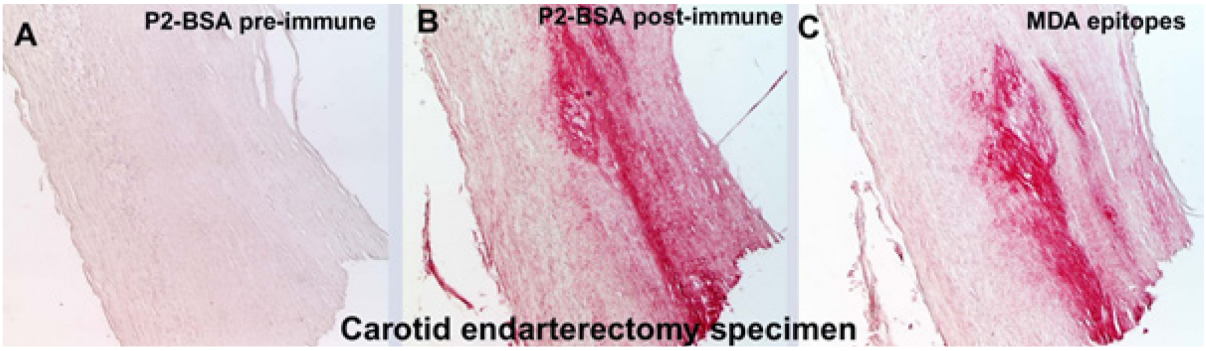

Fig. 12: MDA-mimotope immunization induces MDA-specific Ab responses

Immunohistochemical staining of human carotid endarterectomy specimens. Sections were stained with pooled pre-immune **(A)** or post-immune plasma **(B)** of P2-BSA immunized mice, or with the MDA-LDL specific mAb MDA2 **(C)**. Positive staining is indicated by red color and nuclei are counterstained with hematoxylin. (magnification 200x)

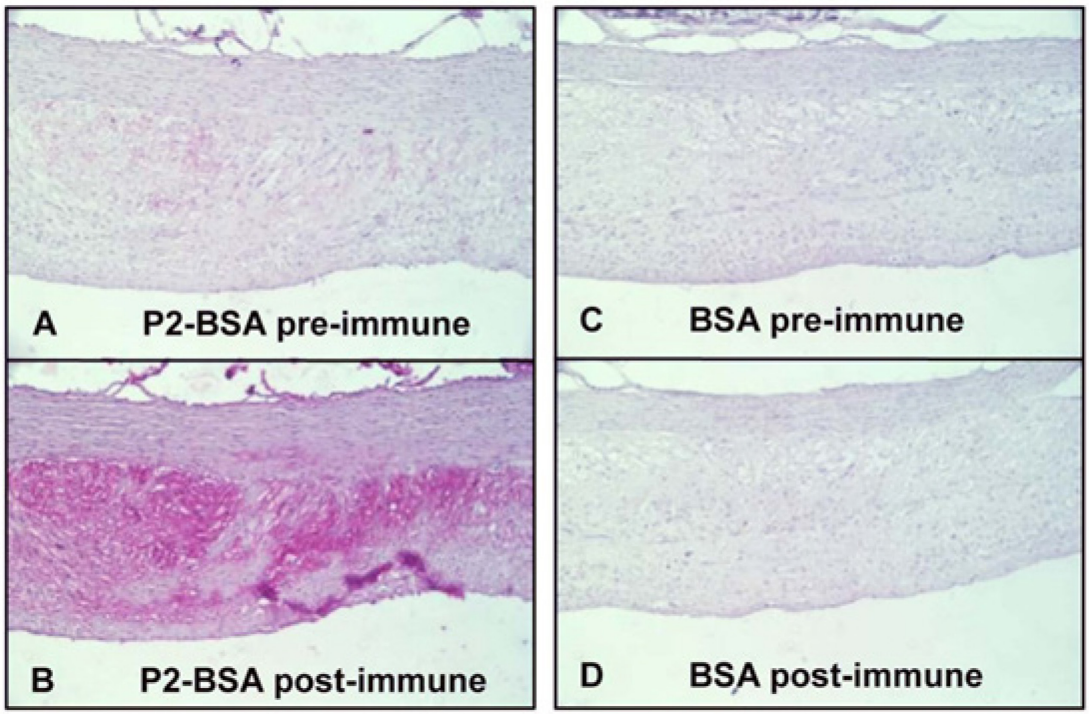

Fig. 13: Antibodies induced by mimotope immunization stain rabbit atherosclerotic lesions

Immunohistochemical staining of atherosclerotic lesions. Atherosclerotic lesions of WHHL rabbits were obtained as described in Methods and stained with pooled pre-immune **(A, C)** or post-immune plasma **(B, D)** of P2-BSA immunized **(A, B)** or BSA-immunized **(C, D)** mice. Positive staining is indicated by red color and nuclei are counterstained with hematoxylin, (magnification 100x).

4.25 Mimotopes are recognized by human antibodies

Previous studies have documented the presence of autoAbs to MDA-LDL in human sera in various clinical settings, and it has been demonstrated that these autoAbs are hapten-specific, i.e. recognized MDA-epitopes independent of the carrier. Given the highly specific nature of P1 and P2 as MDA-mimotopes in mice, I next asked if the newly identified mimotopes would be equally recognized by human autoAbs, as was MDA-LDL. I first tested whether the human MDA-LDL specific monoclonal Ab IK17, which was generated by Ab phage display, also binds the synthetic peptide mimotopes. Indeed, IK17 bound to MAA-BSA and P1 and P2 in a dose-dependent manner (Fig. 14), suggesting that both P1 and P2 could serve as MDA-mimotopes for human autoAbs. I further evaluated whether MDA-mimotopes

are recognized by the B-cell derived MDA-specific recombinant Ab CLL69C. Indeed, the human CLL69C mAb bound to MAA-BSA as well as to MDA-mimotopes, but not to a control peptide (Fig. 14 B and data not shown). Another recombinant mAb, CLL69B, did not bind to MDA-mimotopes and MAA-BSA and was used as a negative control Ab in these assays (Fig. 14 B). Binding of CLL69C to the linear MDA-mimotope P1 was highest and inhibited by increasing concentrations of MAA-BSA, but not BSA, indicating high specificity of this interaction (Fig. 14C). The binding of human mAbs to MDA-mimotopes suggests that the peptides also serve as MDA-mimotopes for human autoAbs.

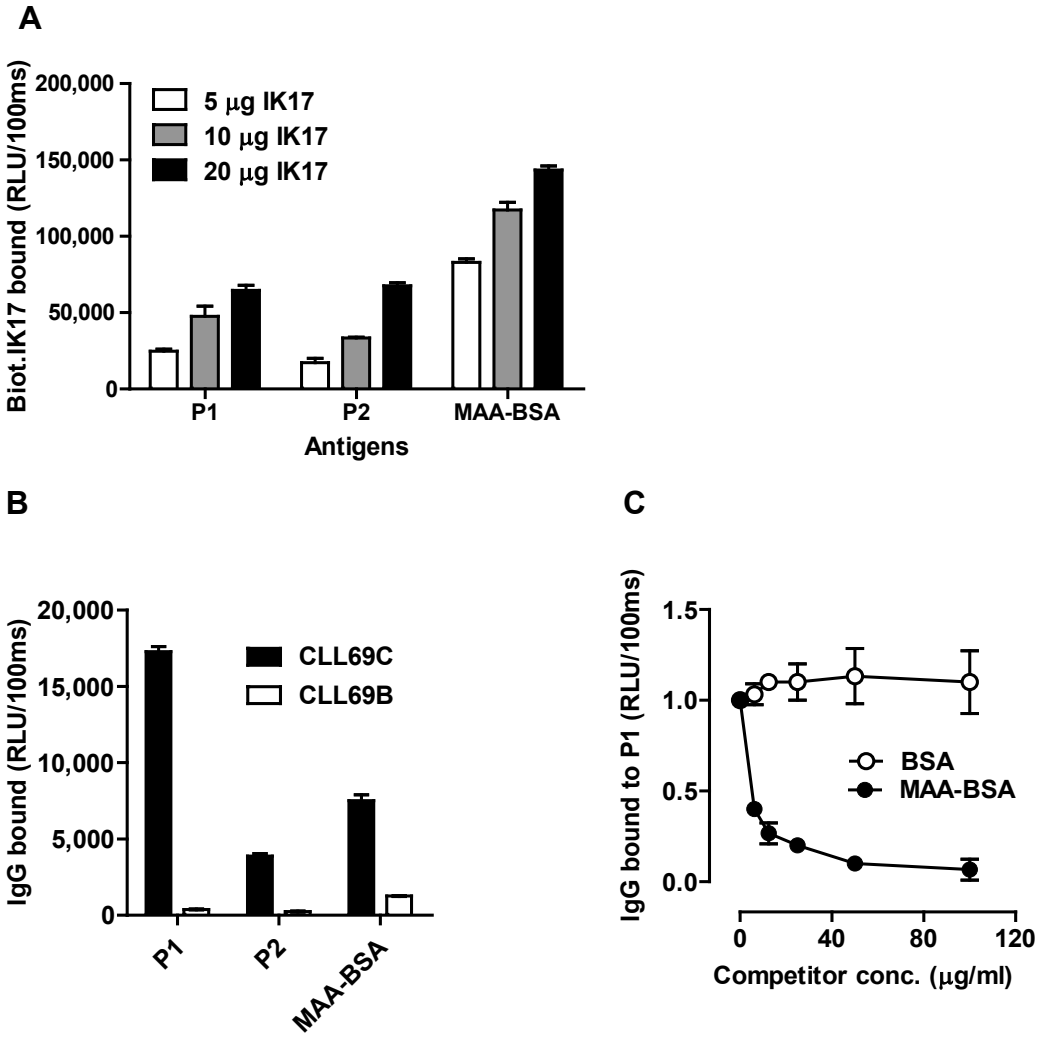

Fig. 14: Mimotopes are bound by the human MDA-specific IgG Abs.

(A) ELISA for binding of the human monoclonal Fab IK17. P1, P2, and MAA-BSA were coated onto microtiter plates, and biotinylated IK17 (Biot. IK17) was added at indicated concentrations. Binding was detected by chemiluminescent detection using AP-conjugated

neutravidin. Values are given as relative light units (RLU) per 100 ms and represent the mean±SD of triplicate determinations. **(B, C)** ELISA for binding of CLL69 Abs to P1, P2, MAA-BSA and control peptide. Antigens were coated at 5-10 µg/mL. Binding of CLL69B and C (1/10 dilution) was determined by chemiluminescent ELISA. Values are given as relative light units (RLU) per 100 ms and represent the mean of triplicate determinations. All data are representative of at least 2-3 independent experiments. **(D)** Immunocompetition assays for the specificity of CLL69C binding to P1. P1 was coated at 10 µg/mL and binding of LRO4 was determined in the absence or presence of soluble BSA or MAA-BSA at indicated concentrations. Data are expressed as a ratio of binding in the presence of competitor (B) divided by the binding in the absence of competitor (B_0) and represent the mean±SD of triplicate determinations.

To directly validate the binding of human autoAbs to MDA-mimotopes, I used plasma from a previous study (172) of middle-aged healthy volunteers (n=18) sampled at 4 different time points over 210 days, and determined Ab binding to P1 and P2 as well as to MDA-LDL in parallel assays. Plasma of all individuals contained both IgG and IgM titers to P1 and P2, respectively (Fig. 15 A-D). Moreover, the Ab titers to MDA-LDL in each plasma sample paralleled the titers to P1 and P2, resulting in significant correlations of IgG and IgM titers to P1 and P2 vs. titers to MDA-LDL (Fig. 15 A-D). I further validated the specificity of P1-reactive Abs for MDA-adducts in immunocompetion assays, which demonstrated that the binding of both IgM and IgG Abs to plated P1 was nearly completely inhibited by increasing concentrations of soluble MAA-BSA (Fig. 15 E and F). Thus, P1 and P2 serve as highly specific mimics of MDA-LDL for human antibodies as well.

I further analyzed disease-associated changes in MDA-specific Abs titers over a 7-month period using P1 and P2 as antigens. The dynamics of OxLDL-specific Abs titers over time in patients with MI have been measured previously by Tsimikas et al., and an initial 30% and 50% increase over baseline in anti-OxLDL IgG and IgM titers has been found, respectively (172) (Fig. 16). When I tested these same plasma samples for Abs binding to P1 and P2, I found an even greater increase in both IgG and IgM titers to P1 and to a lesser degree to P2 following a myocardial infarction (Fig. 17). IgM titers to P1 and P2 returned towards baseline after 210 days, whereas IgG titers to both mimotopes remained increased even after 7 months.

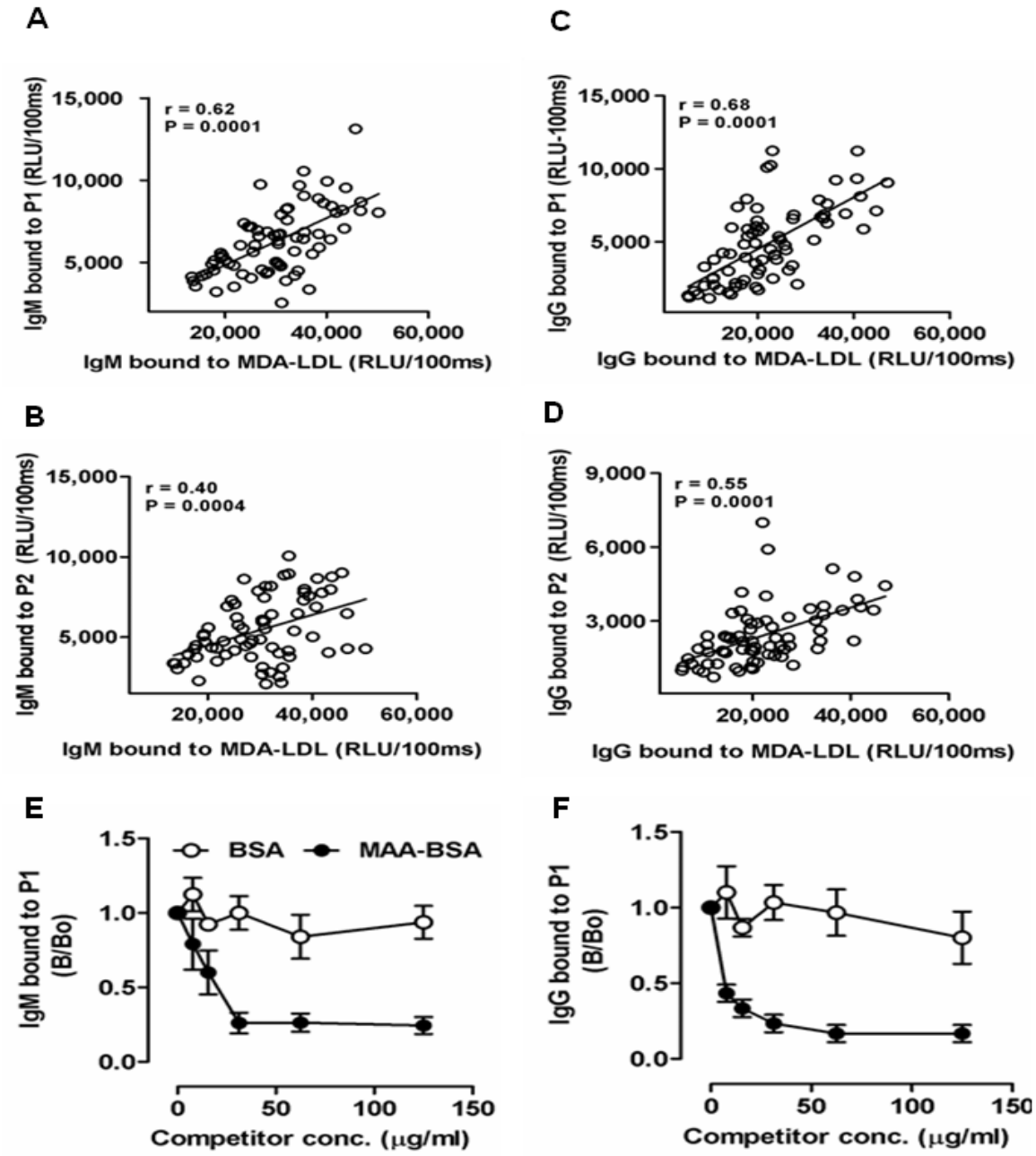

Fig. 15: Mimotopes are recognized by human autoAbs and mimic MDA-LDL.

(A-D) Correlation of mimotope and MDA-LDL specific Ab titers in human plasma. Plasma of middle-aged healthy volunteers (n=18) was obtained in a previous study (172) and Ab titers to P1, P2, and MDA-LDL were measured at 1:400 dilution by chemiluminescent ELISA as described in Methods. **(A, B)** Correlation of IgM titers to MDA-LDL with IgM titers to **(A)** P1 and **(B)** P2. **(C, D)** Correlation of IgG titer to MDA-LDL with IgG titers to **(C)** P1 and **(D)** P2. Values are given as RLU per 100 ms and represent the mean of triplicate determinations. Data points represent measurements of titers obtained from each of the 18 subjects at four different times: 0, 30, 120, and 210 days. Correlations were calculated by analyzing all data from all subjects using non-parametric Spearman's rank correlation (r = spearman rank correlation coefficient). **(E, F)** Immunocompetition assays for specificity of IgG and IgM Abs to P1. Pooled human plasma of healthy subjects (n=26) was obtained in a previous study (171) was diluted 1:1,000 and incubated with or without increasing concentrations of BSA or

MAA-BSA. Subsequently, samples were pelleted and binding of **(E)** IgM and **(F)** IgG Abs to coated P1 was determined in supernatants. Data are expressed as B/B_0 and represent the mean±SD of triplicate determinations.

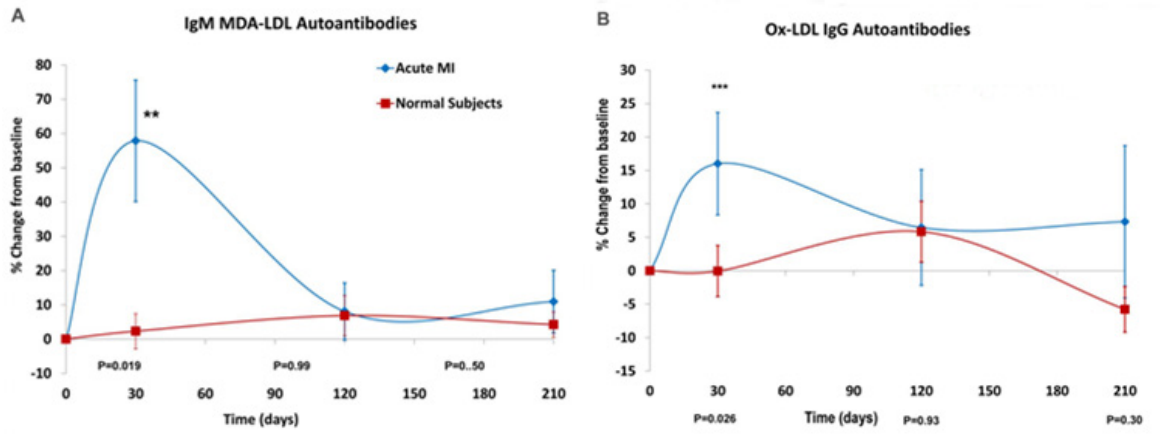

Fig.16: OxLDL specific Abs increased in patients with acute MI

Percent change from baseline in individual IgM and IgG OxLDL autoantibody titers in patients with acute MI and in health subjects. Adapted from Tsimikas et al. (172) with permission.

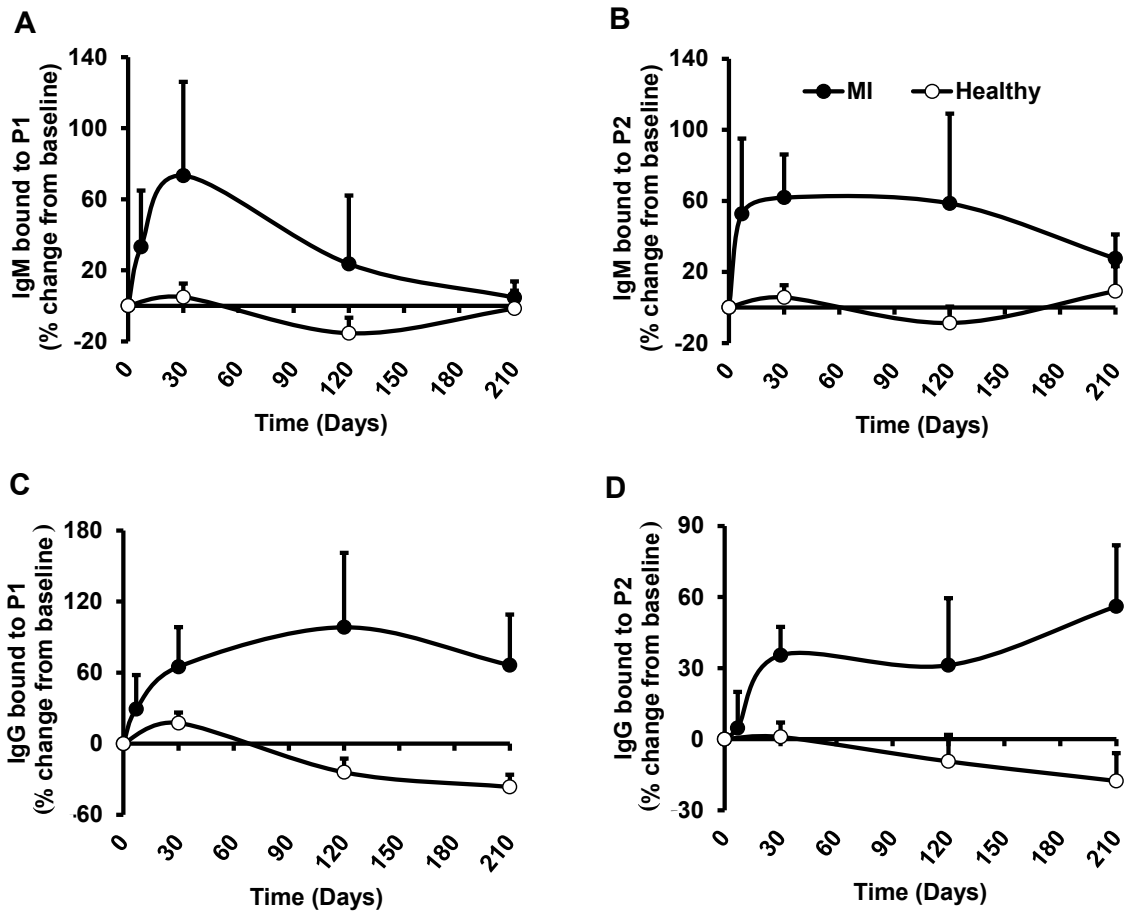

Fig. 17: **Dynamics of mimotope-specific Ab titers in plasma of patients after MI.**

(A-D) ELISA for binding of IgG and IgM Ab titers to P1 and P2 in plasma of patients suffering an MI (n=7) and of healthy controls (n=18). Plasma was obtained at various time points after MI in a previous study (172). Samples were diluted 1:400 and binding of **(A, B)** IgM and **(C, D)** IgG to coated P1 (10 µg/mL; **A, C**) and P2 (5 µg/mL; **B, D**) was determined by chemiluminescent ELISA as described in Methods. Shown are relative mean percent changes over time in Ab binding compared to values obtained at baseline.

In another previous study, I examined autoAb titers in plasma from patients with stable angina collected immediately before and sequentially up to 6 months after PCI (169). In this study a significant drop in both IgG and IgM titers to MDA-LDL that was paralleled by an increase in immune complexes with apoB containing lipoproteins has been reported. By six hours, these values had returned to baseline, and over the next few weeks there was a rise in both IgG and IgM titers with IgG titers persisting for more than 6 months ((169) and reproduced in Fig. 18).

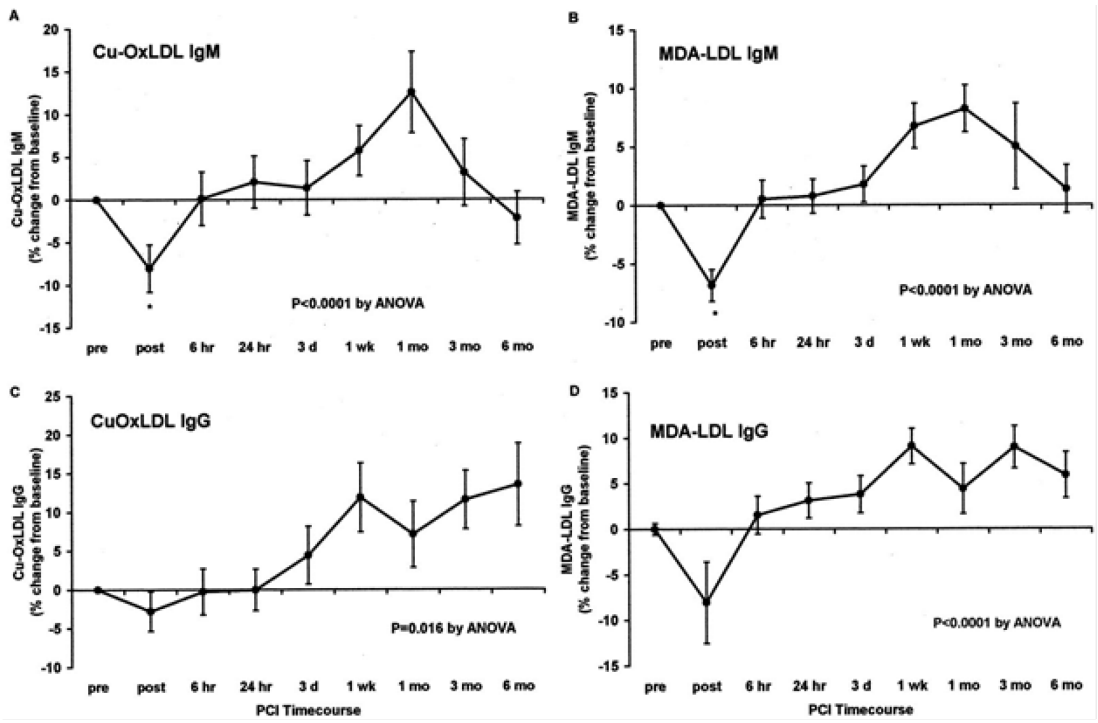

Fig. 18: OxLDL specific Abs after PCI increased in patients with stable angina.

Mean percent change from pre-PCI levels of OxLDL Abs autoantibody titers in patients with stable angina. Reprinted from Tsimikas et al. (169) with permission.

Remarkably, utilizing the P1 and P2 mimotopes as antigens faithfully reproduced these patterns of changes in both IgG and IgM Ab responses in these plasma samples (Fig. 19 A-D). Anti-P1 IgM and IgG autoAbs positively correlated with previously (169) determined anti-MDA-LDL titers ($r = 0.75$, $p < 0.0001$ and $r = 0.39$, $p<0.0001$ respectively), as did anti-P2 ($r = 0.56$, $p< 0.0001$ $r= 0.29$, $p<0.0001$ respectively).

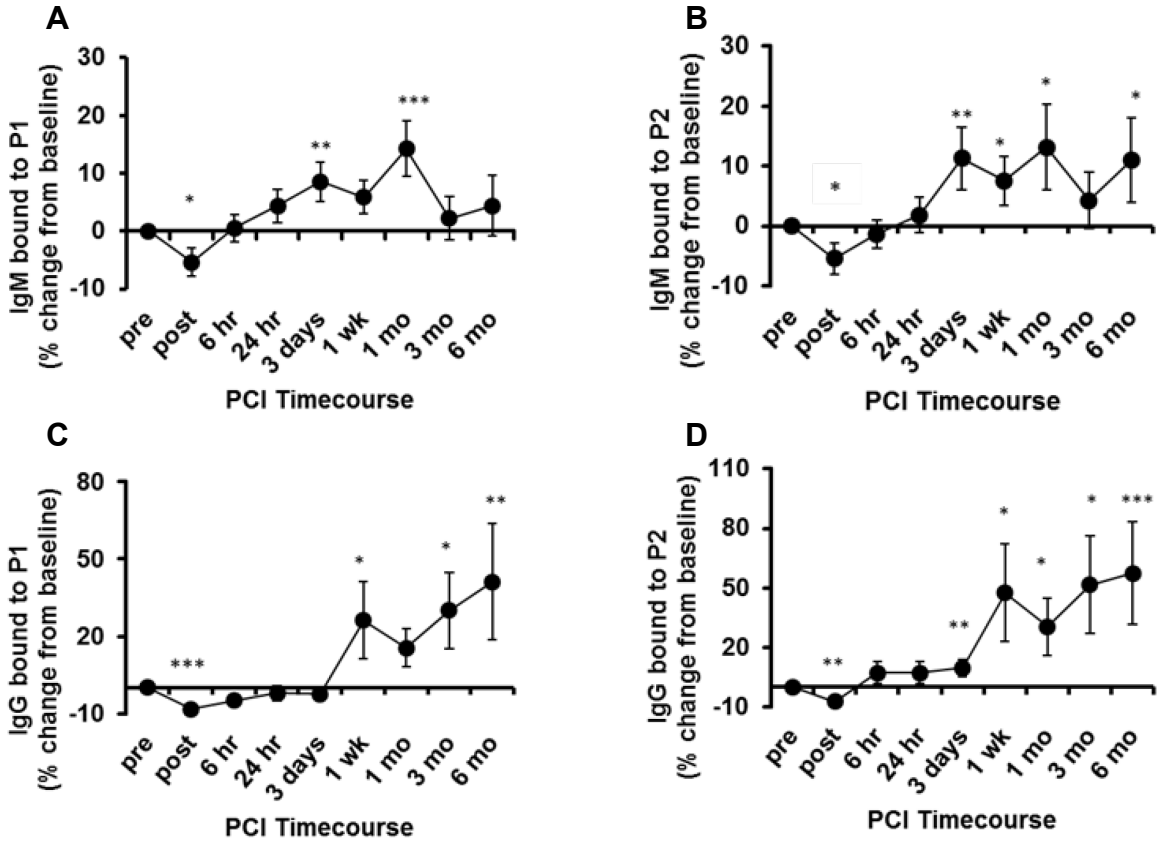

Fig. 19: Plasma antibody binding to mimotopes over time in patients undergoing PCI.

(A-D) ELISA for binding of plasma IgG and IgM to P1 and P2 in patients that underwent PCI. Sequential plasma samples were obtained following PCI (169). Samples were diluted 1:400 and binding of (A, B) IgM and **(C, D)** IgG to coated P1 (10 µg/mL; **A, C**) and P2 (5 µg/mL; **B, D**) was determined by chemiluminescent ELISA. Shown are relative mean percent changes in Ab binding compared to values obtained at baseline (pre-PCI). $*P < 0.05$, $**P < 0.01$, $***P < 0.001$. These values are similar to titers against MDA-LDL as originally observed (169) and reproduced in Fig. 18.

Taken together, these data demonstrate that mimotope-specific Ab titers behave similarly to MDA-LDL specific titers following an acute MI or PCI, and they suggest that as a consequence of MI or PCI, antigens are released that trigger an adaptive immune response, which cross-reacts with the newly identified peptide mimotopes. These findings demonstrate that P1 and P2 are mimotopes of disease-relevant antigens.

5. DISCUSSION

In this study, I report the identification and characterization of novel peptides mimicking the OSE MDA, which is present in MDA-LDL and on the surface of dying cells. Based on sequences obtained from three rounds of biopanning, I synthesized 12-mer (P1) and 7-mer (P2) peptides encoded by the consensus sequences of phagotopes of positive, i.e. LRO4-binding phages from the Ph.D.-12 and Ph.D.-C7C library, respectively. Both peptides were bound by the MDA-specific murine mAb LRO4, as well as by the MDA-specific human recombinant IgG CLL69C and the Fab IK17 Fab in a highly specific manner. Moreover, another MDA-specific murine monoclonal IgM antibody, EN1, encoded by a different complementarity-determining region 3 than LRO4, also bound both MDA mimotopes. The fact that different murine and human MDA-specific mAbs bind the same mimotopes further demonstrate that the selected peptides are faithful mimics of MDA-epitopes.

Our findings identify for the first time simple peptides that mimic lipid peroxidation derived structures. This is noteworthy, as oxidized lipid derivatives are notoriously unstable structures. Peptide mimotopes for PC of capsular polysaccharides have been described before (177-179). However, these are different from the MDA-mimotopes described here. Importantly, MDA-mimotopes are not recognized by the mAb EO6, which has specificity for PC. Thus, the identified peptides are highly specific mimics of MDA epitopes of MDA-LDL, which itself is a complex antigen with different types of MDA-neoantigens. Recently, MAA-epitopes have been identified as dominant epitopes of MDA-modifications (110) and our own unpublished studies). Indeed, the newly found mimotopes seem to mimic MAA-epitopes in MDA-LDL, as binding of autoAbs to P1 in pooled plasma of healthy subjects was inhibited by MAA-BSA, indicating that the mimotope-specific autoAbs in human plasma have specificity for MAA. These data suggest that the peptide mimotopes predominantly represent the fluorescent MAA type epitopes that occur following MDA modification of proteins. Thus, not all MDA-LDL reactive antibodies and/or proteins may bind to the mimotopes. Nevertheless, this fine specificity may be useful in future studies as they more specifically define a restricted set of “MDA-reactive” antibodies to an immunodominant set of MAA modifications.

During the screening of phagotopes, all phages with linear or cyclic mimotopes inhibited the antigen-antibody interaction in phage competition ELISAs. However, the

synthetic linear peptide P1 compared to the cyclic P2, when suspended in solution did not inhibit binding of LRO4 to MDA-LDL. This can be explained by the fact that the cyclic P2 peptides form a circular ring that provides little conformational freedom, whereas linear peptides may attain multiple conformations in different immunoassays (173-175). The cyclic P2 mimotope inhibited the antigen-antibody interaction in solid phase as well as in solution. Nevertheless, both peptides are faithful antigenic mimics of MDA-epitopes.

Further evidence for the molecular mimicry between peptides and MDA-epitopes was provided by experimental immunization approaches of mice with P2 mimotopes, which demonstrated the induction of MDA-reactive Abs. These Abs were particularly directed against the advanced MAA-adducts, which are immunodominant and the cognate antigen of LRO4. Because it has been reported that not all peptides with high antigenicity can induce cross-reactive immune response (180-185) and no good criteria for the selection of mimetics of non-proteineous antigens for the induction of cross-reactive immune response exist, I used the P2 peptide carrying the consensus sequence of all 7-mer phagotopes to test the immunogenicity and *in vivo* cross-reactivity with MDA. In addition to the peptide sequence itself (186-188), the choice of carrier protein, the peptide/carrier ratio (189-194), as well as choice of the adjuvant (195) can affect immunogenicity. Therefore, two separate approaches were carried out. I initially used KLH as carrier. Immunization with P2-KLH resulted in the induction of Abs with specificity for MAA-BSA, but only moderately higher compared to the Abs induced by immunization with KLH alone, which also resulted in a non-specific stimulation of MAA-specific Abs. Subsequent analyses of the plasma from immunized mice unmasked the specific binding to short MAA-modified peptides, but not unmodified peptides, of the induced Abs, demonstrating specificity for the MAA-hapten. In a second experiment, I used another comparatively less immunogenic carrier, BSA, together with Freund's adjuvant. This approach resulted in a more robust induction of IgG Abs specific to MAA-BSA and MDA-LDL, demonstrating molecular mimicry between P2 and MDA-adducts. Moreover, immunization of mice with P2 mimotopes resulted in the induction of MDA-LDL-specific Ab titers, which specifically recognized epitopes in human carotid atherosclerotic lesions. Thus, the synthetic peptides mimic OSEs that occur *in vivo* and that accumulate in atherosclerotic lesions.

Because it has been demonstrated that MDA-specific Abs bind to the surface of apoptotic cells (140, 143, 176), I tested the ability of P2 to inhibit the binding of LRO4 to apoptotoic cells. Indeed, I further confirmed the *in vivo* relevance of the peptide mimotopes by

demonstrating that P2 fully competed the binding of LRO4 to the surface of apoptotic cells. Thus, the peptide mimotopes mimic MDA-epitopes present on the surface of apoptotic cells. This is important, as naturally occurring auto-antibodies IgM, such as LRO4, play an essential role in tissue homeostasis as well as in modulation and regulation of cellular properties (88, 139). It has been reported that clearance of auto antigens in late apoptotic and secondary necrotic cells formed during the injury and apoptosis is assisted by IgM Abs through the activation of the classical pathway (146-149). Recently, it has also been shown that IgM Abs are required for the efficient engulfment and clearance of injected apoptotic cells *in vivo* and their presence is essential for the apoptosis mediated immunomodulatory effects such as the induction of IL-10 secreting B cells and the suppression of inflammatory processes (150). My studies also identified peptide mimotopes of a critically important ligand on dying cells that mediate recognition by natural IgM mediating housekeeping functions.

These well-defined OSE mimotopes have significant potential in biotheranostic applications in humans by providing standardized, chemically defined antigens. Tsimikas et al. have conducted extensive studies documenting the presence and predictive value of autoAbs to MDA-LDL in humans with CVD (e.g. (128, 131)). One of the major limitations of such studies is preparing a reproducible MDA-LDL, which is generated by MDA modification of freshly isolated LDL. The newly generated MDA-mimotopes now identify for the first time a reliable surrogate for MDA-LDL, and more specifically, for MAA-type autoantibodies. The availability of these small peptide mimotopes will greatly enhance the reproducibility and facilitate the standardization of assays for the determination of such autoAbs. As an example of their utility, I demonstrated the ability of P1 and P2 to act as surrogates for MDA-LDL in autoAb assays. Both sera of healthy subjects and patients with CVD contained autoAbs titers against the peptide mimotopes, which correlated positively with MDA-LDL specific titers. I further showed that previously demonstrated dynamic changes in these titers to MDA-LDL following MI or PCI could be faithfully reproduced using P1 or P2 as antigens. For example, in response to PCI, there was an immediate drop in Ab titers, consistent with binding to OSE antigens released into the circulation, followed thereafter by long-term rises in Ab titers, consistent with anamnestic responses to OSEs, likely reflecting the extent of injury. These data exactly parallel previous demonstrations of the Ab dynamics against MDA-LDL as antigen (169, 172).

Other applications of OSE mimotopes may be in molecular imaging and use as immunogens in atheroprotective vaccines. In prior studies, (196). It has been demonstrated that OSE in

atherosclerotic lesions can be targeted and imaged with human and murine oxidation-specific antibodies carried by MRI nanoparticles. These nanoparticles accumulate within macrophages, allowing visualization of active lesions. In an analogous manner, OSE mimotopes may be bound to similar nanoparticles and used as imaging agents, where they would target scavenger receptors on activated macrophages. This approach may be complementary to using OSE-monoclonal antibodies, which would bind to extracellular epitopes, as for example, on OxLDL, whereas OSE mimotopes might more specifically image macrophages.

Another use would be as an immunogen in atheroprotective vaccines. Witztum et al. and others have demonstrated the atheroprotective effect of immunization strategies using MDA-LDL in animal models (29). Use of such an antigen in human studies would be impractical. In this study, I demonstrated that immunization with P2-conjugated BSA gave rise to anti-MDA-LDL Abs and these Abs immunostained atherosclerotic lesions, suggesting its potential as an immunogen for such a vaccine. Future studies will be needed to evaluate its potential to induce atheroprotective immunity.

In conclusion, our studies have identified two peptides that mimic epitopes of MDA-LDL. I provide several lines of evidence documenting the capacity of these peptides to mimic epitopes relevant to atherogenesis. Because both mimotopes are recognized by MDA-specific autoAbs in human sera, they represent for the first time highly reproducible and standardized antigens for the determination of anti-MDA-LDL Abs. Thus, future studies using these mimotopes as antigens may provide a reliable assay to evaluate the role of MDA-specific Abs as biomarkers for CVD. Finally, in conjunction with different carriers, the newly identified peptides can also be used as immunogens to study the mechanistic role of MDA-specific immune responses in immunization studies, and may provide the basis for potential atheroprotective vaccine preparations.

6. STUDY LIMITATIONS AND FUTURE DIRECTIONS

The results presented here confirm the aim of my thesis and from this several questions emerge for consideration.

1) During biopanning of the phage display peptide libraries many peptide sequences were identified and their consensus sequences were synthesized. However, each individual peptide sequence identified might represent a potential candidate for mimicking MDA-epitope that could be even more immunogenic than other candidate peptides. Moreover, it is not known what amino acid residues are exactly required for mimotope-paratope interaction. To understand the exact nature of the mimicry molecular modeling simulations would be required to compare the spatial alignment of MDA-mimotopes with MDA-LDL.

2) The replacement or rearrangement of side residues by alanine-scanning could also further improve the affinity of Ab binding to these mimotopes. Moreover, antigen design including the addition of multiple peptide mimotopes, e.g. multiple antigenic peptides (MAP), in series may improve the affinity as well as immunogenicity of mimotopes.

3) Although my studies identify MDA-mimotopes as surrogate for MDA-LDL, I did not directly compare the utility of mimotopes vs. MDA-LDL as antigens for the determination of autoAbs in large clinical cohorts. Only a side-by-side comparison of both antigens will define the mimotopes as potentially superior antigens and mimotope-specific autoAbs as novel more reliable biomarkers.

4) Moreover, the absence of a 100% correlation between titers to MDA-LDL and P1/P2 in some subjects may reflect subtle differences in disease relevant autoAbs that are masked by the use of the heterogeneous “MDA-LDL” as antigen. Future studies will be needed to determine if the use of these peptides as antigens can unmask the clinical utility of such antibody measurements as biomarker of CVD or other inflammatory settings in studies that have reported negative results.

5) Immunization studies with peptide mimotopes induced MDA-specific Abs. However, the effectiveness of such vaccination approaches in decreasing lesions formation can only be investigated using atherosclerosis-prone animal models. In addition, changing the formulation of the peptide-based immunogens, such as using multiple antigenic peptides with or without addition of T or B cell epitopes, as well as the inclusion of Th1/2-biasing adjuvants may provide mechanistic insights into the functional role of MDA-specific immune responses.

7. APPENDEX

7.1 Appendix A. Phage display peptide libraries and mimotopes

Phage display has been widely used due to its power, versatility, low cost and ease of use. The phage display peptide technology has been used in many applications such as drug discovery/design (receptor agonist or antagonists) (197-202), development of vaccines (177, 179, 203-208), investigation of the immune response (185, 208-213), discovery of agents for targeted delivery of drugs and gene therapy (214), analysis of protein protein interactions (215-222), epitope mapping (223), identification of novel substrates and inhibitors for the active and allosteric sites of the enzymes (224-227)

Phage display is a molecular biology technique where DNA of peptide libraries are fused to the DNA of phage coat proteins (228) thereby making a direct physical link between the DNA sequences and their encoding peptides. Upon expression of phage DNA, peptides with phage coat proteins are also expressed outside the phage (229). Phage display libraries consist of millions of variable and short peptides (Scott, 1992). The number of unique sequences in libraries depend on the number of residues in the displayed peptide. In phage display technology, many outer phage coat proteins (pIII, pVI, pVII, pVIII and pIX) have been used to express peptides. Among all phage coat proteins, pIII and pVIII are the most effective and widely used to display combinatorial peptides.

M13 filamentous bacteriophage has been widely used as a vehicle for display of peptides with variable length (228, 230-232). It is a male-specific virus and contains covalently closed single stranded DNA genome (233) that encodes five coat proteins per phage. Phage protein VIII (pVIII) is the most abundant protein with approximately 2800 copies per phage. Among other proteins, pIII and pVI are displayed on one end and pVII and pIX on other end of phage (234). Due to the avidity effect high copy display of pVIII-fused peptides are useful for selection of low affinity peptide ligands (235), whereas the low valency of pIII displayed libraries is useful for the discovery of ligands with higher affinity (Kd of 10 μM or better).

A mimotope is a peptide that mimics an antibody epitope. The term was first used by Geysen et al. (236) and defined a mimotope as “a molecule able to bind to the antigen-

combining site of an antibody molecule, not necessarily identical with the epitope inducing the antibody, but an acceptable mimic of the essential features of the epitope".

In case of monoclonal antibodies, the epitopes on the target protein may be either continuous linear, consisting of a stretch of 4-8 adjacent amino acids, or nonlinear conformational, consisting of residues that are located far apart in the sequence and are brought together by protein folding (237). Scot et al. and Stephan et al. first reported the use of phage display random libraries to map known linear epitopes of antibodies specific against different antigens. (238, 239). In X-ray crystallographic studies of antigen-antibody complexes, it has been shown that only 3-5 residues contribute most strongly to the binding energy of the complex (240, 241).

Mimotopes of various protein antigens including DNA (242, 243) and non-protein antigens such as polysaccharides (177-179, 244) have been characterized. Peptide mimotopes of protein antigens selected from phage display peptide libraries can be assessed by comparison of their sequence with the target antigen sequence. In case of conformational epitopes, it is extremely difficult to identify homology between the mimotopes and the antigen. Availability of the three dimensional structure (3D) of the antigens using different computational approaches (245-248) with different algorithms and programs have facilitated the mapping of conformational epitopes (248-254). When the 3D structure of an antigen is not available, alignment of the consensus sequence obtained after biopanning of phage display to the primary sequence of the antigen also provides valuable information about the folded structure of the antigen (255-258). However, in case of non-protein antigens such as lipids structural alignments are not possible.

The design of mimotopes is very important for the mimotope-Ab interaction. It has been reported that dimerization or cyclization of peptides increases their binding to the antibody as well as their immunogenic potential (259-261). Not all peptides are immunogenic and this property of peptides depends not only on the design and sequence of peptides (262) but also on strain of immunized mice (263). To classify mimotope as an immunogen, it should be capable to induce antibodies that cross react with the original cognate antigen.

8. REFERENCES

1. Lloyd-Jones, D., R. J. Adams, T. M. Brown, M. Carnethon, S. Dai, G. De Simone, T. B. Ferguson, E. Ford, K. Furie, C. Gillespie, A. Go, K. Greenlund, N. Haase, S. Hailpern, P. M. Ho, V. Howard, B. Kissela, S. Kittner, D. Lackland, L. Lisabeth, A. Marelli, M. M. McDermott, J. Meigs, D. Mozaffarian, M. Mussolino, G. Nichol, V. L. Roger, W. Rosamond, R. Sacco, P. Sorlie, R. Stafford, T. Thom, S. Wasserthiel-Smoller, N. D. Wong, and J. Wylie-Rosett. 2010. Executive summary: heart disease and stroke statistics--2010 update: a report from the American Heart Association. *Circulation* **121**: 948-954.

2. Joan, S. 2008. Global Mortality Trends. *JAMA* **299**: 2737.

3. Murphy, S. L., X. Jiaquan, and K. D. Kochanek. 2012. National vital statistics reports. Deaths: Preliminary data for 2012. www.cdc.gov/nchs/data/nvsr/nvsr53/nvsr53_05.pdf

4. Glass, C. K., and J. L. Witztum. 2001. Atherosclerosis. the road ahead. *Cell* **104**: 503-516.

5. Kockx, M. M. 1998. Apoptosis in the atherosclerotic plaque: quantitative and qualitative aspects. *Arterioscler Thromb Vasc Biol* **18**: 1519-1522.

6. Van Vre, E. A., H. Ait-Oufella, A. Tedgui, and Z. Mallat. 2012. Apoptotic cell death and efferocytosis in atherosclerosis. *Arterioscler Thromb Vasc Biol* **32**: 887-893.

7. Falk, E., P. K. Shah, and V. Fuster. 1995. Coronary plaque disruption. *Circulation* **92**: 657-671.

8. Mann, J. M., and M. J. Davies. 1996. Vulnerable Plaque: Relation of Characteristics to Degree of Stenosis in Human Coronary Arteries. *Circulation* **94**: 928-931.

9. Hansson, G. K. 2005. Inflammation, atherosclerosis, and coronary artery disease. *N Engl J Med* **352**: 1685-1695.

10. Galkina, E., and K. Ley. 2009. Immune and inflammatory mechanisms of atherosclerosis (*). *Annu Rev Immunol* **27**: 165-197.

11. Binder, C. J. 2010. Natural IgM antibodies against oxidation-specific epitopes. *J Clin Immunol* **30 Suppl 1**: S56-60.

12. Hansson, G. K., and A. Hermansson. 2011. The immune system in atherosclerosis. *Nat Immunol* **12**: 204-212.

13. Wilson, P. W., R. B. D'Agostino, D. Levy, A. M. Belanger, H. Silbershatz, and W. B. Kannel. 1998. Prediction of coronary heart disease using risk factor categories. *Circulation* **97**: 1837-1847.

14. Libby, P., P. M. Ridker, and G. K. Hansson. 2009. Inflammation in atherosclerosis: from pathophysiology to practice. *J Am Coll Cardiol* **54**: 2129-2138.

15. Skalen, K., M. Gustafsson, E. K. Rydberg, L. M. Hulten, O. Wiklund, T. L. Innerarity, and J. Boren. 2002. Subendothelial retention of atherogenic lipoproteins in early atherosclerosis. *Nature* **417**: 750-754.

16. Harrison, D., K. K. Griendling, U. Landmesser, B. Hornig, and H. Drexler. 2003. Role of oxidative stress in atherosclerosis. *Am J Cardiol* **91**: 7A-11A.

17. Heinecke, J. W. 1997. Mechanisms of oxidative damage of low density lipoprotein in human atherosclerosis. *Curr Opin Lipidol* **8**: 268-274.

18. Steinberg, D., S. Parthasarathy, T. E. Carew, J. C. Khoo, and J. L. Witztum. 1989. Beyond cholesterol. Modifications of low-density lipoprotein that increase its atherogenicity. *N Engl J Med* **320**: 915-924.

19. Witztum, J. L. 1994. The oxidation hypothesis of atherosclerosis. *Lancet* **344**: 793-795.

20. Cybulsky, M. I., and M. A. Gimbrone, Jr. 1991. Endothelial expression of a mononuclear leukocyte adhesion molecule during atherogenesis. *Science* **251**: 788-791.

21. Nakashima, Y., E. W. Raines, A. S. Plump, J. L. Breslow, and R. Ross. 1998. Upregulation of VCAM-1 and ICAM-1 at atherosclerosis-prone sites on the endothelium in the ApoE-deficient mouse. *Arterioscler Thromb Vasc Biol* **18**: 842-851.

22. Walpola, P. L., A. I. Gotlieb, M. I. Cybulsky, and B. L. Langille. 1995. Expression of ICAM-1 and VCAM-1 and monocyte adherence in arteries exposed to altered shear stress. *Arterioscler Thromb Vasc Biol* **15**: 2-10.

23. Boring, L., J. Gosling, M. Cleary, and I. F. Charo. 1998. Decreased lesion formation in CCR2-/- mice reveals a role for chemokines in the initiation of atherosclerosis. *Nature* **394**: 894-897.

24. Cybulsky, M. I., K. Iiyama, H. Li, S. Zhu, M. Chen, M. Iiyama, V. Davis, J. C. Gutierrez-Ramos, P. W. Connelly, and D. S. Milstone. 2001. A major role for VCAM-1, but not ICAM-1, in early atherosclerosis. *J Clin Invest* **107**: 1255-1262.

25. Galkina, E., and K. Ley. 2007. Vascular adhesion molecules in atherosclerosis. *Arterioscler Thromb Vasc Biol* **27**: 2292-2301.

26. Gosling, J., S. Slaymaker, L. Gu, S. Tseng, C. H. Zlot, S. G. Young, B. J. Rollins, and I. F. Charo. 1999. MCP-1 deficiency reduces susceptibility to atherosclerosis in mice that overexpress human apolipoprotein B. *J Clin Invest* **103**: 773-778.

27. Ait-Oufella, H., S. Taleb, Z. Mallat, and A. Tedgui. 2011. Recent advances on the role of cytokines in atherosclerosis. *Arterioscler Thromb Vasc Biol* **31**: 969-979.

28. Smith, J. D., E. Trogan, M. Ginsberg, C. Grigaux, J. Tian, and M. Miyata. 1995. Decreased atherosclerosis in mice deficient in both macrophage colony-stimulating factor (op) and apolipoprotein E. *Proc Natl Acad Sci U S A* **92**: 8264-8268.

29. Amir, S., and C. J. Binder. 2010. Experimental immunotherapeutic approaches for atherosclerosis. *Clin Immunol* **134**: 66-79.

30. Steinbrecher, U. P., S. Parthasarathy, D. S. Leake, J. L. Witztum, and D. Steinberg. 1984. Modification of low density lipoprotein by endothelial cells involves lipid peroxidation and degradation of low density lipoprotein phospholipids. *Proc Natl Acad Sci U S A* **81**: 3883-3887.

31. Fogelman, A. M., I. Shechter, J. Seager, M. Hokom, J. S. Child, and P. A. Edwards. 1980. Malondialdehyde alteration of low density lipoproteins leads to cholesteryl ester accumulation in human monocyte-macrophages. *Proc Natl Acad Sci U S A* **77**: 2214-2218.

32. Yamada, Y., T. Doi, T. Hamakubo, and T. Kodama. 1998. Scavenger receptor family proteins: roles for atherosclerosis, host defence and disorders of the central nervous system. *Cell Mol Life Sci* **54**: 628-640.

33. McLaren, J. E., D. R. Michael, T. G. Ashlin, and D. P. Ramji. 2011. Cytokines, macrophage lipid metabolism and foam cells: implications for cardiovascular disease therapy. *Prog Lipid Res* **50**: 331-347.

34. Binder, C. J., M. K. Chang, P. X. Shaw, Y. I. Miller, K. Hartvigsen, A. Dewan, and J. L. Witztum. 2002. Innate and acquired immunity in atherogenesis. *Nat Med* **8**: 1218-1226.

35. Lahoute, C., O. Herbin, Z. Mallat, and A. Tedgui. 2011. Adaptive immunity in atherosclerosis: mechanisms and future therapeutic targets. *Nat Rev Cardiol* **8**: 348-358.

36. Weismann, D., and C. J. Binder. 2012. The innate immune response to products of phospholipid peroxidation. *Biochim Biophys Acta*.

37. Hartvigsen, K., M. Y. Chou, L. F. Hansen, P. X. Shaw, S. Tsimikas, C. J. Binder, and J. L. Witztum. 2009. The role of innate immunity in atherogenesis. *J Lipid Res* **50 Suppl**: S388-393.

38. Lundberg, A. M., and G. K. Hansson. 2010. Innate immune signals in atherosclerosis. *Clin Immunol* **134**: 5-24.

39. Akira, S., S. Uematsu, and O. Takeuchi. 2006. Pathogen recognition and innate immunity. *Cell* **124**: 783-801.

40. Medzhitov, R., and C. A. Janeway, Jr. 2002. Decoding the patterns of self and nonself by the innate immune system. *Science* **296**: 298-300.

41. Miller, Y. I., S. H. Choi, P. Wiesner, L. Fang, R. Harkewicz, K. Hartvigsen, A. Boullier, A. Gonen, C. J. Diehl, X. Que, E. Montano, P. X. Shaw, S. Tsimikas, C. J.

Binder, and J. L. Witztum. 2011. Oxidation-specific epitopes are danger-associated molecular patterns recognized by pattern recognition receptors of innate immunity. *Circ Res* **108**: 235-248.

42. Pluddemann, A., C. Neyen, and S. Gordon. 2007. Macrophage scavenger receptors and host-derived ligands. *Methods* **43**: 207-217.

43. Kzhyshkowska, J., C. Neyen, and S. Gordon. 2012. Role of macrophage scavenger receptors in atherosclerosis. *Immunobiology* **217**: 492-502.

44. Greaves, D. R., and S. Gordon. 2009. The macrophage scavenger receptor at 30 years of age: current knowledge and future challenges. *J Lipid Res* **50 Suppl**: S282-286.

45. Guy, E., S. Kuchibhotla, R. Silverstein, and M. Febbraio. 2007. Continued inhibition of atherosclerotic lesion development in long term Western diet fed CD36o /apoEo mice. *Atherosclerosis* **192**: 123-130.

46. Kuchibhotla, S., D. Vanegas, D. J. Kennedy, E. Guy, G. Nimako, R. E. Morton, and M. Febbraio. 2008. Absence of CD36 protects against atherosclerosis in ApoE knock-out mice with no additional protection provided by absence of scavenger receptor A I/II. *Cardiovasc Res* **78**: 185-196.

47. Manning-Tobin, J. J., K. J. Moore, T. A. Seimon, S. A. Bell, M. Sharuk, J. I. Alvarez-Leite, M. P. de Winther, I. Tabas, and M. W. Freeman. 2009. Loss of SR-A and CD36 activity reduces atherosclerotic lesion complexity without abrogating foam cell formation in hyperlipidemic mice. *Arterioscler Thromb Vasc Biol* **29**: 19-26.

48. Suzuki, H., Y. Kurihara, M. Takeya, N. Kamada, M. Kataoka, K. Jishage, O. Ueda, H. Sakaguchi, T. Higashi, T. Suzuki, Y. Takashima, Y. Kawabe, O. Cynshi, Y. Wada, M. Honda, H. Kurihara, H. Aburatani, T. Doi, A. Matsumoto, S. Azuma, T. Noda, Y. Toyoda, H. Itakura, Y. Yazaki, and T. Kodama. 1997. A role for macrophage scavenger receptors in atherosclerosis and susceptibility to infection. *Nature* **386**: 292-296.

49. Moore, K. J., V. V. Kunjathoor, S. L. Koehn, J. J. Manning, A. A. Tseng, J. M. Silver, M. McKee, and M. W. Freeman. 2005. Loss of receptor-mediated lipid uptake via scavenger receptor A or CD36 pathways does not ameliorate atherosclerosis in hyperlipidemic mice. *J Clin Invest* **115**: 2192-2201.

50. Febbraio, M., E. A. Podrez, J. D. Smith, D. P. Hajjar, S. L. Hazen, H. F. Hoff, K. Sharma, and R. L. Silverstein. 2000. Targeted disruption of the class B scavenger receptor CD36 protects against atherosclerotic lesion development in mice. *J Clin Invest* **105**: 1049-1056.

51. Curtiss, L. K., and P. S. Tobias. 2009. Emerging role of Toll-like receptors in atherosclerosis. *J Lipid Res* **50 Suppl**: S340-345.

52. Seneviratne, A. N., B. Sivagurunathan, and C. Monaco. 2012. Toll-like receptors and macrophage activation in atherosclerosis. *Clin Chim Acta* **413**: 3-14.

53. Liu, X., T. Ukai, H. Yumoto, M. Davey, S. Goswami, F. C. Gibson, 3rd, and C. A. Genco. 2008. Toll-like receptor 2 plays a critical role in the progression of atherosclerosis that is independent of dietary lipids. *Atherosclerosis* **196**: 146-154.

54. Shinohara, M., K. Hirata, T. Yamashita, T. Takaya, N. Sasaki, R. Shiraki, T. Ueyama, N. Emoto, N. Inoue, M. Yokoyama, and S. Kawashima. 2007. Local overexpression of toll-like receptors at the vessel wall induces atherosclerotic lesion formation: synergism of TLR2 and TLR4. *Arterioscler Thromb Vasc Biol* **27**: 2384-2391.

55. Ding, Y., S. Subramanian, V. N. Montes, L. Goodspeed, S. Wang, C. Y. Han, A. S. Teresa, 3rd, J. Kim, K. D. O'Brien, and A. Chait. 2012. Toll-Like Receptor 4 Deficiency Decreases Atherosclerosis But Does Not Protect Against Inflammation in Obese Low-Density Lipoprotein Receptor-Deficient Mice. *Arterioscler Thromb Vasc Biol*.

56. Kiechl, S., E. Lorenz, M. Reindl, C. J. Wiedermann, F. Oberhollenzer, E. Bonora, J. Willeit, and D. A. Schwartz. 2002. Toll-like receptor 4 polymorphisms and atherogenesis. *N Engl J Med* **347**: 185-192.

57. Yang, I. A., J. W. Holloway, and S. Ye. 2003. TLR4 Asp299Gly polymorphism is not associated with coronary artery stenosis. *Atherosclerosis* **170**: 187-190.

58. Stewart, C. R., L. M. Stuart, K. Wilkinson, J. M. van Gils, J. Deng, A. Halle, K. J. Rayner, L. Boyer, R. Zhong, W. A. Frazier, A. Lacy-Hulbert, J. El Khoury, D. T. Golenbock, and K. J. Moore. 2010. CD36 ligands promote sterile inflammation through assembly of a Toll-like receptor 4 and 6 heterodimer. *Nat Immunol* **11**: 155-161.

59. Weismann, D., and C. J. Binder. 2012. The innate immune response to products of phospholipid peroxidation. *Biochim Biophys Acta*: 10.1016/j.bbamem.2012.1001.1018.

60. de Villartay, J. P. 2009. V(D)J recombination deficiencies. *Adv Exp Med Biol* **650**: 46-58.

61. Hansson, G. K., and L. Jonasson. 2009. The discovery of cellular immunity in the atherosclerotic plaque. *Arterioscler Thromb Vasc Biol* **29**: 1714-1717.

62. Lu, X., D. Lu, U. Narayan, and V. V. Kakkar. 2011. The role of T-helper cells in atherosclerosis. *Cardiovasc Hematol Agents Med Chem* **9**: 25-41.

63. Stemme, S., B. Faber, J. Holm, O. Wiklund, J. L. Witztum, and G. K. Hansson. 1995. T lymphocytes from human atherosclerotic plaques recognize oxidized low density lipoprotein. *Proc Natl Acad Sci U S A* **92**: 3893-3897.

64. Binder, C. J., K. Hartvigsen, M. K. Chang, M. Miller, D. Broide, W. Palinski, L. K. Curtiss, M. Corr, and J. L. Witztum. 2004. IL-5 links adaptive and natural immunity specific for epitopes of oxidized LDL and protects from atherosclerosis. *J Clin Invest* **114**: 427-437.

65. Huber, S. A., P. Sakkinen, C. David, M. K. Newell, and R. P. Tracy. 2001. T helper-cell phenotype regulates atherosclerosis in mice under conditions of mild hypercholesterolemia. *Circulation* **103**: 2610-2616.

66. Eid, R. E., D. A. Rao, J. Zhou, S. F. Lo, H. Ranjbaran, A. Gallo, S. I. Sokol, S. Pfau, J. S. Pober, and G. Tellides. 2009. Interleukin-17 and interferon-gamma are produced concomitantly by human coronary artery-infiltrating T cells and act synergistically on vascular smooth muscle cells. *Circulation* **119**: 1424-1432.

67. Liu, Z., F. Lu, H. Pan, Y. Zhao, S. Wang, S. Sun, J. Li, X. Hu, and L. Wang. 2012. Correlation of peripheral Th17 cells and Th17-associated cytokines to the severity of carotid artery plaque and its clinical implication. *Atherosclerosis* **221**: 232-241.

68. Smith, E., K. M. Prasad, M. Butcher, A. Dobrian, J. K. Kolls, K. Ley, and E. Galkina. 2010. Blockade of interleukin-17A results in reduced atherosclerosis in apolipoprotein E-deficient mice. *Circulation* **121**: 1746-1755.

69. van Es, T., G. H. van Puijvelde, O. H. Ramos, F. M. Segers, L. A. Joosten, W. B. van den Berg, I. M. Michon, P. de Vos, T. J. van Berkel, and J. Kuiper. 2009. Attenuated atherosclerosis upon IL-17R signaling disruption in LDLr deficient mice. *Biochem Biophys Res Commun* **388**: 261-265.

70. Gao, Q., Y. Jiang, T. Ma, F. Zhu, F. Gao, P. Zhang, C. Guo, Q. Wang, X. Wang, C. Ma, Y. Zhang, W. Chen, and L. Zhang. 2010. A critical function of Th17 proinflammatory cells in the development of atherosclerotic plaque in mice. *J Immunol* **185**: 5820-5827.

71. Taleb, S., M. Romain, B. Ramkhelawon, C. Uyttenhove, G. Pasterkamp, O. Herbin, B. Esposito, N. Perez, H. Yasukawa, J. Van Snick, A. Yoshimura, A. Tedgui, and Z. Mallat. 2009. Loss of SOCS3 expression in T cells reveals a regulatory role for interleukin-17 in atherosclerosis. *J Exp Med* **206**: 2067-2077.

72. Butcher, M., and E. Galkina. 2011. Current views on the functions of interleukin-17A-producing cells in atherosclerosis. *Thromb Haemost* **106**: 787-795.

73. Usui, F., H. Kimura, T. Ohshiro, K. Tatsumi, A. Kawashima, A. Nishiyama, Y. Iwakura, S. Ishibashi, and M. Takahashi. 2012. Interleukin-17 deficiency reduced vascular inflammation and development of atherosclerosis in Western diet-induced apoE-deficient mice. *Biochem Biophys Res Commun* **420**: 72-77.

74. Ait-Oufella, H., B. L. Salomon, S. Potteaux, A. K. Robertson, P. Gourdy, J. Zoll, R. Merval, B. Esposito, J. L. Cohen, S. Fisson, R. A. Flavell, G. K. Hansson, D. Klatzmann, A. Tedgui, and Z. Mallat. 2006. Natural regulatory T cells control the development of atherosclerosis in mice. *Nat Med* **12**: 178-180.

75. van Es, T., G. H. van Puijvelde, A. C. Foks, K. L. Habets, I. Bot, E. Gilboa, T. J. Van Berkel, and J. Kuiper. 2010. Vaccination against Foxp3(+) regulatory T cells aggravates atherosclerosis. *Atherosclerosis* **209**: 74-80.

76. Mallat, Z., A. Gojova, V. Brun, B. Esposito, N. Fournier, F. Cottrez, A. Tedgui, and H. Groux. 2003. Induction of a regulatory T cell type 1 response reduces the

development of atherosclerosis in apolipoprotein E-knockout mice. *Circulation* **108**: 1232-1237.

77. Mor, A., D. Planer, G. Luboshits, A. Afek, S. Metzger, T. Chajek-Shaul, G. Keren, and J. George. 2007. Role of naturally occurring CD4+ CD25+ regulatory T cells in experimental atherosclerosis. *Arterioscler Thromb Vasc Biol* **27**: 893-900.

78. Robertson, A. K., M. Rudling, X. Zhou, L. Gorelik, R. A. Flavell, and G. K. Hansson. 2003. Disruption of TGF-beta signaling in T cells accelerates atherosclerosis. *J Clin Invest* **112**: 1342-1350.

79. Pinderski Oslund, L. J., C. C. Hedrick, T. Olvera, A. Hagenbaugh, M. Territo, J. A. Berliner, and A. I. Fyfe. 1999. Interleukin-10 blocks atherosclerotic events in vitro and in vivo. *Arterioscler Thromb Vasc Biol* **19**: 2847-2853.

80. Mallat, Z., A. Gojova, C. Marchiol-Fournigault, B. Esposito, C. Kamate, R. Merval, D. Fradelizi, and A. Tedgui. 2001. Inhibition of transforming growth factor-beta signaling accelerates atherosclerosis and induces an unstable plaque phenotype in mice. *Circ Res* **89**: 930-934.

81. Mallat, Z., S. Besnard, M. Duriez, V. Deleuze, F. Emmanuel, M. F. Bureau, F. Soubrier, B. Esposito, H. Duez, C. Fievet, B. Staels, N. Duverger, D. Scherman, and A. Tedgui. 1999. Protective role of interleukin-10 in atherosclerosis. *Circ Res* **85**: e17-24.

82. Veldhoen, M., C. Uyttenhove, J. van Snick, H. Helmby, A. Westendorf, J. Buer, B. Martin, C. Wilhelm, and B. Stockinger. 2008. Transforming growth factor-beta 'reprograms' the differentiation of T helper 2 cells and promotes an interleukin 9-producing subset. *Nat Immunol* **9**: 1341-1346.

83. King, C. 2009. New insights into the differentiation and function of T follicular helper cells. *Nat Rev Immunol* **9**: 757-766.

84. Doran, A. C., M. J. Lipinski, S. N. Oldham, J. C. Garmey, K. A. Campbell, M. D. Skaflen, A. Cutchins, D. J. Lee, D. K. Glover, K. A. Kelly, E. V. Galkina, K. Ley, J. L. Witztum, S. Tsimikas, T. P. Bender, and C. A. McNamara. 2012. B-cell aortic homing and atheroprotection depend on Id3. *Circ Res* **110**: e1-12.

85. Zhou, X., and G. K. Hansson. 1999. Detection of B cells and proinflammatory cytokines in atherosclerotic plaques of hypercholesterolaemic apolipoprotein E knockout mice. *Scand J Immunol* **50**: 25-30.

86. Aubry, M. C., D. L. Riehle, W. D. Edwards, H. Maradit-Kremers, V. L. Roger, T. J. Sebo, and S. E. Gabriel. 2004. B-Lymphocytes in plaque and adventitia of coronary arteries in two patients with rheumatoid arthritis and coronary atherosclerosis: preliminary observations. *Cardiovasc Pathol* **13**: 233-236.

87. Baumgarth, N. 2011. The double life of a B-1 cell: self-reactivity selects for protective effector functions. *Nat Rev Immunol* **11**: 34-46.

88. Gronwall, C., J. Vas, and G. J. Silverman. 2012. Protective Roles of Natural IgM Antibodies. *Front Immunol* **3**: 66.

89. Caligiuri, G., A. Nicoletti, B. Poirier, and G. K. Hansson. 2002. Protective immunity against atherosclerosis carried by B cells of hypercholesterolemic mice. *J Clin Invest* **109**: 745-753.

90. Major, A. S., S. Fazio, and M. F. Linton. 2002. B-lymphocyte deficiency increases atherosclerosis in LDL receptor-null mice. *Arterioscler Thromb Vasc Biol* **22**: 1892-1898.

91. Ait-Oufella, H., O. Herbin, J. D. Bouaziz, C. J. Binder, C. Uyttenhove, L. Laurans, S. Taleb, E. Van Vre, B. Esposito, J. Vilar, J. Sirvent, J. Van Snick, A. Tedgui, T. F. Tedder, and Z. Mallat. 2010. B cell depletion reduces the development of atherosclerosis in mice. *J Exp Med* **207**: 1579-1587.

92. Kyaw, T., C. Tay, A. Khan, V. Dumouchel, A. Cao, K. To, M. Kehry, R. Dunn, A. Agrotis, P. Tipping, A. Bobik, and B. H. Toh. 2010. Conventional B2 B cell depletion ameliorates whereas its adoptive transfer aggravates atherosclerosis. *J Immunol* **185**: 4410-4419.

93. Martin, F., and J. F. Kearney. 2001. B1 cells: similarities and differences with other B cell subsets. *Curr Opin Immunol* **13**: 195-201.

94. Kyaw, T., C. Tay, H. Hosseini, P. Kanellakis, T. Gadowski, F. MacKay, P. Tipping, A. Bobik, and B. H. Toh. 2012. Depletion of B2 but not B1a B cells in BAFF receptor-deficient ApoE mice attenuates atherosclerosis by potently ameliorating arterial inflammation. *PLoS One* **7**: e29371.

95. Sage, A. P., D. Tsiantoulas, L. Baker, J. Harrison, L. Masters, D. Murphy, C. Loinard, C. J. Binder, and Z. Mallat. 2012. BAFF Receptor Deficiency Reduces the Development of Atherosclerosis in Mice. *Arterioscler Thromb Vasc Biol*.

96. Kyaw, T., C. Tay, S. Krishnamurthi, P. Kanellakis, A. Agrotis, P. Tipping, A. Bobik, and B. H. Toh. 2011. B1a B lymphocytes are atheroprotective by secreting natural IgM that increases IgM deposits and reduces necrotic cores in atherosclerotic lesions. *Circ Res* **109**: 830-840.

97. Lewis, M. J., T. H. Malik, M. R. Ehrenstein, J. J. Boyle, M. Botto, and D. O. Haskard. 2009. Immunoglobulin M is required for protection against atherosclerosis in low-density lipoprotein receptor-deficient mice. *Circulation* **120**: 417-426.

98. Hansson, G. K., A. K. Robertson, and C. Söderberg-Nauclér. 2006. Inflammation and atherosclerosis. *Annu Rev Pathol.* **1**: 329.

99. Palinski, W., M. E. Rosenfeld, S. Yla-Herttuala, G. C. Gurtner, S. S. Socher, S. W. Butler, S. Parthasarathy, T. E. Carew, D. Steinberg, and J. L. Witztum. 1989. Low density lipoprotein undergoes oxidative modification in vivo. *Proc Natl Acad Sci U S A* **86**: 1372-1376.

100. Horkko, S., C. J. Binder, P. X. Shaw, M. K. Chang, G. Silverman, W. Palinski, and J. L. Witztum. 2000. Immunological responses to oxidized LDL. *Free Radic Biol Med* **28**: 1771-1779.

101. Esterbauer, H., R. J. Schaur, and H. Zollner. 1991. Chemistry and biochemistry of 4-hydroxynonenal, malonaldehyde and related aldehydes. *Free Radic Biol Med* **11**: 81-128.

102. Uchida, K., K. Sakai, K. Itakura, T. Osawa, and S. Toyokuni. 1997. Protein modification by lipid peroxidation products: formation of malondialdehyde-derived N(epsilon)-(2-propenol)lysine in proteins. *Arch Biochem Biophys* **346**: 45-52.

103. Itakura, K., and K. Uchida. 2001. Evidence that malondialdehyde-derived aminoenimine is not a fluorescent age pigment. *Chem Res Toxicol* **14**: 473-475.

104. Itakura, K., K. Uchida, and T. Osawa. 1996. A novel fluorescent malondialdehyde-lysine adduct. *Chem Phys Lipids* **84**: 75-79.

105. Tuma, D. J., G. M. Thiele, D. Xu, L. W. Klassen, and M. F. Sorrell. 1996. Acetaldehyde and malondialdehyde react together to generate distinct protein adducts in the liver during long-term ethanol administration. *Hepatology* **23**: 872-880.

106. Tuma, D. J., M. L. Kearley, G. M. Thiele, S. Worrall, A. Haver, L. W. Klassen, and M. F. Sorrell. 2001. Elucidation of reaction scheme describing malondialdehyde-acetaldehyde-protein adduct formation. *Chem Res Toxicol* **14**: 822-832.

107. Xu, D., G. M. Thiele, M. L. Kearley, M. D. Haugen, L. W. Klassen, M. F. Sorrell, and D. J. Tuma. 1997. Epitope characterization of malondialdehyde-acetaldehyde adducts using an enzyme-linked immunosorbent assay. *Chem Res Toxicol* **10**: 978-986.

108. Kearley, M. L., A. Patel, J. Chien, and D. J. Tuma. 1999. Observation of a new nonfluorescent malondialdehyde-acetaldehyde-protein adduct by 13C NMR spectroscopy. *Chem Res Toxicol* **12**: 100-105.

109. Tuma, D. J. 2002. Role of malondialdehyde-acetaldehyde adducts in liver injury. *Free Radic Biol Med* **32**: 303-308.

110. Duryee, M. J., L. W. Klassen, C. S. Schaffert, D. J. Tuma, C. D. Hunter, R. P. Garvin, D. R. Anderson, and G. M. Thiele. 2010. Malondialdehyde–acetaldehyde adduct is the dominant epitope after MDA modification of proteins in atherosclerosis. *Free Radical Biol. Med.* **49**: 1480-1486.

111. Thiele, G. M., M. J. Duryee, M. S. Willis, M. F. Sorrell, T. L. Freeman, D. J. Tuma, and L. W. Klassen. 2004. Malondialdehyde-acetaldehyde (MAA) modified proteins induce pro-inflammatory and pro-fibrotic responses by liver endothelial cells. *Comp Hepatol* **3 Suppl 1**: S25.

112. Yamada, S., S. Kumazawa, T. Ishii, T. Nakayama, K. Itakura, N. Shibata, M. Kobayashi, K. Sakai, T. Osawa, and K. Uchida. 2001. Immunochemical detection of a lipofuscin-like fluorophore derived from malondialdehyde and lysine. *J Lipid Res* **42**: 1187-1196.

113. Yla-Herttuala, S., W. Palinski, S. W. Butler, S. Picard, D. Steinberg, and J. L. Witztum. 1994. Rabbit and human atherosclerotic lesions contain IgG that recognizes epitopes of oxidized LDL. *Arterioscler Thromb* **14**: 32-40.

114. Yla-Herttuala, S., W. Palinski, M. E. Rosenfeld, S. Parthasarathy, T. E. Carew, S. Butler, J. L. Witztum, and D. Steinberg. 1989. Evidence for the presence of oxidatively modified low density lipoprotein in atherosclerotic lesions of rabbit and man. *J Clin Invest* **84**: 1086-1095.

115. Shaw, P. X., S. Horkko, M. K. Chang, L. K. Curtiss, W. Palinski, G. J. Silverman, and J. L. Witztum. 2000. Natural antibodies with the T15 idiotype may act in atherosclerosis, apoptotic clearance, and protective immunity. *J Clin Invest* **105**: 1731-1740.

116. Tsimikas, S., W. Palinski, and J. L. Witztum. 2001. Circulating autoantibodies to oxidized LDL correlate with arterial accumulation and depletion of oxidized LDL in LDL receptor-deficient mice. *Arterioscler Thromb Vasc Biol* **21**: 95-100.

117. Cyrus, T., D. Pratico, L. Zhao, J. L. Witztum, D. J. Rader, J. Rokach, G. A. FitzGerald, and C. D. Funk. 2001. Absence of 12/15-lipoxygenase expression decreases lipid peroxidation and atherogenesis in apolipoprotein e-deficient mice. *Circulation* **103**: 2277-2282.

118. Pratico, D., R. K. Tangirala, S. Horkko, J. L. Witztum, W. Palinski, and G. A. FitzGerald. 2001. Circulating autoantibodies to oxidized cardiolipin correlate with isoprostane F(2alpha)-VI levels and the extent of atherosclerosis in ApoE-deficient mice: modulation by vitamin E. *Blood* **97**: 459-464.

119. Puurunen, M., M. Manttari, V. Manninen, L. Tenkanen, G. Alfthan, C. Ehnholm, O. Vaarala, K. Aho, and T. Palosuo. 1994. Antibody against oxidized low-density lipoprotein predicting myocardial infarction. *Arch Intern Med* **154**: 2605-2609.

120. Dotevall, A., J. Hulthe, A. Rosengren, O. Wiklund, and L. Wilhelmsen. 2001. Autoantibodies against oxidized low-density lipoprotein and C-reactive protein are associated with diabetes and myocardial infarction in women. *Clin Sci (Lond)* **101**: 523-531.

121. Maggi, E., R. Chiesa, G. Melissano, R. Castellano, D. Astore, A. Grossi, G. Finardi, and G. Bellomo. 1994. LDL oxidation in patients with severe carotid atherosclerosis. A study of in vitro and in vivo oxidation markers. *Arterioscler Thromb* **14**: 1892-1899.

122. Fang, J. C., S. Kinlay, D. Behrendt, H. Hikita, J. L. Witztum, A. P. Selwyn, and P. Ganz. 2002. Circulating autoantibodies to oxidized LDL correlate with impaired coronary endothelial function after cardiac transplantation. *Arterioscler Thromb Vasc Biol* **22**: 2044-2048.

123. Hulthe, J. 2004. Antibodies to oxidized LDL in atherosclerosis development--clinical and animal studies. *Clin Chim Acta* **348**: 1-8.

124. Salonen, J. T., S. Yla-Herttuala, R. Yamamoto, S. Butler, H. Korpela, R. Salonen, K. Nyyssonen, W. Palinski, and J. L. Witztum. 1992. Autoantibody against oxidised LDL and progression of carotid atherosclerosis. *Lancet* **339**: 883-887.

125. Hulthe, J., O. Wiklund, E. Hurt-Camejo, and G. Bondjers. 2001. Antibodies to oxidized LDL in relation to carotid atherosclerosis, cell adhesion molecules, and phospholipase A(2). *Arterioscler Thromb Vasc Biol.* **21**: 269-274.

126. van de Vijver, L. P., R. Steyger, G. van Poppel, J. M. Boer, D. A. Kruijssen, J. C. Seidell, and H. M. Princen. 1996. Autoantibodies against MDA-LDL in subjects with severe and minor atherosclerosis and healthy population controls. *Atherosclerosis* **122**: 245-253.

127. Ahmed, E., J. Trifunovic, B. Stegmayr, G. Hallmans, and A. K. Lefvert. 1999. Autoantibodies against oxidatively modified LDL do not constitute a risk factor for stroke: a nested case-control study. *Stroke* **30**: 2541-2546.

128. Tsimikas, S., E. S. Brilakis, R. J. Lennon, E. R. Miller, J. L. Witztum, J. P. McConnell, K. S. Kornman, and P. B. Berger. 2007. Relationship of IgG and IgM autoantibodies to oxidized low density lipoprotein with coronary artery disease and cardiovascular events. *J Lipid Res* **48**: 425-433.

129. Gounopoulos, P., E. Merki, L. F. Hansen, S. H. Choi, and S. Tsimikas. 2007. Antibodies to oxidized low density lipoprotein: epidemiological studies and potential clinical applications in cardiovascular disease. *Minerva Cardioangiol* **55**: 821-837.

130. Lopes-Virella, M. F., and G. Virella. 2010. Clinical significance of the humoral immune response to modified LDL. *Clin Immunol* **134**: 55-65.

131. Ravandi, A., S. M. Boekholdt, Z. Mallat, P. J. Talmud, J. J. Kastelein, N. J. Wareham, E. R. Miller, J. Benessiano, A. Tedgui, J. L. Witztum, K. T. Khaw, and S. Tsimikas. 2011. Relationship of IgG and IgM autoantibodies and immune complexes to oxidized LDL with markers of oxidation and inflammation and cardiovascular events: results from the EPIC-Norfolk Study. *J Lipid Res* **52**: 1829-1836.

132. Tsimikas, S. 2006. Oxidative biomarkers in the diagnosis and prognosis of cardiovascular disease. *Am J Cardiol* **98**: 9P-17P.

133. Binder, C. J., S. Horkko, A. Dewan, M. K. Chang, E. P. Kieu, C. S. Goodyear, P. X. Shaw, W. Palinski, J. L. Witztum, and G. J. Silverman. 2003. Pneumococcal vaccination decreases atherosclerotic lesion formation: molecular mimicry between Streptococcus pneumoniae and oxidized LDL. *Nat Med* **9**: 736-743.

134. Inoue, T., T. Uchida, H. Kamishirado, K. Takayanagi, T. Hayashi, and S. Morooka. 2001. Clinical significance of antibody against oxidized low density lipoprotein in patients with atherosclerotic coronary artery disease. *J Am Coll Cardiol* **37**: 775-779.

135. Hulthe, J., L. Bokemark, and B. Fagerberg. 2001. Antibodies to oxidized LDL in relation to intima-media thickness in carotid and femoral arteries in 58-year-old subjectively clinically healthy men. *Arterioscler Thromb Vasc Biol.* **21**: 101-107.

136. Karvonen, J., M. Paivansalo, Y. A. Kesaniemi, and S. Horkko. 2003. Immunoglobulin M type of autoantibodies to oxidized low-density lipoprotein has an inverse relation to carotid artery atherosclerosis. *Circulation* **108**: 2107-2112.

137. Meraviglia, M. V., E. Maggi, G. Bellomo, M. Cursi, G. Fanelli, and F. Minicucci. 2002. Autoantibodies against oxidatively modified lipoproteins and progression of carotid restenosis after carotid endarterectomy. *Stroke* **33**: 1139-1141.

138. Baumgarth, N., J. W. Tung, and L. A. Herzenberg. 2005. Inherent specificities in natural antibodies: a key to immune defense against pathogen invasion. *Springer Semin Immunopathol* **26**: 347-362.

139. Lutz, H. U., C. J. Binder, and S. Kaveri. 2009. Naturally occurring auto-antibodies in homeostasis and disease. *Trends Immunol* **30**: 43-51.

140. Chou, M. Y., L. Fogelstrand, K. Hartvigsen, L. F. Hansen, D. Woelkers, P. X. Shaw, J. Choi, T. Perkmann, F. Backhed, Y. I. Miller, S. Horkko, M. Corr, J. L. Witztum, and C. J. Binder. 2009. Oxidation-specific epitopes are dominant targets of innate natural antibodies in mice and humans. *J Clin Invest* **119**: 1335-1349.

141. Palinski, W., S. Horkko, E. Miller, U. P. Steinbrecher, H. C. Powell, L. K. Curtiss, and J. L. Witztum. 1996. Cloning of monoclonal autoantibodies to epitopes of oxidized lipoproteins from apolipoprotein E-deficient mice. Demonstration of epitopes of oxidized low density lipoprotein in human plasma. *J Clin Invest* **98**: 800-814.

142. Horkko, S., D. A. Bird, E. Miller, H. Itabe, N. Leitinger, G. Subbanagounder, J. A. Berliner, P. Friedman, E. A. Dennis, L. K. Curtiss, W. Palinski, and J. L. Witztum. 1999. Monoclonal autoantibodies specific for oxidized phospholipids or oxidized phospholipid-protein adducts inhibit macrophage uptake of oxidized low-density lipoproteins. *J Clin Invest* **103**: 117-128.

143. Chang, M. K., C. Bergmark, A. Laurila, S. Horkko, K. H. Han, P. Friedman, E. A. Dennis, and J. L. Witztum. 1999. Monoclonal antibodies against oxidized low-density lipoprotein bind to apoptotic cells and inhibit their phagocytosis by elicited macrophages: evidence that oxidation-specific epitopes mediate macrophage recognition. *Proc Natl Acad Sci U S A* **96**: 6353-6358.

144. Karsten, H., M. Y. Chou, L. F. Hansen, A. Gonen, E. N. Montano, X. Que, C. J. Binder, and J. L. Witztum. 2009. Anti-inflammatory and Antiatherogenic Properties of 5 Monoclonal Malondialdehyde-Modified LDL-Specific IgM. *Arterioscler Thromb Vasc Biol. 2009 Annual Conference, Washington DC,* **29**: e9-e130.

145. Amir, S., K. Hartvigsen, A. Gonen, G. Leibundgut, X. Que, E. Jensen-Jarolim, O. Wagner, S. Tsimikas, J. L. Witztum, and C. J. Binder. 2012. Peptide mimotopes of malondialdehyde epitopes for clinical applications in cardiovascular disease. *J Lipid Res* **53**: 1316-1326.

146. Zwart, B., C. Ciurana, I. Rensink, R. Manoe, C. Erik Hack, and L. A. Aarden. 2004. Complement Activation by Apoptotic Cells Occurs Predominantly via IgM and is Limited to Late Apoptotic (Secondary Necrotic) Cells. *Autoimmunity* **37**: 95-102.

147. Quartier, P., P. K. Potter, M. R. Ehrenstein, M. J. Walport, and M. Botto. 2005. Predominant role of IgM-dependent activation of the classical pathway in the clearance of dying cells by murine bone marrow-derived macrophages in vitro. *Eur J Immunol* **35**: 252-260.

148. Chen, Y., Y. B. Park, E. Patel, and G. J. Silverman. 2009. IgM antibodies to apoptosis-associated determinants recruit C1q and enhance dendritic cell phagocytosis of apoptotic cells. *J Immunol* **182**: 6031-6043.

149. Ogden, C. A., R. Kowalewski, Y. Peng, V. Montenegro, and K. B. Elkon. 2005. IGM is required for efficient complement mediated phagocytosis of apoptotic cells in vivo. *Autoimmunity* **38**: 259-264.

150. Notley, C. A., M. A. Brown, G. P. Wright, and M. R. Ehrenstein. 2011. Natural IgM is required for suppression of inflammatory arthritis by apoptotic cells. *J Immunol* **186**: 4967-4972.

151. de Jager, S. C., and J. Kuiper. 2011. Vaccination strategies in atherosclerosis. *Thromb Haemost* **106**: 796-803.

152. Chyu, K. Y., J. Nilsson, and P. K. Shah. 2011. Immune mechanisms in atherosclerosis and potential for an atherosclerosis vaccine. *Discovery medicine* **11**: 403-412.

153. Palinski, W., E. Miller, and J. L. Witztum. 1995. Immunization of low density lipoprotein (LDL) receptor-deficient rabbits with homologous malondialdehyde-modified LDL reduces atherogenesis. *Proc Natl Acad Sci U S A* **92**: 821-825.

154. Ameli, S., A. Hultgardh-Nilsson, J. Regnstrom, F. Calara, J. Yano, B. Cercek, P. K. Shah, and J. Nilsson. 1996. Effect of immunization with homologous LDL and oxidized LDL on early atherosclerosis in hypercholesterolemic rabbits. *Arterioscler Thromb Vasc Biol* **16**: 1074-1079.

155. George J, Afek A, Gilburd B, Levkovitz H, Shaish A, Goldberg I, Kopolovic Y, Wick G, Shoenfeld Y, and H. D. 1998. Hyperimmunization of apo-E-deficient mice with homologous malondialdehyde low-density lipoprotein suppresses early atherogenesis. *Atherosclerosis* **138**: 147-152.

156. Freigang, S., S. Horkko, E. Miller, J. L. Witztum, and W. Palinski. 1998. Immunization of LDL receptor-deficient mice with homologous malondialdehyde-modified and native LDL reduces progression of atherosclerosis by mechanisms other than induction of high titers of antibodies to oxidative neoepitopes. *Arterioscler Thromb Vasc Biol* **18**: 1972-1982.

157. Zhou, X., G. Caligiuri, A. Hamsten, A. K. Lefvert, and G. K. Hansson. 2001. LDL immunization induces T-cell-dependent antibody formation and protection against atherosclerosis. *Arterioscler Thromb Vasc Biol* **21**: 108-114.

158. Zhou, X., A. K. Robertson, M. Rudling, P. Parini, and G. K. Hansson. 2005. Lesion development and response to immunization reveal a complex role for CD4 in atherosclerosis. *Circ Res* **96**: 427-434.

159. Virella, G., and M. F. Lopes-Virella. 2008. Atherogenesis and the humoral immune response to modified lipoproteins. *Atherosclerosis* **200**: 239-246.

160. Schiopu, A., J. Bengtsson, I. Söderberg, S. Janciauskiene, S. Lindgren, M. P. Ares, P. K. Shah, R. Carlsson, J. Nilsson, and G. N. Fredrikson. 2004. Recombinant human antibodies against aldehyde-modified apolipoprotein B-100 peptide sequences inhibit atherosclerosis. *Circulation.* **110**: 2047-2052.

161. Schiopu, A., B. Frendéus, B. Jansson, I. Söderberg, I. Ljungcrantz, Z. Araya, P. K. Shah, R. Carlsson, J. Nilsson, and G. N. Fredrikson. 2007. Recombinant antibodies to an oxidized low-density lipoprotein epitope induce rapid regression of atherosclerosis in apobec-1(-/-)/low-density lipoprotein receptor(-/-) mice. *J. Am. Coll. Cardiol.* **50**: 2313-2318.

162. Goncalves, I., M. Nitulescu, M. P. Ares, G. N. Fredrikson, B. Jansson, Z. C. Li, and J. Nilsson. 2009. Identification of the target for therapeutic recombinant anti-apoB-100 peptide antibodies in human atherosclerotic lesions. *Atherosclerosis* **205**: 96-100.

163. Tsimikas, S., A. Miyanohara, K. Hartvigsen, E. Merki, P. X. Shaw, M. Y. Chou, J. Pattison, M. Torzewski, J. Sollors, T. Friedmann, N. C. Lai, H. K. Hammond, G. S. Getz, C. A. Reardon, A. C. Li, C. L. Banka, and J. L. Witztum. 2011. Human oxidation-specific antibodies reduce foam cell formation and atherosclerosis progression. *J Am Coll Cardiol* **58**: 1715-1727.

164. Palinski, W., S. Yla-Herttuala, M. E. Rosenfeld, S. W. Butler, S. A. Socher, S. Parthasarathy, L. K. Curtiss, and J. L. Witztum. 1990. Antisera and monoclonal antibodies specific for epitopes generated during oxidative modification of low density lipoprotein. *Arteriosclerosis* **10**: 325-335.

165. Tuominen, A., Y. I. Miller, L. F. Hansen, Y. A. Kesaniemi, J. L. Witztum, and S. Horkko. 2006. A natural antibody to oxidized cardiolipin binds to oxidized low-density lipoprotein, apoptotic cells, and atherosclerotic lesions. *Arterioscler Thromb Vasc Biol* **26**: 2096-2102.

166. Shaw, P. X., S. Horkko, S. Tsimikas, M. K. Chang, W. Palinski, G. J. Silverman, P. P. Chen, and J. L. Witztum. 2001. Human-derived anti-oxidized LDL autoantibody blocks uptake of oxidized LDL by macrophages and localizes to atherosclerotic lesions in vivo. *Arterioscler Thromb Vasc Biol* **21**: 1333-1339.

167. Perschinka, H., B. Wellenzohn, W. Parson, R. van der Zee, J. Willeit, S. Kiechl, and G. Wick. 2007. Identification of atherosclerosis-associated conformational heat shock protein 60 epitopes by phage display and structural alignment. *Atherosclerosis* **194**: 79-87.

168. Petit, M. A., C. Jolivet-Reynaud, E. Peronnet, Y. Michal, and C. Trepo. 2003. Mapping of a conformational epitope shared between E1 and E2 on the serum-derived human hepatitis C virus envelope. *J Biol Chem* **278**: 44385-44392.

169. Tsimikas, S., H. K. Lau, K. R. Han, B. Shortal, E. R. Miller, A. Segev, L. K. Curtiss, J. L. Witztum, and B. H. Strauss. 2004. Percutaneous coronary intervention results in acute increases in oxidized phospholipids and lipoprotein(a): short-term and long-term

immunologic responses to oxidized low-density lipoprotein. *Circulation* **109**: 3164-3170.

170. Friguet, B., A. F. Chaffotte, L. Djavadi-Ohaniance, and M. E. Goldberg. 1985. Measurements of the true affinity constant in solution of antigen-antibody complexes by enzyme-linked immunosorbent assay. *J Immunol Methods* **77**: 305-319.

171. Faghihnia, N., S. Tsimikas, E. R. Miller, J. L. Witztum, and R. M. Krauss. 2010. Changes in lipoprotein(a), oxidized phospholipids, and LDL subclasses with a low-fat high-carbohydrate diet. *J Lipid Res* **51**: 3324-3330.

172. Tsimikas, S., C. Bergmark, R. W. Beyer, R. Patel, J. Pattison, E. Miller, J. Juliano, and J. L. Witztum. 2003. Temporal increases in plasma markers of oxidized low-density lipoprotein strongly reflect the presence of acute coronary syndromes. *J Am Coll Cardiol* **41**: 360-370.

173. Shin, J. S., J. Yu, J. Lin, L. Zhong, K. L. Bren, and M. H. Nahm. 2002. Peptide mimotopes of pneumococcal capsular polysaccharide of 6B serotype: a peptide mimotope can bind to two unrelated antibodies. *J Immunol* **168**: 6273-6278.

174. Dyson, H. J., and P. E. Wright. 1991. Defining solution conformations of small linear peptides. *Annu Rev Biophys Biophys Chem* **20**: 519-538.

175. Haro, I., and M. J. Gomara. 2004. Design of synthetic peptidic constructs for the vaccine development against viral infections. *Curr Protein Pept Sci* **5**: 425-433.

176. Chang, M. K., C. J. Binder, Y. I. Miller, G. Subbanagounder, G. J. Silverman, J. A. Berliner, and J. L. Witztum. 2004. Apoptotic cells with oxidation-specific epitopes are immunogenic and proinflammatory. *J Exp Med* **200**: 1359-1370.

177. Buchwald, U. K., A. Lees, M. Steinitz, and L. A. Pirofski. 2005. A peptide mimotope of type 8 pneumococcal capsular polysaccharide induces a protective immune response in mice. *Infect Immun* **73**: 325-333.

178. Harris, S. L., A. S. Dagtas, and B. Diamond. 2002. Regulating the isotypic and idiotypic profile of an anti-PC antibody response: lessons from peptide mimics. *Mol Immunol* **39**: 263-272.

179. Monzavi-Karbassi, B., G. Cunto-Amesty, P. Luo, and T. Kieber-Emmons. 2002. Peptide mimotopes as surrogate antigens of carbohydrates in vaccine discovery. *Trends Biotechnol* **20**: 207-214.

180. Latzka, J., S. Gaier, G. Hofstetter, N. Balazs, U. Smole, S. Ferrone, O. Scheiner, H. Breiteneder, H. Pehamberger, and S. Wagner. 2011. Specificity of Mimotope-Induced Anti-High Molecular Weight-Melanoma Associated Antigen (HMW-MAA) Antibodies Does Not Ensure Biological Activity. *PLoS One* **6**: e19383.

181. Hafner, C., S. Wagner, D. Allwardt, A. B. Riemer, O. Scheiner, H. Pehamberger, and H. Breiteneder. 2005. Cross-reactivity of mimotopes with a monoclonal antibody against the high molecular weight melanoma-associated antigen (HMW-MAA) does not predict cross-reactive immunogenicity. *Melanoma Res* **15**: 111-117.

182. Youn, J. H., H. J. Myung, A. Liav, D. Chatterjee, P. J. Brennan, I. H. Choi, S. N. Cho, and J. S. Shin. 2004. Production and characterization of peptide mimotopes of phenolic glycolipid-I of Mycobacterium leprae. *FEMS Immunol Med Microbiol* **41**: 51-57.

183. Valadon, P., G. Nussbaum, J. Oh, and M. D. Scharff. 1998. Aspects of antigen mimicry revealed by immunization with a peptide mimetic of Cryptococcus neoformans polysaccharide. *J Immunol* **161**: 1829-1836.

184. El Kasmi, K. C., S. Deroo, D. M. Theisen, N. H. Brons, and C. P. Muller. 1999. Crossreactivity of mimotopes and peptide homologues of a sequential epitope with a monoclonal antibody does not predict crossreactive immunogenicity. *Vaccine* **18**: 284-290.

185. Beenhouwer, D. O., R. J. May, P. Valadon, and M. D. Scharff. 2002. High affinity mimotope of the polysaccharide capsule of Cryptococcus neoformans identified from an evolutionary phage peptide library. *J Immunol* **169**: 6992-6999.

186. Hudecz, F. 2001. Manipulation of epitope function by modification of peptide structure: a minireview. *Biologicals* **29**: 197-207.

187. Manca, F., J. A. Habeshaw, A. G. Dalgleish, D. Fenoglio, G. Li Pira, and E. E. Sercarz. 1993. Role of flanking variable sequences in antigenicity of consensus regions of HIV gp120 for recognition by specific human T helper clones. *Eur J Immunol* **23**: 269-274.

188. Stittelaar, K. J., P. Hoogerhout, W. Ovaa, R. R. van Binnendijk, M. C. Poelen, P. Roholl, C. A. van Els, A. D. Osterhaus, and E. J. Wiertz. 2001. In vitro processing and presentation of a lipidated cytotoxic T-cell epitope derived from measles virus fusion protein. *Vaccine* **20**: 249-261.

189. Gonzalez, S., E. Caballero, R. Silva, and R. Pajon. 2001. Effect of P64k presensitization on its efficacy as an immunological carrier in mice. *Biochem Biophys Res Commun* **282**: 376-379.

190. Herzenberg, L. A., and T. Tokuhisa. 1980. Carrier-priming leads to hapten-specific suppression. *Nature* **285**: 664-667.

191. Jegerlehner, A., M. Wiesel, K. Dietmeier, F. Zabel, D. Gatto, P. Saudan, and M. F. Bachmann. 2010. Carrier induced epitopic suppression of antibody responses induced by virus-like particles is a dynamic phenomenon caused by carrier-specific antibodies. *Vaccine* **28**: 5503-5512.

192. Renjifo, X., S. Wolf, P. P. Pastoret, H. Bazin, J. Urbain, O. Leo, and M. Moser. 1998. Carrier-induced, hapten-specific suppression: a problem of antigen presentation? *J Immunol* **161**: 702-706.

193. Schutze, M. P., E. Deriaud, G. Przewlocki, and C. LeClerc. 1989. Carrier-induced epitopic suppression is initiated through clonal dominance. *J Immunol* **142**: 2635-2640.

194. Schutze, M. P., C. Leclerc, M. Jolivet, F. Audibert, and L. Chedid. 1985. Carrier-induced epitopic suppression, a major issue for future synthetic vaccines. *J Immunol* **135**: 2319-2322.

195. Brunner, R., E. Jensen-Jarolim, and I. Pali-Scholl. 2010. The ABC of clinical and experimental adjuvants--a brief overview. *Immunol Lett* **128**: 29-35.

196. Briley-Saebo, K. C., Y. S. Cho, and S. Tsimikas. 2011. Imaging of oxidation-specific epitopes in atherosclerosis and macrophage-rich vulnerable plaques. *Curr Cardiovasc Imaging Rep* **4**: 4-16.

197. Cwirla, S. E., P. Balasubramanian, D. J. Duffin, C. R. Wagstrom, C. M. Gates, S. C. Singer, A. M. Davis, R. L. Tansik, L. C. Mattheakis, C. M. Boytos, P. J. Schatz, D. P. Baccanari, N. C. Wrighton, R. W. Barrett, and W. J. Dower. 1997. Peptide Agonist of the Thrombopoietin Receptor as Potent as the Natural Cytokine. *Science* **276**: 1696-1699.

198. Wrighton, N. C., F. X. Farrell, R. Chang, A. K. Kashyap, F. P. Barbone, L. S. Mulcahy, D. L. Johnson, R. W. Barrett, L. K. Jolliffe, and W. J. Dower. 1996. Small peptides as potent mimetics of the protein hormone erythropoietin. *Science* **273**: 458-464.

199. Schooltink, H., and S. Rose-John. 2005. Designing cytokine variants by phage-display. *Comb Chem High Throughput Screen* **8**: 173-179.

200. Molek, P., B. Strukelj, and T. Bratkovic. 2011. Peptide phage display as a tool for drug discovery: targeting membrane receptors. *Molecules* **16**: 857-887.

201. Rodi, D. J., R. W. Janes, H. J. Sanganee, R. A. Holton, B. A. Wallace, and L. Makowski. 1999. Screening of a library of phage-displayed peptides identifies human bcl-2 as a taxol-binding protein. *J Mol Biol* **285**: 197-203.

202. Segers, F. M., H. Yu, T. J. Molenaar, P. Prince, T. Tanaka, T. J. van Berkel, and E. A. Biessen. 2012. Design and validation of a specific scavenger receptor class AI binding peptide for targeting the inflammatory atherosclerotic plaque. *Arterioscler Thromb Vasc Biol* **32**: 971-978.

203. Wagner, S., C. Hafner, D. Allwardt, J. Jasinska, S. Ferrone, C. C. Zielinski, O. Scheiner, U. Wiedermann, H. Pehamberger, and H. Breiteneder. 2005. Vaccination with a human high molecular weight melanoma-associated antigen mimotope induces a humoral response inhibiting melanoma cell growth in vitro. *J Immunol* **174**: 976-982.

204. Jiang, B., W. Liu, H. Qu, L. Meng, S. Song, T. Ouyang, and C. Shou. 2005. A novel peptide isolated from a phage display peptide library with trastuzumab can mimic antigen epitope of HER-2. *J Biol Chem* **280**: 4656-4662.

205. Zhou, B., P. Wirsching, and K. D. Janda. 2002. Human antibodies against spores of the genus Bacillus: a model study for detection of and protection against anthrax and the bioterrorist threat. *Proc Natl Acad Sci U S A* **99**: 5241-5246.

206. De Berardinis, P., and N. L. Haigwood. 2004. New recombinant vaccines based on the use of prokaryotic antigen-display systems. *Expert Rev Vaccines* **3**: 673-679.

207. Jensen-Jarolim, E., and J. Singer. 2011. Cancer vaccines inducing antibody production: more pros than cons. *Expert Rev Vaccines* **10**: 1281-1289.

208. Wu, Y., Q. Zhang, D. Sales, A. E. Bianco, and A. Craig. 2010. Vaccination with peptide mimotopes produces antibodies recognizing bacterial capsular polysaccharides. *Vaccine* **28**: 6425-6435.

209. Zhou, M., I. Kostoula, B. Brill, E. Panou, M. Sakarellos-Daitsiotis, and U. Dietrich. 2012. Prime boost vaccination approaches with different conjugates of a new HIV-1 gp41 epitope encompassing the membrane proximal external region induce neutralizing antibodies in mice. *Vaccine* **30**: 1911-1916.

210. Riemer, A. B., M. Klinger, S. Wagner, A. Bernhaus, L. Mazzucchelli, H. Pehamberger, O. Scheiner, C. C. Zielinski, and E. Jensen-Jarolim. 2004. Generation of Peptide mimics of the epitope recognized by trastuzumab on the oncogenic protein Her-2/neu. *J Immunol* **173**: 394-401.

211. Hartmann, C., N. Muller, A. Blaukat, J. Koch, I. Benhar, and W. S. Wels. 2010. Peptide mimotopes recognized by antibodies cetuximab and matuzumab induce a functionally equivalent anti-EGFR immune response. *Oncogene* **29**: 4517-4527.

212. Wierzbicki, A., M. Gil, M. Ciesielski, R. A. Fenstermaker, Y. Kaneko, H. Rokita, J. T. Lau, and D. Kozbor. 2008. Immunization with a mimotope of GD2 ganglioside induces CD8+ T cells that recognize cell adhesion molecules on tumor cells. *J Immunol* **181**: 6644-6653.

213. Hafner, C., S. Wagner, J. Jasinska, D. Allwardt, O. Scheiner, K. Wolff, H. Pehamberger, U. Wiedermann, and H. Breiteneder. 2005. Epitope-specific antibody response to Mel-CAM induced by mimotope immunization. *J Invest Dermatol* **124**: 125-131.

214. Sergeeva, A., M. G. Kolonin, J. J. Molldrem, R. Pasqualini, and W. Arap. 2006. Display technologies: application for the discovery of drug and gene delivery agents. *Adv Drug Deliv Rev* **58**: 1622-1654.

215. Tong, A. H., B. Drees, G. Nardelli, G. D. Bader, B. Brannetti, L. Castagnoli, M. Evangelista, S. Ferracuti, B. Nelson, S. Paoluzi, M. Quondam, A. Zucconi, C. W. Hogue, S. Fields, C. Boone, and G. Cesareni. 2002. A combined experimental and computational strategy to define protein interaction networks for peptide recognition modules. *Science* **295**: 321-324.

216. Laura, R. P., A. S. Witt, H. A. Held, R. Gerstner, K. Deshayes, M. F. Koehler, K. S. Kosik, S. S. Sidhu, and L. A. Lasky. 2002. The Erbin PDZ domain binds with high affinity and specificity to the carboxyl termini of delta-catenin and ARVCF. *J Biol Chem* **277**: 12906-12914.

217. Landgraf, C., S. Panni, L. Montecchi-Palazzi, L. Castagnoli, J. Schneider-Mergener, R. Volkmer-Engert, and G. Cesareni. 2004. Protein interaction networks by proteome peptide scanning. *PLoS Biol* **2**: E14.

218. Abram, C. L., D. F. Seals, I. Pass, D. Salinsky, L. Maurer, T. M. Roth, and S. A. Courtneidge. 2003. The adaptor protein fish associates with members of the ADAMs family and localizes to podosomes of Src-transformed cells. *J Biol Chem* **278**: 16844-16851.

219. Beckmann, C., J. D. Waggoner, T. O. Harris, G. S. Tamura, and C. E. Rubens. 2002. Identification of novel adhesins from Group B streptococci by use of phage display reveals that C5a peptidase mediates fibronectin binding. *Infect Immun* **70**: 2869-2876.

220. Heilmann, C., M. Herrmann, B. E. Kehrel, and G. Peters. 2002. Platelet-binding domains in 2 fibrinogen-binding proteins of Staphylococcus aureus identified by phage display. *J Infect Dis* **186**: 32-39.

221. Sidhu, S. S., W. J. Fairbrother, and K. Deshayes. 2003. Exploring protein-protein interactions with phage display. *Chembiochem* **4**: 14-25.

222. Hertveldt, K., T. Belien, and G. Volckaert. 2009. General M13 phage display: M13 phage display in identification and characterization of protein-protein interactions. *Methods Mol Biol* **502**: 321-339.

223. Rowley, M. J., K. O'Connor, and L. Wijeyewickrema. 2004. Phage display for epitope determination: a paradigm for identifying receptor-ligand interactions. *Biotechnol Annu Rev* **10**: 151-188.

224. Pande, J., M. M. Szewczyk, and A. K. Grover. 2010. Phage display: concept, innovations, applications and future. *Biotechnol Adv* **28**: 849-858.

225. Montigiani, S., R. Muller, and R. E. Kontermann. 2003. Inhibition of cell proliferation and induction of apoptosis by novel tetravalent peptides inhibiting DNA binding of E2F. *Oncogene* **22**: 4943-4952.

226. Sedlacek, R., and E. Chen. 2005. Screening for protease substrate by polyvalent phage display. *Comb Chem High Throughput Screen* **8**: 197-203.

227. Kay, B. K., and P. T. Hamilton. 2001. Identification of enzyme inhibitors from phage-displayed combinatorial peptide libraries. *Comb Chem High Throughput Screen* **4**: 535-543.

228. Smith, G. P. 1985. Filamentous fusion phage: novel expression vectors that display cloned antigens on the virion surface. *Science* **228**: 1315-1317.

229. Burritt, J. B., C. W. Bond, K. W. Doss, and A. J. Jesaitis. 1996. Filamentous phage display of oligopeptide libraries. *Anal Biochem* **238**: 1-13.

230. Rodi, D. J., and L. Makowski. 1999. Phage-display technology--finding a needle in a vast molecular haystack. *Curr. Opin. Biotec.* **10**: 87-93.

231. Parmley, S. F., and G. P. Smith. 1988. Antibody-selectable filamentous fd phage vectors: affinity purification of target genes. *Gene* **73**: 305-318.

232. Smith, G. P., and J. K. Scott. 1993. Libraries of peptides and proteins displayed on filamentous phage. *Methods Enzymol* **217**: 228-257.

233. Cabilly, S. 1998. The basic structure of filamentous phage and its use in the display of combinatorial peptide libraries. *Methods Mol Biol* **87**: 129-136.

234. Smith, G. P. 1988. Filamentous phages as cloning vectors. *Biotechnology* **10**: 61-83.

235. Gram, H., L. A. Marconi, C. F. Barbas, T. A. Collet, R. A. Lerner, and A. S. Kang. 1992. In vitro selection and affinity maturation of antibodies from a naive combinatorial immunoglobulin library. *Proc Natl Acad Sci U S A* **89**: 3576-3580.

236. Geysen, H. M., S. J. Rodda, and T. J. Mason. 1986. A priori delineation of a peptide which mimics a discontinuous antigenic determinant. *Mol Immunol* **23**: 709-715.

237. Yip, Y. L., and R. L. Ward. 1999. Epitope discovery using monoclonal antibodies and phage peptide libraries. *Combinatorial chemistry & high throughput screening* **2**: 125-138.

238. Scott, J. K., and G. P. Smith. 1990. Searching for peptide ligands with an epitope library. *Science* **249**: 386-390.

239. Stephen, C. W., and D. P. Lane. 1992. Mutant conformation of p53. Precise epitope mapping using a filamentous phage epitope library. *J Mol Biol* **225**: 577-583.

240. Amit, A. G., R. A. Mariuzza, S. E. Phillips, and R. J. Poljak. 1986. Three-dimensional structure of an antigen-antibody complex at 2.8 A resolution. *Science* **233**: 747-753.

241. Kay, B. K., A. V. Kurakin, and R. Hyde-DeRuyscher. 1998. From peptides to drugs via phage display. *Drug Discov Today* **3**: 370-378.

242. Sun, Y., K. Y. Fong, M. C. Chung, and Z. J. Yao. 2001. Peptide mimicking antigenic and immunogenic epitope of double-stranded DNA in systemic lupus erythematosus. *Int Immunol* **13**: 223-232.

243. Wun, H. L., D. T. Leung, K. C. Wong, Y. L. Chui, and P. L. Lim. 2001. Molecular mimicry: anti-DNA antibodies may arise inadvertently as a response to antibodies generated to microorganisms. *Int Immunol* **13**: 1099-1107.

244. Knittelfelder, R., A. B. Riemer, and E. Jensen-Jarolim. 2009. Mimotope vaccination--from allergy to cancer. *Expert Opin Biol Ther* **9**: 493-506.

245. Denisova, G. F., D. A. Denisov, and J. L. Bramson. 2010. Applying bioinformatics for antibody epitope prediction using affinity-selected mimotopes - relevance for vaccine design. *Immunome Res* **6 Suppl 2**: S6.

246. Negi, S. S., and W. Braun. 2009. Automated detection of conformational epitopes using phage display Peptide sequences. *Bioinform Biol Insights* **3**: 71-81.

247. Huang, Y. X., Y. L. Bao, S. Y. Guo, Y. Wang, C. G. Zhou, and Y. X. Li. 2008. Pep-3D-Search: a method for B-cell epitope prediction based on mimotope analysis. *BMC Bioinformatics* **9**: 538.

248. Schreiber, A., M. Humbert, A. Benz, and U. Dietrich. 2005. 3D-Epitope-Explorer (3DEX): localization of conformational epitopes within three-dimensional structures of proteins. *J Comput Chem* **26**: 879-887.

249. Halperin, I., H. Wolfson, and R. Nussinov. 2003. SiteLight: binding-site prediction using phage display libraries. *Protein Sci* **12**: 1344-1359.

250. Enshell-Seijffers, D., D. Denisov, B. Groisman, L. Smelyanski, R. Meyuhas, G. Gross, G. Denisova, and J. M. Gershoni. 2003. The mapping and reconstitution of a conformational discontinuous B-cell epitope of HIV-1. *J Mol Biol* **334**: 87-101.

251. Huang, J., A. Gutteridge, W. Honda, and M. Kanehisa. 2006. MIMOX: a web tool for phage display based epitope mapping. *BMC Bioinformatics* **7**: 451.

252. Szalai, K., J. Fuhrmann, T. Pavkov, M. Scheidl, J. Wallmann, K. H. Bramswig, S. Vrtala, O. Scheiner, W. Keller, J. M. Saint-Remy, D. Neumann, I. Pali-Scholl, and E. Jensen-Jarolim. 2008. Mimotopes identify conformational B-cell epitopes on the two major house dust mite allergens Der p 1 and Der p 2. *Mol Immunol* **45**: 1308-1317.

253. Luzzago, A., F. Felici, A. Tramontano, A. Pessi, and R. Cortese. 1993. Mimicking of discontinuous epitopes by phage-displayed peptides, I. Epitope mapping of human H ferritin using a phage library of constrained peptides. *Gene* **128**: 51-57.

254. Untersmayr, E., K. Szalai, A. B. Riemer, W. Hemmer, I. Swoboda, B. Hantusch, I. Scholl, S. Spitzauer, O. Scheiner, R. Jarisch, G. Boltz-Nitulescu, and E. Jensen-Jarolim. 2006. Mimotopes identify conformational epitopes on parvalbumin, the major fish allergen. *Mol Immunol* **43**: 1454-1461.

255. Poloni, F., G. Romagnoli, M. Cianfriglia, and F. Felici. 1995. Isolation of antigenic mimics of MDR1-P-glycoprotein by phage-displayed peptide libraries. *Int J Cancer* **61**: 727-731.

256. Birkenmeier, G., A. A. Osman, G. Kopperschlager, and T. Mothes. 1997. Epitope mapping by screening of phage display libraries of a monoclonal antibody directed against the receptor binding domain of human alpha2-macroglobulin. *FEBS Lett* **416**: 193-196.

257. Orlandi, R., C. Formantici, S. Menard, C. M. Boyer, J. R. Wiener, and M. Colnaghi. 1997. A linear region of a monoclonal antibody conformational epitope mapped on p185HER2 oncoprotein. *Biol Chem* **378**: 1387-1392.

258. Lin, C. W., and S. C. Wu. 2004. Identification of mimotopes of the Japanese encephalitis virus envelope protein using phage-displayed combinatorial peptide library. *J Mol Microbiol Biotechnol* **8**: 34-42.

259. Oomen, C. J., P. Hoogerhout, B. Kuipers, G. Vidarsson, L. van Alphen, and P. Gros. 2005. Crystal structure of an Anti-meningococcal subtype P1.4 PorA antibody provides basis for peptide-vaccine design. *J Mol Biol* **351**: 1070-1080.

260. Jakab, A., G. Schlosser, M. Feijlbrief, S. Welling-Wester, M. Manea, M. Vila-Perello, D. Andreu, F. Hudecz, and G. Mezo. 2009. Synthesis and antibody recognition of cyclic epitope peptides, together with their dimer and conjugated derivatives based on residues 9-22 of herpes simplex virus type 1 glycoprotein D. *Bioconjug Chem* **20**: 683-692.

261. Coulon, S., J. Y. Metais, M. Chartier, J. P. Briand, and D. Baty. 2004. Cyclic peptides selected by phage display mimic the natural epitope recognized by a monoclonal anti-colicin A antibody. *J Pept Sci* **10**: 648-658.

262. Francis, M. J., G. Z. Hastings, F. Brown, J. McDermed, Y. A. Lu, and J. P. Tam. 1991. Immunological evaluation of the multiple antigen peptide (MAP) system using the major immunogenic site of foot-and-mouth disease virus. *Immunology* **73**: 249-254.

263. Leclerc, C., P. Martineau, B. Charlot, F. Delpeyroux, S. van der Werf, and M. Hofnung. 1997. Control by Ig genes of the responsiveness to a neutralization viral B cell epitope. *J Immunol* **158**: 3252-3258.

9. LIST OF ABBREVIATIONS

AA	acetaldehyde
AutoAbs	autoantibodies
APCs	antigen presenting cells
4-HNE	4-hydroxynonenal
apoB	apolipoprotein B
apoE	apolipoprotein E
BPRs	Biopanning rounds
BSA	bovine serum albumin
CFA	complete Freunds adjuvant
CFH	complement factor H
CRP	c-reactive protein
CuOx	copper sulfate–oxidized
DAMPs	danger-associated molecular patterns
ELISA	enzyme-linked immunosorbent assay
Ig	immunoglobulin
IL-	interleukin-
LDL	low-density lipoprotein
LDLR	low-density lipoprotein receptor
LOX-1	lectin-type oxidized LDL receptor 1
mAbs	monoclonal antibodies
MAA	malondialdehyde-acetaldehyde
MDA	malondialdehyde
MDHDC	4-methyl-1,4-dihydropyridine-3,5-dicarbaldehyde
MI	myocardial infarction
Nab(s)	natural antibodies
NEB	New England Biolabs
OSE	oxidation-specific epitopes
PAMPs	Pathogen-associated molecular patterns
PC	phosphocholine (PC)
PCI	percutaneous coronary intervention
PFU	plaque forming
Ph.D.-12	dodecameric phage display peptide library
Ph.D.-C7C	heptameric phage display cyclic peptide library
PRRs	pattern recognition receptor
PUFAs	polyunsaturated fatty acid
RLU	relative light units
SEM	standard error of the mean
TLRs	Toll-like receptors
TNF	tumor necrosis factor

10. PUBLICATIONS BASED ON THE THESIS

Part of this thesis has been published as a review article "Experimental immunotherapeutic approaches for atherosclerosis" in Clinical Immunology, 2010, by S. Amir and C. J. Binder (29). The dissertation author was the primary investigator and author of this paper.

Part of this thesis has been published as original article "Peptide Mimotopes of malondialdehyde-epitopes for the clinical applications in cardiovascular disease.", in the Journal of Lipid Research, 2012, by S.Amir, K. Hartvigsen, G.Leibundgut, X.Que, E. Jensen-Jarolim, O.Wagner, S.Tsimikas, J.L.Witztum and C.J.Binder. The dissertation author was the primary investigator and author of this paper.

Fig. 16 and 18 were reproduced in "Peptide Mimotopes to Oxidation-Specific Epitopes for Clinical Applications in Cardiovascular Disease". Permission from publishers were acquired for the inclusion.

11. ACKNOWLEDGEMENTS

I would like to express a warm gratitude to all the people who have made this thesis possible and who have encouraged and supported me during my PhD studies, especially the following people:

A special thank you to my main supervisors and mentors **Prof. Dr. Oswald Wagner** and **Prof. DDr. Christoph J. Binder** for giving me the opportunity to do my PhD studies in your lab.

Prof. DDr. Christoph J. Binder, my main supervisor at the Medical University of Vienna, for inspiring me to be creative and innovative and providing me with the critical and enlightening comments. Many thanks also for your creativity; expertise in atherosclerosis and immunology. My thesis and project would not have been realized without your valuable inputs, constructive criticisms and guidance.

Prof. Dr. L. **Joseph Witztum**, my co-supervisor and mentor at the University of California San Diego, for your immense knowledge in the field of atherosclerosis, lipidology, vaccinology and for always taking time to answer my questions, quickly and straight to the point. Thank you for all the interesting discussions about both science and life.

Prof. Dr. Sotirios Tsimikas for bringing the clinical views into research, your extensive knowledge in human atherosclerosis and for providing the precious human samples from different published human cohorts.

Dr. Karsten Hartvigsen, Thanks for providing EN1 antibody and the MDA-modified short peptides and for providing expertise and valuable input to my research-.

Dr.Xuchu Que, Thanks for providing CLL69 antibodies and productive discussions about different experimental approaches relevant to my hypothesis.

I convey my sincere thanks to **Prof. Dr. Erika Jensen-Jarolim, DDr. Yury I. Miller Dr. Krisztina Szalai** and **Dr. Arvand Haschemi** for their valuable suggestions and useful discussions. Special thanks to **Sabrina Gruber, Clara Jana Lui Busch, Nikolina Papac-Milicevic** for reviewing thesis and the manuscript for publication.

I thank all my colleagues from Vienna **(David Weismann, Dimitris Tsiantoulas, Larissa Cardilo dos Reis, Laura Göderle, Maria Ozsvar-Kozma)** and from San Diego

(Ayelet Gonen, Felicidad Almazan, Gregor Leibundgut, Philipp Wiesner) who gave me scientific help and technical support.

I would like to acknowledge my family (M.Sharif, M. Saleem Uddin, M. Shahbaz Uddin, Samina Majid and Ghazala Saleem) for providing constant support.

12. FUNDING

This work was supported by the doctoral program Cell Communication in Health and Disease (CCHD), funded by the Austrian Science Fund and the Medical University of Vienna; by the SFB Lipotox F30 of the Austrian Science Fund (CJB); NIH grants HL088093 (CJB, ST, JLW), RO1 HL086599 (KH, JLW), and the Fondation Leducq (CJB,ST,JLW).

13. AUTHOR'S CURRICULUM VITAE

Personal Information

Name	Shahzada Amir, MD., M.Sc.
Date of Birth	July 10th, 1980
Nationality	Pakistan
Address	KILM Department of Laboratory Medicine \ Ce-M-M- Center for Molecular Medicine of the Austrian Academy of Sciences Medical University of Vienna Lazarettgasse 14 1090 Vienna Austria
E-mail	shahzada.amir@meduniwien.ac.at

Education

2007 - Present	Student in the international CCHD-PhD program (2007-2012), Medical University of Vienna, Vienna, Austria. International MD Post-Doc scholar (2010-2011), University of California San Diego, San Diego, USA
2005-2007	International master in Molecular Bio-Engineering. Biotechnology Centre (BIOTEC), Technical University of Dresden, Dresden, Germany
2003-2005	Clinical Residency in General Surgery, Grodno University Hospital, Grodno State Medical University, Grodno, Belarus
1997-2003	Doctor of Medicine (M.D.) in Human Medicine (with Distinction), Grodno State Medical University, Grodno, Belarus
1996-1997	Preparatory Course for Human Medicine, Belorussian State Polytechnic Academy, Minsk, Belarus
1994-1996	Intermediate Course (Pre-Medicine), Zamindar College Gujrat, Gujrat, Pakistan

Research Experience

10. 2007 – 06.2012	PhD student: "Identification and characterization of malondialdehyde peptide mimotopes" Supervisor: Prof. Christoph J. Binder Medical University of Vienna and Center for Molecular Medicine of the Austrian Academy of Sciences, Vienna, Austria
6. 2010 – 4. 2011	Research visit at the University of California San Diego, San Diego, USA Laboratory of Prof. Joseph L. Witztum
9. 2006 – 6. 2007	Master Thesis: "Isolation and characterization of cardiac resident stem cells" Supervisor: Prof. Dr. Ursula Ravens, Dr. Denis Corbeil Inst. of Pharmacology, Medical University of Dresden, Dreseden, Germany

Peer reviewed Publications

S. Amir., and C. J. Binder. 2010. **Experimental immunotherapeutic approaches for atherosclerosis**. *Clin Immunol* 134:66-79.

S.Amir, K. Hartvigsen, G.Leibundgut, X.Que, E. Jensen-Jarolim, O.Wagner, S.Tsimikas, J.L.Witztum and C.J.Binder. 2012. **Peptide Mimotopes of malondialdehyde-epitopes for the clinical applications in cardiovascular disease.** *J Lipid Res*. 53:1316-1326.

A. Haschemi., P. Kosma., L. Gille., C. Evans., C. F. Burant., P. Starkl., B. Knapp., R. Haas., J. A. Schmid., C. Jandl., S. Amir., G. Lubec., J. Park., H. Esterbauer.,M. Bilban., L. Brizuela., A. J. Pospisilik., L. E. Otterbein., O. Wagner. 2012. **The Sedoheptulose Kinase CARKL Directs Macrophage Polarization Through Control of Glucose Metabolism**. *Cell Meta.*- In press.

Conferences

2012	Young Scientist Association (YSA) Conference, Medical University of Vienna, Austria. *Poster presentation.*
2011	Scientific Sessions - American Heart Association, Orlando, USA. *Poster presentation.*
2009	Young Scientist Association Conference, Medical University of Vienna, Austria. *Poster presentation.*
2008	European Vascular Genomics Network Summer School, Cracow, Poland. *Poster presentation.*

Awards

2012	**Best YSA-poster presentation Award**, Medical University of Vienna, Austria
2007- 2012	**CCHD PhD Fellowship,** Medical University of Vienna, Austria
2003-2005	**Studentship for postgraduate students,** Grodno State Medical University, Belarus
2001-2003	**Excellent Student Award/Scholarship,** Grodno State Medical University, Belarus
2002	**Young scientists & student conference award,** Grodno, Belarus